

Supplementary Material: Switchable Access to Amines and Imines from Reductive Coupling of Nitroarenes with Alcohols Catalyzed by Biomass-Derived Cobalt Nanoparticles

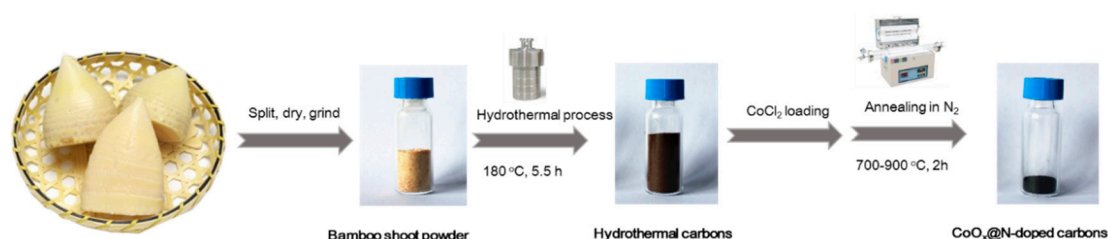
Tao Song ¹, Yanan Duan ¹, Xiufang Chen ^{1,*} and Yong Yang ^{1,*}

1. General considerations

Unless otherwise noted, all reagents were purchased commercially from Sigma-Aldrich, or Aladdin and used as received without further purification. The fresh bamboo shoots were obtained from Anhui Taiping Test Centre, International Centre for Bamboo and Rattan, Anhui Province, China. All operations were carried out in an argon atmosphere using glovebox and Schlenk techniques unless otherwise specified. Anhydrous tetrahydrofuran (THF), hexanes and toluene were obtained from an argon purged solvent purification system comprised of columns of activated alumina and molecular sieves. Gas chromatography analysis was performed on an Agilent HP-7890 instrument with a flame ionization detector (FID) and an HP-5MS capillary column (30 m, 0.25 mm i.d., 0.25 μ m film thicknesses) using helium as the carrier gas. Gas chromatography-mass spectrometry analysis was carried out on an Agilent HP-7890 instrument with an Agilent HP-5975 with triple-axis detector and HP-5 capillary column using helium carrier gas. NMR spectra were received using DRX-400, or DRX-600, Chemical shifts are reported in ppm relative to the residual solvent signal (CDCl₃: 7.26 ppm (¹H), 77.16 ppm (¹³C), Multiplicities were reported using the following abbreviations: s = singlet, d = doublet, dd = doublet of doublets, t = triplet, q = quartet, m = multiplet, brs = broad singlet. High-resolution mass data were recorded on Bruke Maxis UHR TOF mass spectrometers in ESI mode.

2. Preparation of the nanostructured Co nanoparticles catalyst

The functionalized hydrochars were firstly prepared by hydrothermal method using bamboo shoots as raw material. The fresh bamboo shoots were cut into slices, dried and ground into a powder. 2 g of the dried bamboo shoots were added to 20 mL of deionized water in a 100 mL Teflon-inner stainless steel autoclave, which was sealed and heated at 180 °C for 5.5 h. The resulting solids were obtained by filtration, washed thoroughly using distilled water to remove any soluble metals, and dried by vacuum freeze-drying. After that, 0.5 g of the obtained hydrochars were mixed with 15 mL of CoCl₂ aqueous solution (0.2 mmol Co) and the suspension was stirred at 60 °C for 2 h and then dried at 100 °C for 10 h to remove water. Afterward, the solids were grinded to fine powders and heated to 700, 800 or 900 °C at a rate of 5 °C/min and maintained at this temperature for 2 h under N₂ atmosphere. The Co based N-doped porous carbon catalysts were named as CoO_x@NC-T, where T represents the calcination temperature, as shown in Scheme S1. For comparison, Co based commercial activated carbon (CoO_x@C-800) was also synthesized under a similar process, which was calcined at 800 °C for 2 h under N₂ atmosphere.



Scheme S1. The schematic illustration of the fabrication of CoO_x@NC catalyst.

3. Characterization of the as-prepared catalysts

The X-ray diffraction (XRD) powder patterns were recorded on a Bruker D8 Advance X-ray diffraction diffractometer, equipped with CuK α radiation ($\lambda = 1.5147 \text{ \AA}$). The magnetic hysteresis loop was measured by using a Quantum Design SQUID-VSM magnetometer. The morphology of the catalysts was examined using a Tecnai G2 F30 high-resolution transmission electron microscope (HRTEM) and a FEI Tecnai G2 F20 scanning transmission electron microscope (STEM). Nitrogen adsorption–desorption data were obtained using a Micromeritics ASAP 2020 static volumetric sorption analyzer. The specific surface area of the samples was calculated using the Brunauer–Emmett–Teller (BET) method. The micropore volume was calculated using a t-plot method. The pore size distribution was determined using non-local density functional theory (DFT). The X-ray photoelectron spectroscopy (XPS) data were obtained using a Thermo ESCALAB250 instrument with a monochromatized Al K α line source. All the binding energies obtained were calibrated based on the C 1s peak at 284.6 eV. The elemental composition analysis was conducted using a Vario El elemental analyzer. Inductively coupled plasma atomic emission spectroscopy (ICP-AES) measurements were taken on a Perkin Elmer Optima 5300 DV instrument. Fourier transformed infrared (FT-IR) spectra was recorded on a Thermo Nicolet FTIR Spectrometer. Raman spectra were collected on a Horiba Jobin Yvon LabRAM HR800 Raman spectrometer system using a 532 nm wavelength laser at room temperature. Magnetic measurement was carried out using a SQUID MPMS-XL5 from Quantum Design with the field range of -3 to 3 T in hysteresis mode. The sample was prepared in a gelatine capsule held in a plastic straw under protective atmosphere. The raw data were corrected for the diamagnetic part of the sample holder.

4. Test of as-prepared catalysts

4.1. General procedure for imine synthesis

A 25 mL sealed tube was charged with a magnetic stirring bar, 20 mg (10 mol%) catalyst and 67.2 mg (0.6 mmol) *t*BuOK, the tube was then sealed with a rubber septum and was evacuated for a while to remove air, then the tube was refilled with N₂ followed by injection of 0.2 mmol nitrocompounds, 0.6 mmol alcohols, 5 mL toluene via syringe into the tube and the reaction was loaded into a preheated oil bath at 120°C for 15 h. After completion of the reaction, the reaction mixture was filtered or separated using external magnet. The liquid was analysed by GC and GC-MS to determine the conversion and selectivity using dodecane as an internal standard. The products were purified by column chromatography or recrystallization and structurally confirmed by NMR.

4.2. General procedure for amine synthesis

A 25 mL sealed tube was charged with a magnetic stirring bar, 20 mg (10 mol%) catalyst and 89.6 mg (0.8 mmol) *t*BuOK, the tube was then sealed with a rubber septum and was evacuated for a while to remove air, then the tube was refilled with N₂ followed by injection of 0.2 mmol nitrocompounds, 0.8 mmol alcohols, 5 mL toluene via syringe into the tube and the reaction was loaded into a preheated oil bath at 120°C for 15h. After completion of the reaction, the reaction mixture was filtered or separated using external magnet. The liquid was analysed by GC and GC-MS to determine the conversion and selectivity using dodecane as an internal standard. The products were purified by column chromatography or recrystallization and structurally confirmed by NMR.

4.3. Catalyst recycling

The model reaction was chosen to investigate the recyclability of the novel cobalt nanocomposite catalyst. A 25 mL sealed tube was charged with a magnetic stirring bar, 20 mg (10 mol%) catalyst and 67.5 mg (0.6 mmol) *t*BuOK, the tube was then sealed with a rubber septum and was evacuated for a while to remove air, then 0.2 mmol nitrobenzene, 0.6 mmol benzyl alcohol, 5 mL toluene were injected via syringe into the tube and the reaction was stirred at 120 °C for 15 h. After completion of the reaction, tube was cooled to room temperature and the yield was determined by GC using dodecane

as an internal standard, the reaction mixture was centrifuged (10000 rpm and 15 min) or was separated by external magnet (the magnet was placed at the bottom of the tube for 30 min) and the liquid was carefully decanted out. 5 mL of ethanol and 5 mL water were added and the resulting mixture was stirred for 10 min by followed by centrifugation again to remove any residuals on the catalyst. Such operation was repeated for 3 times. Finally, the obtained black solid was dried under vacuum at 40°C overnight for successive use.

5. Characterization results

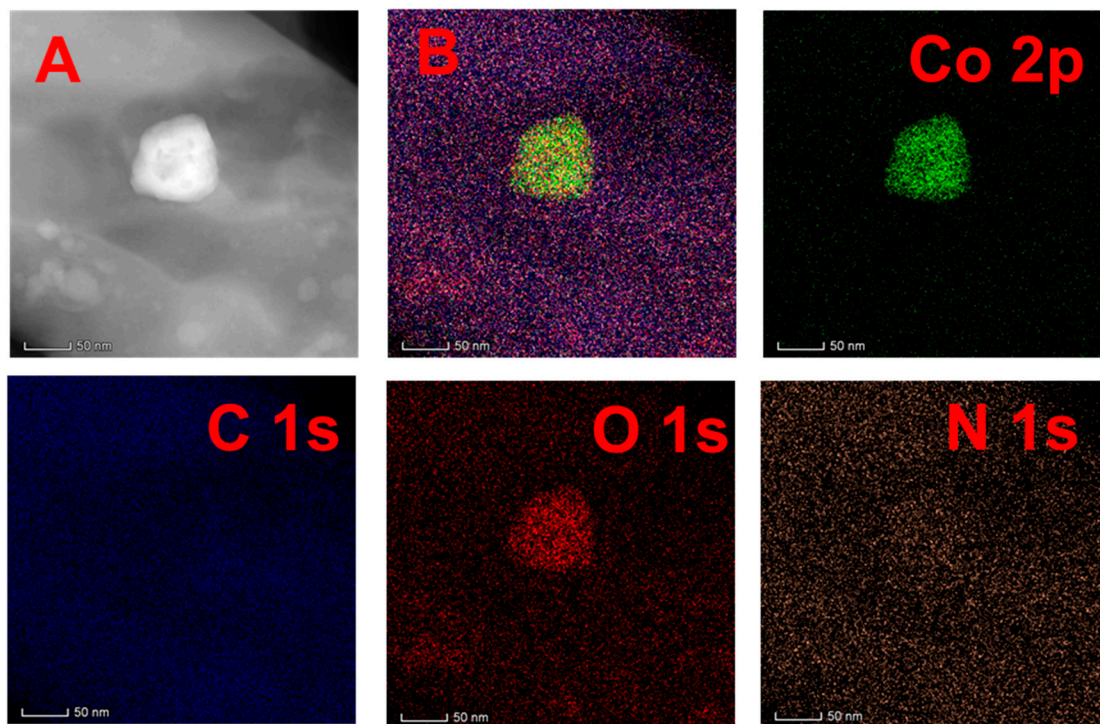


Figure S1. High-angle annular dark-field scanning transmission electron microscopy (HAADF-STEM) image and elemental mapping of Co, C, O, and N for the catalyst CoO_x@NC-800.

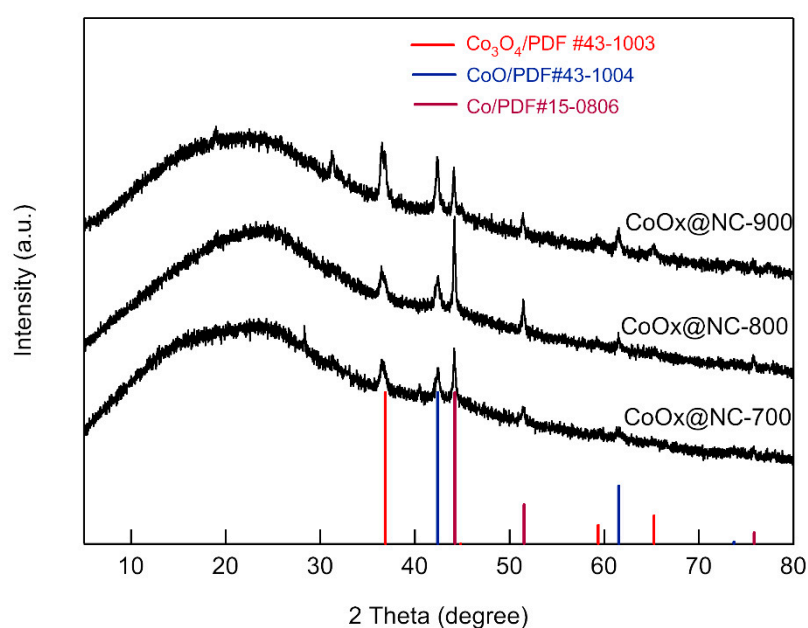


Figure S2. XRD patterns of CoO_x@NC-700, CoO_x@NC-800, and CoO_x@NC-900.

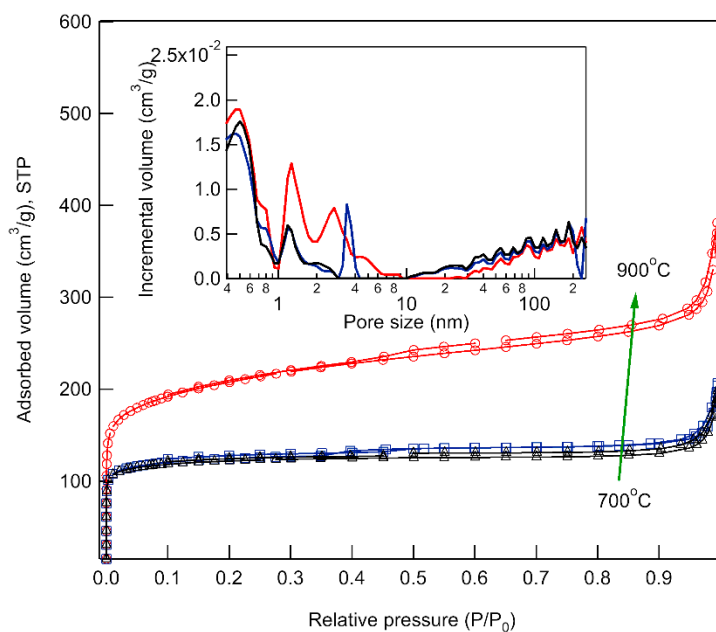


Figure S3. N₂ sorption isotherms and pore size distribution calculated using a nonlocal density function theory (NLDFT) method for the catalysts CoO_x@NC-700, CoO_x@NC-800, and CoO_x@NC-900.

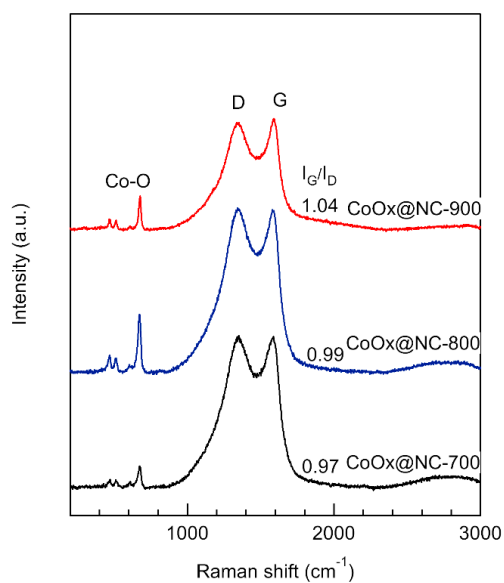


Figure S4. Raman spectra of the catalysts CoO_x@NC-700, CoO_x@NC-800, and CoO_x@NC-900.

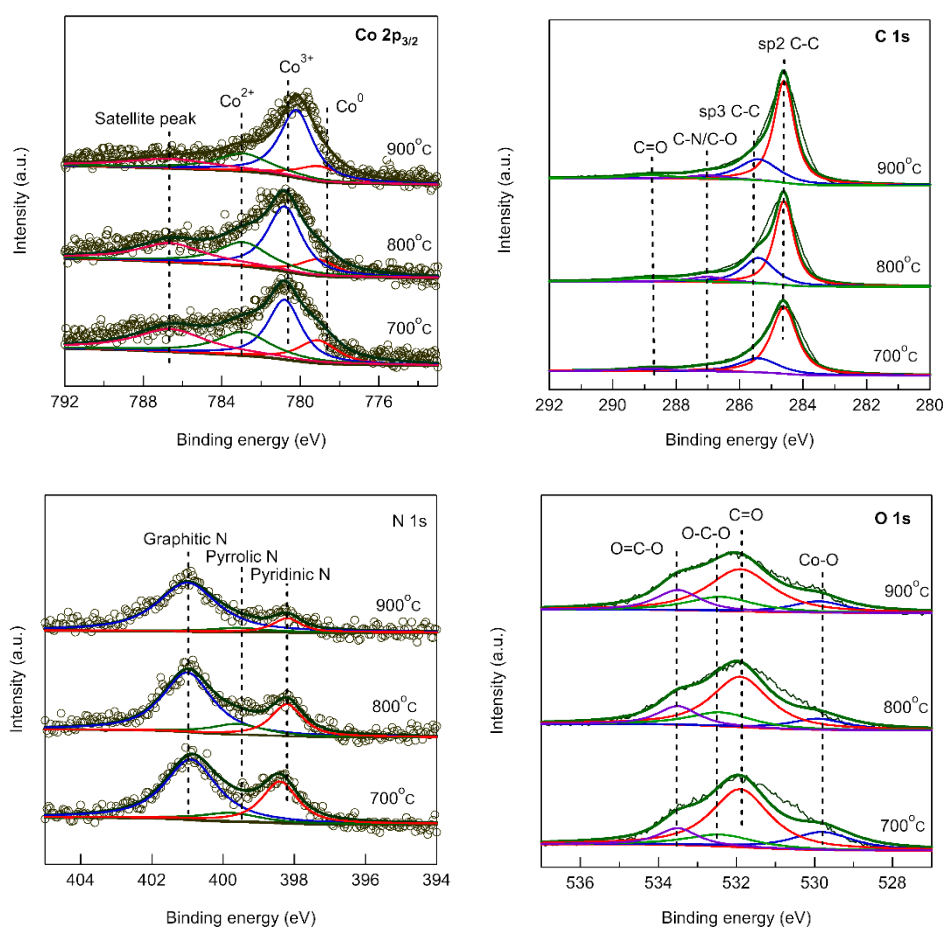


Figure S5. Co 2p_{3/2}, C 1s, N 1s and O 1s XPS spectra of the catalysts CoO_x@NC-700, CoO_x@NC-800, and CoO_x@NC-900.

Table S1. Chemical composition of the catalysts CoO_x@NC-T by elemental analysis.

Sample	C (%) ^a	N (%) ^a	O (%) ^a	Co content (wt%) _b
CoO _x @NC-700	67.34	4.00	16.53	5.48
CoO _x @NC-800	66.67	2.97	16.76	5.39
CoO _x @NC-900	64.21	1.74	17.73	8.30
Co@C-800	-	-	-	4.96

^a Calculated from the results of elemental analysis. ^b Determined by ICP-AES.

Table S2. The textural properties of the catalysts CoO_x@NC-T.

Sample	Surface area (m ² /g) ^a	Pore volume (cm ³ /g) ^b
CoO _x @NC-700	462.9	0.307
CoO _x @NC-800	471.7	0.319
CoO _x @NC-900	763.3	0.589

^a BET surface area calculated from the linear part of the BET plot ($P/P_0 = 0.1-0.2$). ^b Total pore volume, taken from the volume of N₂ adsorbed at $P/P_0 = 0.99$.

Table S3. The nitrogen types and respective contents in the carbon matrix for the catalysts CoO_x@NC-T by XPS analysis.

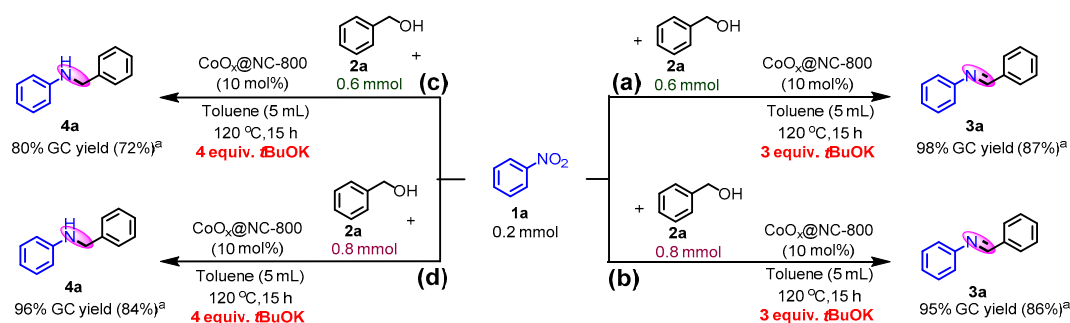
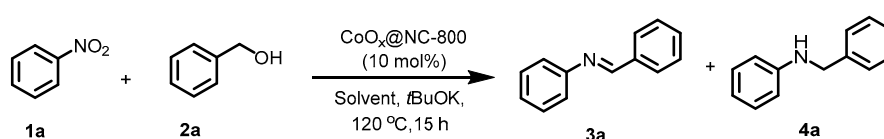
Sample	Graphitic N (401.2 eV)	Pyrrolic N or Co-N _x (399.6 eV)	Pyridinic N (398.2 eV)
CoO _x @NC-700	61%	10%	29%
CoO _x @NC-800	66%	12%	22%
CoO _x @NC-900	83%	7%	11%

Table S4. The different cobalt phases and respective contents in the catalysts CoO_x@NC-T by XPS analysis.

Catalyst	Co ⁰ (778.9 eV)	CoO (782.9 eV)	Co ₃ O ₄ (780.8 eV)
CoO _x @NC-700	21%	32%	47%
CoO _x @NC-800	15%	32%	53%
CoO _x @NC-900	17%	26%	57%

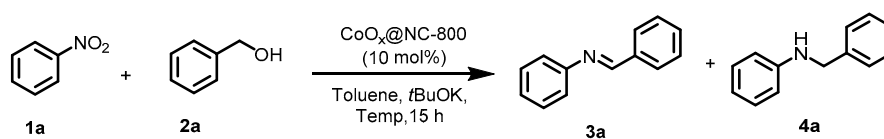
6. Catalytic studies

6.1. Conditions optimization

**Scheme S2.** Switchable product selectivity for coupling of nitrobenzene and benzyl alcohol catalyzed by CoO_x@NC-800 by simple modification of reaction conditions. ^aIsolated yield.**Table S5.** Screening of solvents^[a].

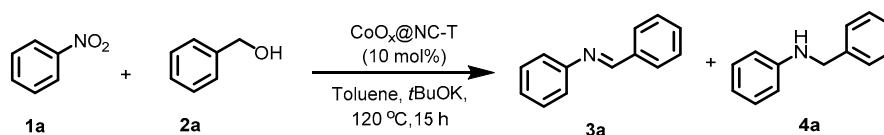
Entry	Solvent	Conversion (%)	Selectivity (%)		
			3a	4a	others
1	THF	71	38	4	58
2	Dioxane	78	22	0	78
3	n-Hexane	28	23	5	0
4	Toluene	100	98	2	0

^[a] Reaction conditions: nitrobenzene (0.2 mmol), benzyl alcohol (0.6 mmol), CoO_x@NC-800 (10 mol%), *t*BuOK (0.6 mmol), Solvent (5 mL), 120 °C, 15 h. [b] Determined by GC using dodecane as an internal standard and conversion based on the conversion of nitrobenzene.

Table S6. Screening of reaction temperature^[a].

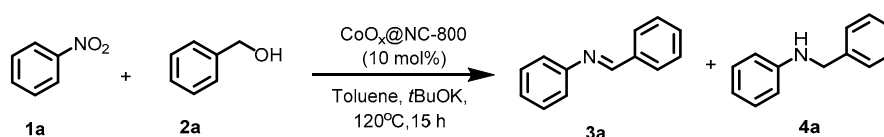
Entry	Temperature	Conversion (%)	Selectivity (%)	
			3a	4a
1	120	100	98	2
2	100	68	61	0
3	80	44	34	0

^[a] Reaction conditions: nitrobenzene (0.2 mmol), benzyl alcohol (0.6 mmol), CoO_x@NC-800t (10 mol%), *t*BuOK (0.6 mmol), Toluene (5 mL), 120 °C, 15 h. [b] Determined by GC using dodecane as an internal standard and conversion based on the conversion of nitrobenzene.

Table S7. Screening of CoO_x@NC-T catalysts^[a].

Entry	Catalyst	Conversion (%)	Selectivity (%)	
			3a	4a
1	CoO _x @NC-700	100	85	15
2	CoO _x @NC-800	100	98	2
3	CoO _x @NC-700	78	95	5

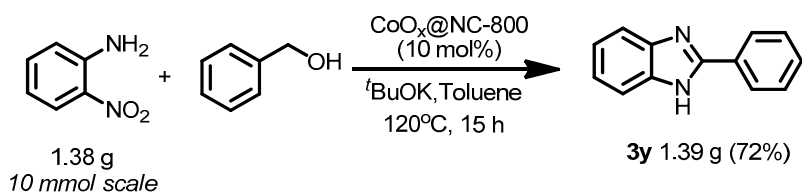
^[a] Reaction conditions: nitrobenzene (0.2 mmol), benzyl alcohol (0.6 mmol), CoO_x@NC-T (10 mol%), *t*BuOK (0.6 mmol), Toluene (5 mL), 120 °C, 15 h. [b] Determined by GC using dodecane as an internal standard and conversion based on the conversion of nitrobenzene.

Table S8. Effect of amount of benzyl alcohol^[a].

Entry	2a (equiv.)	Conversion (%)	Selectivity (%)	
			3a	4a
1	2	43	100	0
2	3	100	98	2
3	4	100	95	5

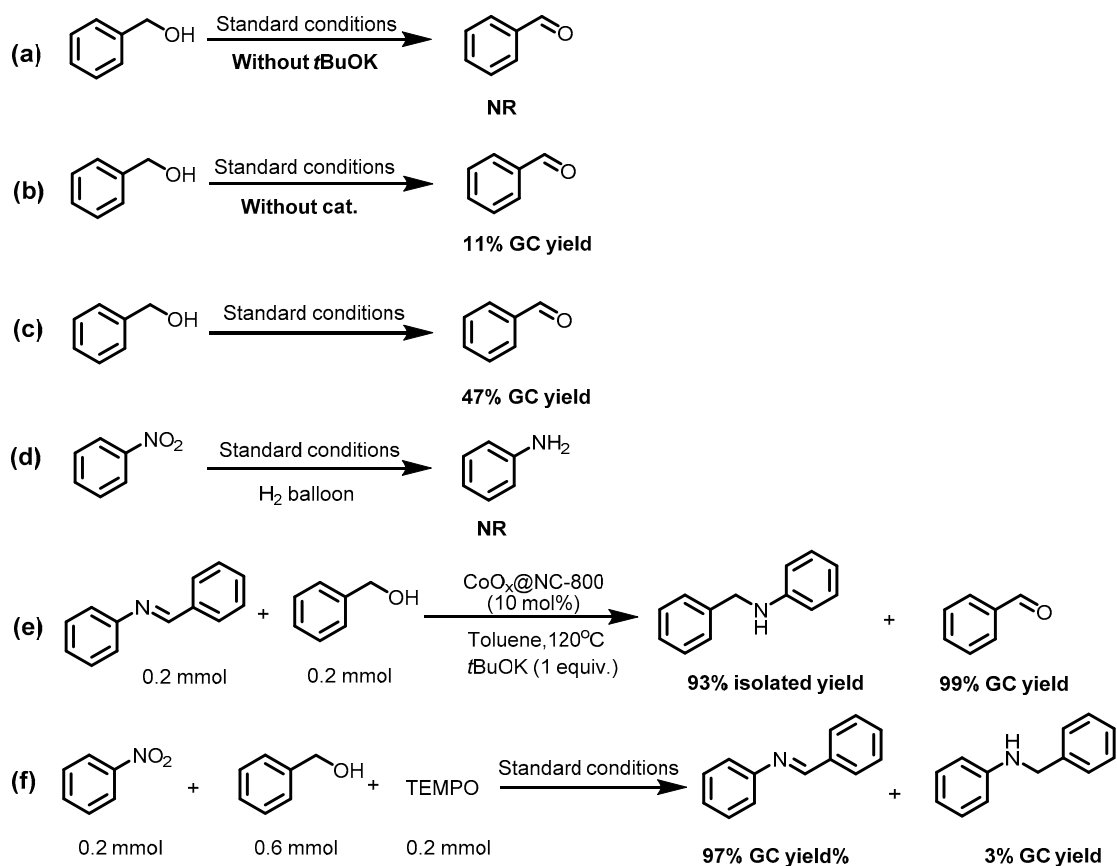
^[a] Reaction conditions: nitrobenzene (0.2 mmol), benzyl alcohol (0.4–0.8 mmol), CoO_x@NC-800 (10 mol%), *t*BuOK (0.6 mmol), Toluene (5 mL), 120 °C, 15 h. [b] Determined by GC using dodecane as an internal standard and conversion based on the conversion of nitrobenzene.

6.2. Gram-scale synthesis of benzoimidazole



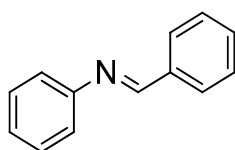
A 500 mL round-bottom flask with economical allihn condenser was charged with a magnetic stirring bar, 1 g (10 mol%) catalyst and 3.36 g (30 mol) *t*BuOK, the bottom was then sealed with a rubber septum and was evacuated for a while to remove air, then 1.38 g (10 mol) 2-nitroaniline, 3.11 mL (30 mol) benzyl alcohol, 250 mL toluene were injected via syringe into the tube and the reaction was refluxed for 20 h. After completion of the reaction, the reaction mixture was filtered and the filtrate was concentrated by rotary evaporator, then 1.39 g benzoimidazole was obtained by recrystallization (MeOH / Ethyl Acetate) and the structure was confirmed by NMR.

6.3. Control experiments

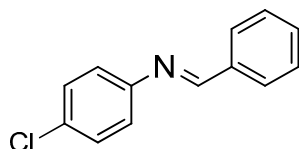


Scheme S3. Control experiments. NR = no reaction.

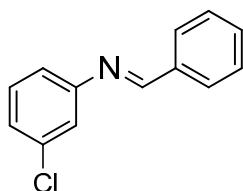
7. Characterization of the obtained products



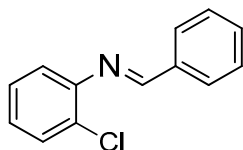
(E)-N-benzylideneaniline (3a)^[1], Light yellow solid; ¹H NMR (400 MHz, CDCl₃): δ 8.37 (s, 1H), 7.79-7.81 (m, 2H), 7.45-7.30 (m, 5H), 7.23-7.11 (m, 3H); ¹³C NMR (101 MHz, CDCl₃): δ 160.4, 152.2, 136.4, 131.5, 129.3, 128.9, 128.9, 126.1, 121.0; The spectroscopic data matched that previously report.^[1]



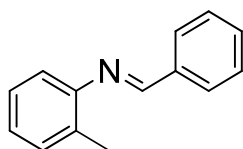
(E)-N-benzylidene-4-chloroaniline (3b)^[1], White solid; ¹H NMR (400 MHz, CDCl₃): δ 8.40 (s, 1H), 7.88 (d, *J* = 6.2 Hz, 2H), 7.50-7.42 (d, *J* = 5.9 Hz, 3H), 7.33 (d, *J* = 8.3 Hz, 2H), 7.13 (d, *J* = 8.2 Hz, 2H); ¹³C NMR (101 MHz, CDCl₃): δ 160.7, 150.5, 135.9, 131.7, 131.5, 129.3, 128.9, 128.9, 122.3; The spectroscopic data matched that previously report.^[1]



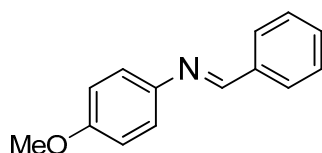
(E)-N-benzylidene-3-chloroaniline (3c)^[1], White solid; ¹H NMR (400 MHz, CDCl₃): δ 8.38 (s, 1H), 8.06-7.69 (m, 2H), 7.451-7.41 (d, *J* = 6.7 Hz, 3H), 7.28 (t, *J* = 8.1 Hz, 1H), 7.18 (d, *J* = 1.4 Hz, 2H), 7.07 (d, *J* = 7.7 Hz, 1H); ¹³C NMR (101 MHz, CDCl₃): δ 161.4, 153.4, 135.9, 134.8, 131.8, 130.2, 129.0, 128.9, 125.9, 120.9, 119.4; The spectroscopic data matched that previously report.^[1]



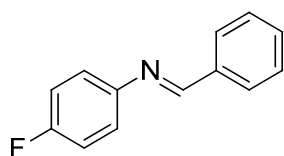
(E)-N-benzylidene-2-chloroaniline (3d)^[2], Yellow oil; ¹H NMR (600 MHz, CDCl₃): δ 8.32 (s, 1H), 7.91 (d, *J* = 7.5 Hz, 2H), 7.55-7.31 (m, 4H), 7.22 (t, *J* = 7.6 Hz, 1H), 7.09 (t, *J* = 7.7 Hz, 1H), 6.97 (d, *J* = 7.8 Hz, 1H); ¹³C NMR (151 MHz, CDCl₃): δ 162.1, 149.6, 135.9, 131.9, 130.0, 129.2, 128.9, 127.9, 127.7, 126.5, 120.1; The spectroscopic data matched that previously report.^[2]



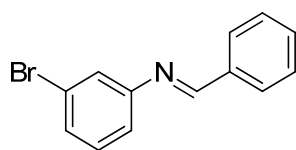
(E)-N-benzylidene-2-methylaniline (3e)^[3], Yellow oil; ¹H NMR (400 MHz, CDCl₃): δ 8.35 (s, 1H), 8.04-7.72 (m, 2H), 7.55-7.34 (m, 3H), 7.30-7.16 (m, 2H), 7.16 -7.05 (m, 1H), 6.91 (d, *J* = 7.8 Hz, 1H), 2.36 (s, 3H); ¹³C NMR (101 MHz, CDCl₃): δ 159.5, 151.2, 136.5, 131.9, 131.3, 130.3, 128.8, 126.8, 125.7, 117.7, 17.9; The spectroscopic data matched that previously report.^[3]



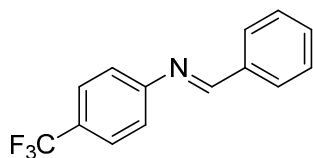
(E)-N-benzylidene-4-methoxyaniline (3f)^[3], White solid; ¹H NMR (400 MHz, CDCl₃): δ 8.45 (s, 1H), 7.98-7.74 (m, 2H), 7.58-7.35 (m, 3H), 7.22 (d, *J* = 8.8 Hz, 2H), 6.91 (d, *J* = 8.9 Hz, 2H), 3.79 (s, 3H); ¹³C NMR (101 MHz, CDCl₃): δ 158.4, 158.3, 144.9, 136.5, 131.1, 128.8, 128.6, 122.3, 114.4, 55.5; The spectroscopic data matched that previously report.^[3]



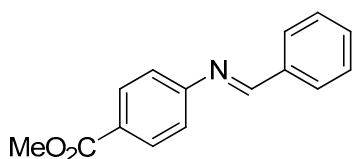
(E)-N-benzylidene-4-fluoroaniline (3g)^[3], Yellow oil; ¹H NMR (600 MHz, CDCl₃): δ 8.43 (s, 1H), 7.89 (d, *J* = 6.0 Hz, 2H), 7.47 (d, *J* = 5.9 Hz, 3H), 7.22-7.14 (m, 2H), 7.07 (t, *J* = 8.3 Hz, 2H); ¹³C NMR (151 MHz, CDCl₃): δ 161.3 (d, *J* = 244.6 Hz), 160.2, 148.08 (d, *J* = 2.4 Hz), 136.1, 131.5, 128.83, 128.81, 122.3 (d, *J* = 8.2 Hz), 115.9 (d, *J* = 22.5 Hz); The spectroscopic data matched that previously report.^[3]



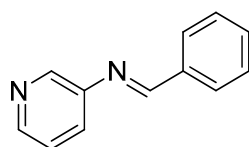
(E)-N-benzylidene-3-bromoaniline (3h)^[3], White solid; ¹H NMR (600 MHz, CDCl₃): δ 8.35 (s, 1H), 7.86 (d, *J* = 7.3 Hz, 2H), 7.52-7.38 (m, 3H), 7.38-7.26 (m, 2H), 7.21 (t, *J* = 7.8 Hz, 1H), 7.10 (d, *J* = 7.8 Hz, 1H); ¹³C NMR (151 MHz, CDCl₃): δ 161.2, 153.4, 135.7, 131.7, 130.4, 128.9, 128.8, 128.6, 123.6, 122.7, 119.9; The spectroscopic data matched that previously report.^[3]



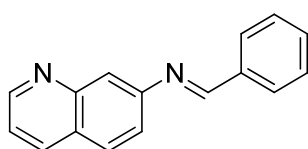
(E)-N-benzylidene-4-(trifluoromethyl)aniline (3i)^[3], White solid; ¹H NMR (400 MHz, CDCl₃): δ 8.34 (s, 1H), 7.90–7.75 (m, 2H), 7.56 (d, *J* = 8.3 Hz, 2H), 7.49–7.33 (m, 3H), 7.26–7.04 (m, 2H); ¹³C NMR (101 MHz, CDCl₃): δ 162.0, 155.2, 135.7, 132.0, 129.1, 128.9, 127.7 (q, *J* = 32.5 Hz), 126.4 (q, *J* = 3.8 Hz), 124.34 (d, *J* = 271.7 Hz), 121.0; The spectroscopic data matched that previously report.^[3]



(E)-methyl 4-(benzylideneamino)benzoate (3j)^[3], Yellow solid; ¹H NMR (400 MHz, CDCl₃): δ 8.34 (s, 1H), 7.99 (d, *J* = 8.3 Hz, 2H), 7.82 (d, *J* = 6.3 Hz, 2H), 7.40 (d, *J* = 6.9 Hz, 3H), 7.12 (d, *J* = 8.3 Hz, 2H), 3.83 (s, 3H); ¹³C NMR (101 MHz, CDCl₃): δ 192.4, 166.8, 161.7, 156.2, 135.8, 131.9, 130.9, 129.1, 128.9, 120.7, 52.1; The spectroscopic data matched that previously report.^[3]

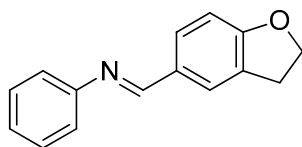


(E)-N-benzylidenepyridin-3-amine (3k), Yellow oil; ¹H NMR (600 MHz, CDCl₃): δ 8.45–8.32 (m, 2H), 8.29 (s, 1H), 7.90–7.70 (m, 2H), 7.42–7.27 (m, 4H), 7.16 (dd, *J* = 8.1, 4.8 Hz, 1H); ¹³C NMR (151 MHz, CDCl₃): δ 162.0, 147.8, 147.1, 142.6, 135.7, 131.9, 129.0, 128.9, 127.8, 123.7; HRMS (*m/z*): calcd. for C₁₂H₁₁N₂ [M+H], 183.0917; found, 183.0917.

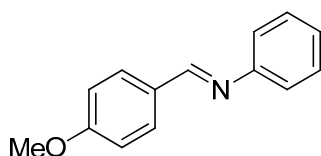


(E)-N-benzylidenequinolin-7-amine (3l), Yellow oil; ¹H NMR (400 MHz, CDCl₃): δ 8.76 (dd, *J* = 4.2, 1.7 Hz, 1H), 8.45 (d, *J* = 4.9 Hz, 1H), 8.07–7.97 (m, 2H), 7.89–7.80 (m, 2H), 7.61–7.50 (m, 1H), 7.43–7.33 (m, 4H), 7.32–7.17 (m, 1H); ¹³C NMR (101 MHz, CDCl₃): δ

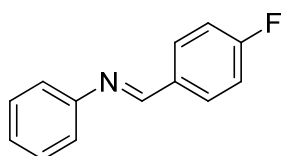
161.3, 150.2, 149.6, 146.9, 136.0, 135.9, 131.7, 130.4, 129.0, 128.9, 128.9, 124.8, 121.5, 117.3; HRMS (m/z): calcd. for $C_{16}H_{13}N_2$ [$M+H$], 233.1073; found, 233.1079.



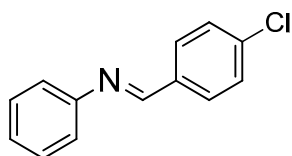
(E)-N-((2,3-dihydrobenzofuran-5-yl)methylene)aniline (3m), Yellow oil; 1H NMR (400 MHz, $CDCl_3$): δ 8.39 (s, 1H), 7.91 (s, 1H), 7.63 (d, $J = 8.0$ Hz, 1H), 7.41 (t, $J = 7.6$ Hz, 2H), 7.33–7.08 (m, 3H), 6.88 (d, $J = 8.2$ Hz, 1H), 4.68 (t, $J = 8.7$ Hz, 2H), 3.29 (t, $J = 8.6$ Hz, 2H); ^{13}C NMR (101 MHz, $CDCl_3$): δ 190.8, 163.3, 159.9, 131.1, 129.2, 128.2, 125.6, 124.8, 120.9, 115.1, 109.4, 72.0, 29.2; HRMS (m/z): calcd. for $C_{15}H_{14}NO$ [$M+H$], 224.1070; found, 224.1073.



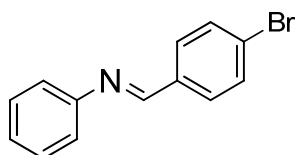
(E)-N-(4-methoxybenzylidene)aniline (3n)^[3], White solid; 1H NMR (600 MHz, $CDCl_3$): δ 8.42 (s, 1H), 7.90 (d, $J = 8.4$ Hz, 2H), 7.43 (t, $J = 7.8$ Hz, 2H), 7.26 (dd, $J = 18.7, 10.9$ Hz, 3H), 7.03 (d, $J = 8.9$ Hz, 2H), 3.91 (d, $J = 7.6$ Hz, 3H); ^{13}C NMR (151 MHz, $CDCl_3$): δ 162.2, 159.7, 152.3, 130.6, 129.2, 125.6, 120.9, 114.2, 55.5; The spectroscopic data matched that previously report.^[3]



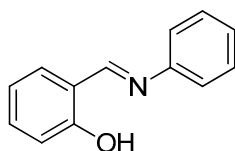
(E)-N-(4-fluorobenzylidene)aniline (3o)^[3], Colourless oil; 1H NMR (400 MHz, $CDCl_3$): δ 8.33 (s, 1H), 7.88–7.78 (m, 2H), 7.31 (t, $J = 7.8$ Hz, 2H), 7.21–6.99 (m, 5H); ^{13}C NMR (101 MHz, $CDCl_3$): δ 164.7 (d, $J = 252.2$ Hz, 1H), 158.8, 151.8, 132.6 (d, $J = 2.8$ Hz), 130.8 (d, $J = 8.8$ Hz, 6H), 129.2, 126.1, 120.8, 115.9 (d, $J = 22.0$ Hz). The spectroscopic data matched that previously report.^[3]



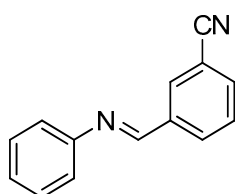
(E)-N-(4-chlorobenzylidene)aniline (3p)^[3], White solid; ¹H NMR (400 MHz, CDCl₃): δ 8.37 (s, 1H), 7.80 (d, *J* = 8.4 Hz, 2H), 7.51–7.32 (m, 4H), 7.26–7.11 (m, 3H); ¹³C NMR (101 MHz, CDCl₃): δ 158.8, 151.7, 137.4, 134.8, 130.0, 129.3, 129.1, 126.3, 120.9; The spectroscopic data matched that previously report.^[3]



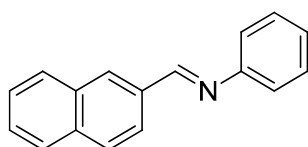
(E)-N-(4-bromobenzylidene)aniline (3q)^[3], White solid; ¹H NMR (400 MHz, CDCl₃): δ 8.33 (s, 1H), 7.69 (d, *J* = 8.4 Hz, 2H), 7.53 (d, *J* = 8.4 Hz, 2H), 7.32 (t, *J* = 7.8 Hz, 2H), 7.21–7.08 (m, 3H); ¹³C NMR (101 MHz, CDCl₃): δ 158.9, 151.7, 135.1, 132.1, 130.2, 129.2, 126.3, 125.9, 120.9; The spectroscopic data matched that previously report.^[3]



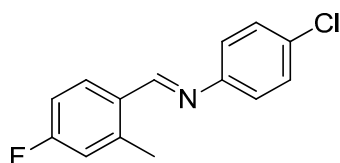
(E)-2-((phenylimino)methyl)phenol (3r)^[4], Yellow solid; ¹H NMR (400 MHz, CDCl₃): δ 13.25 (brs, 1H), 8.54 (d, *J* = 1.5 Hz, 1H), 7.42–7.29 (m, 4H), 7.27–7.17 (m, 3H), 7.00 (dd, *J* = 8.6, 3.7 Hz, 1H), 6.92–6.81 (m, 1H); ¹³C NMR (101 MHz, CDCl₃): δ 162.7, 161.2, 148.5, 133.2, 132.4, 129.5, 126.9, 121.3, 119.3, 119.1, 117.3; The spectroscopic data matched that previously report.^[4]



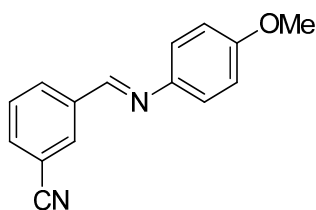
(E)-3-((phenylimino)methyl)benzonitrile (3s)^[5], White solid; ¹H NMR (400 MHz, CDCl₃): δ 8.38 (s, 1H), 8.11 (s, 1H), 8.05 (d, *J* = 7.9 Hz, 1H), 7.72–7.60 (m, 1H), 7.51 (t, *J* = 7.8 Hz, 1H), 7.38 (t, *J* = 7.8 Hz, 2H), 7.29–7.13 (m, 3H); ¹³C NMR (101 MHz, CDCl₃): δ 157.4, 150.9, 137.3, 134.2, 132.8, 132.1, 129.7, 129.4, 126.9, 121.0, 118.4, 113.1; The spectroscopic data matched that previously report.^[5]



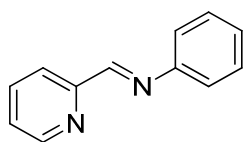
(E)-N-(naphthalen-2-ylmethylene)aniline (3t)^[6], White solid; ¹H NMR (400 MHz, CDCl₃): δ 8.57 (s, 1H), 8.19–8.11 (m, 2H), 7.93–7.78 (m, 3H), 7.58–7.45 (m, 2H), 7.40 (t, *J* = 7.8 Hz, 2H), 7.31–7.16 (m, 3H); ¹³C NMR (101 MHz, CDCl₃): δ 160.4, 152.2, 135.1, 134.0, 133.2, 131.3, 129.3, 128.8, 128.7, 128.0, 127.6, 126.7, 126.1, 123.9, 121.0; The spectroscopic data matched that previously report.^[6]



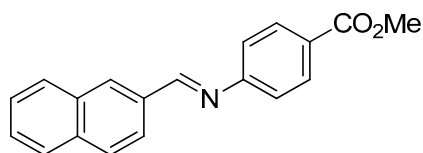
(E)-4-chloro-N-(4-fluoro-2-methylbenzylidene)aniline (3u), White solid; ¹H NMR (400 MHz, CDCl₃): δ 8.69 (s, 1H), 7.82 (d, *J* = 8.4 Hz, 1H), 7.39 (d, *J* = 8.2 Hz, 2H), 7.33–6.98 (m, 4H), 2.56 (s, 3H); ¹³C NMR (101 MHz, CDCl₃): δ 161.5, 157.9, 150.5, 135.5, 134.3, 132.5, 131.8, 129.3, 122.3, 118.2, 113.8, 18.5; HRMS (*m/z*): calcd. for C₁₄H₁₂ClFN [M+H], 248.0637; found, 248.0637.



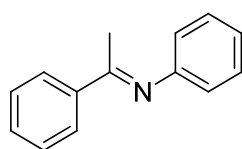
(E)-3-(((4-methoxyphenyl)imino)methyl)benzonitrile (3v)^[5], White solid; ¹H NMR (600 MHz, CDCl₃): δ 8.46 (s, 1H), 8.13 (d, *J* = 49.1 Hz, 2H), 7.63 (d, *J* = 85.2 Hz, 2H), 7.26 (s, 2H), 6.94 (s, 2H), 3.83 (s, 3H); ¹³C NMR (151 MHz, CDCl₃): δ 158.9, 154.9, 143.7, 137.6, 133.8, 132.5, 131.8, 129.6, 122.5, 118.4, 114.5, 113.1, 55.5; The spectroscopic data matched that previously report.^[5]



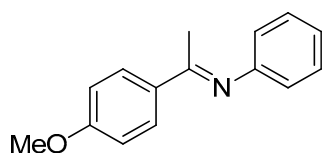
(E)-N-(pyridin-2-ylmethylene)aniline (3w), yellow oil; ¹H NMR (600 MHz, CDCl₃): δ 8.71–8.63 (m, 1H), 8.62 (s, 1H), 8.27–8.07 (m, 1H), 7.85–7.59 (m, 1H), 7.47–7.33 (m, 2H), 7.33–7.14 (m, 4H); ¹³C NMR (151 MHz, CDCl₃): δ 160.6, 154.6, 151.0, 149.7, 136.6, 129.2, 126.7, 125.1, 121.9, 121.2; HRMS (*m/z*): calcd. for C₁₂H₁₁N₂ [M+H], 183.0917; found, 183.0917.



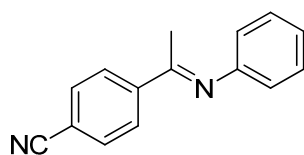
(E)-methyl 4-((naphthalen-2-ylmethylene)amino)benzoate (3x)^[6], Yellow solid; ¹H NMR (400 MHz, CDCl₃): δ 8.61 (s, 1H), 8.29–8.06 (m, 4H), 7.93 (dd, *J* = 15.8, 7.8 Hz, 3H), 7.59 (t, *J* = 6.5 Hz, 2H), 7.29 (d, *J* = 7.7 Hz, 2H), 3.96 (s, 3H); ¹³C NMR (101 MHz, CDCl₃): δ 166.9, 161.7, 156.2, 135.3, 133.5, 133.1, 131.9, 130.9, 128.92, 128.85, 128.01, 127.91, 126.8, 123.9, 120.8, 52.1; The spectroscopic data matched that previously report.^[6]



(E)-N-(1-phenylethylidene)aniline (3y)^[9], white solid; ¹H NMR (400 MHz, CDCl₃): δ 7.98–7.81 (m, 2H), 7.47–7.33 (m, 3H), 7.32–7.22 (m, 2H), 7.07–6.94 (m, 1H), 6.73 (dd, *J* = 8.3, 1.0 Hz, 2H), 2.17 (s, 3H); ¹³C NMR (101 MHz, CDCl₃): 166.4, 152.7, 140.4, 131.4, 129.9, 129.3, 128.1, 124.2, 120.3, 18.3. The spectroscopic data matched that previously report.^[9]

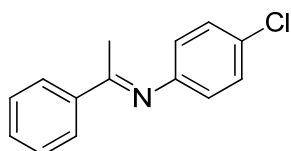


(E)-N-(1-(4-methoxyphenyl)ethylidene)aniline (3z)^[10], white solid; ¹H NMR (400 MHz, CDCl₃): δ 7.95–7.74 (m, 2H), 7.32–7.22 (m, 2H), 7.00 (dd, *J* = 10.6, 4.2 Hz, 1H), 6.92–6.84 (m, 2H), 6.72 (dd, *J* = 8.3, 1.0 Hz, 2H), 3.79 (s, 3H), 2.13 (s, 3H); ¹³C NMR (101 MHz, CDCl₃): δ 164.6, 161.6, 151.8, 132.2, 128.9, 128.8, 123.1, 119.6, 113.6, 55.4, 17.2. The spectroscopic data matched that previously report.^[10]

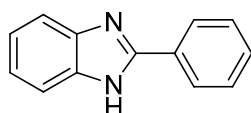


(E)-4-(1-(phenylimino)ethyl)benzonitrile (3aa)^[10], yellow solid; ¹H NMR (400 MHz, CDCl₃): δ 8.1–7.99 (m, 2H), 7.67–7.62 (m, 2H), 7.32–7.28 (m, 2H), 7.07–7.03 (m, 1H), 6.73–

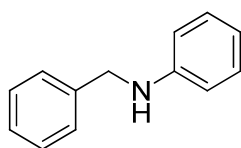
6.70 (m, 1H) 2.17 (s, 3H); ^{13}C NMR (101 MHz, CDCl_3): δ 163.9, 150.8, 143.2, 132.2, 129.1, 127.8, 123.8, 119.1, 118.5, 113.8, 17.3. The spectroscopic data matched that previously report. ^[10]



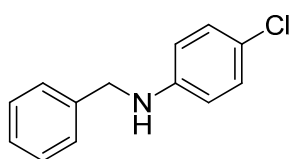
(E)-4-chloro-N-(1-phenylethylidene)aniline (3ab)^[11], yellow solid; ^1H NMR (400 MHz, CDCl_3): δ 7.90–7.88 (m, 2H), 7.40–7.35 (m, 3H), 7.26–7.19 (m, 2H), 6.68–6.60 (m, 2H), 2.17 (s, 3H); ^{13}C NMR (101 MHz, CDCl_3): δ 166.4, 149.2, 139.8, 130.7, 129.0, 128.6, 128.4, 127.2, 17.4. The spectroscopic data matched that previously report. ^[11]



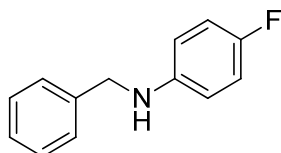
2-phenyl-1H-benzo[d]imidazole^[7], white solid; ^1H NMR (400 MHz, $\text{DMSO}-d_6$): δ 8.34 (d, $J = 7.4$ Hz, 2H), 7.73 (dd, $J = 5.7, 3.2$ Hz, 2H), 7.59 (t, $J = 7.5$ Hz, 2H), 7.51 (t, $J = 7.3$ Hz, 1H), 7.33–7.20 (m, 2H); ^{13}C NMR (151 MHz, $\text{DMSO}-d_6$): δ 151.3, 143.8, 135.2, 130.2, 129.7, 128.9, 126.5, 122.1, 118.7, 111.4; The spectroscopic data matched that previously report. ^[7]



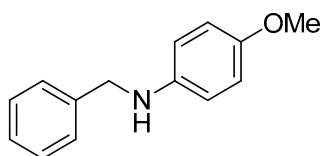
N-benzylaniline (4a)^[8], White solid; ^1H NMR (400 MHz, CDCl_3): δ 7.57–7.48 (m, 4H), 7.48–7.40 (m, 1H), 7.40–7.28 (m, 2H), 6.91 (t, $J = 7.3$ Hz, 1H), 6.80 (dd, $J = 8.5, 0.8$ Hz, 2H), 4.46 (s, 2H), 4.21 (brs, 1H); ^{13}C NMR (101 MHz, CDCl_3): δ 148.3, 139.6, 129.5, 128.8, 127.7, 127.2, 117.8, 113.1, 48.6; The spectroscopic data matched that previously report. ^[8]



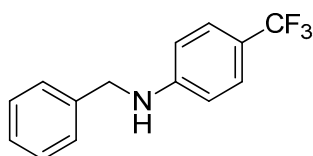
***N*-benzyl-4-chloroaniline (4b)**^[8], White solid; ¹H NMR (400 MHz, CDCl₃): δ 7.26–7.19 (m, 4H), 7.18–7.13 (m, 1H), 7.03–6.89 (m, 2H), 6.49–6.27 (m, 2H), 4.14 (s, 2H), 3.92 (brs, 1H); ¹³C NMR (101 MHz, CDCl₃): δ 146.7, 138.9, 129.2, 128.8, 127.5, 127.5, 122.2, 114.28, 48.4; The spectroscopic data matched that previously report.^[8]



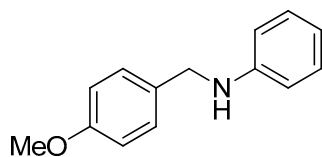
***N*-benzyl-4-fluoroaniline (4c)**^[8], White solid; ¹H NMR (600 MHz, CDCl₃): δ 7.47 (dd, *J* = 6.7, 4.4 Hz, 4H), 7.43–7.36 (m, 1H), 7.04–6.95 (m, 2H), 6.69–6.61 (m, 2H), 4.37 (s, 2H), 3.99 (brs, 1H); ¹³C NMR (151 MHz, CDCl₃): δ 155.9 (d, *J* = 234.9 Hz), 144.6, 139.4, 128.8, 127.6, 127.4, 115.8 (d, *J* = 22.3 Hz), 113.8 (d, *J* = 7.4 Hz), 49.0; The spectroscopic data matched that previously report.^[8]



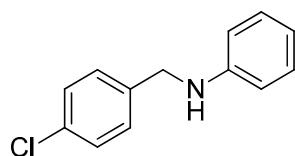
***N*-benzyl-4-methoxyaniline (4d)**^[8], White solid; ¹H NMR (400 MHz, CDCl₃): δ 7.32–7.17 (m, 5H), 6.75–6.64 (m, 2H), 6.65–6.52 (m, 2H), 4.21 (s, 2H), 3.67 (s, 3H); ¹³C NMR (101 MHz, CDCl₃): δ 152.9, 141.19, 138.89, 128.69, 127.9, 127.4, 115.0, 114.9, 55.8, 49.8; The spectroscopic data matched that previously report.^[8]



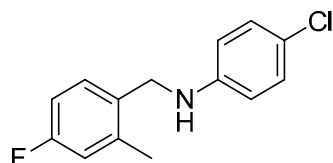
***N*-benzyl-4-(trifluoromethyl)aniline (4e)**^[8], Colourless oil; ¹H NMR (400 MHz, CDCl₃): δ 7.31–7.10 (m, 7H), 6.46 (d, *J* = 8.6 Hz, 2H), 4.23 (brs, 1H), 4.19 (s, 2H); ¹³C NMR (101 MHz, CDCl₃): δ 150.3, 138.3, 128.8, 127.5, 127.46, 126.6 (q, *J* = 3.8 Hz), 124.9 (d, *J* = 270.9 Hz), 119.1 (q, *J* = 32.6 Hz), 112.0, 47.8; The spectroscopic data matched that previously report.^[8]



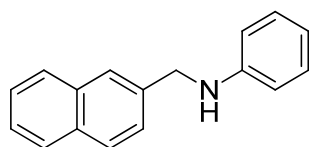
***N*-(4-methoxybenzyl)aniline (4f)**^[8], Yellow solid; ¹H NMR (400 MHz, CDCl₃): δ 7.38 (d, *J* = 8.3 Hz, 2H), 7.32–7.16 (m, 2H), 6.98 (d, *J* = 8.0 Hz, 2H), 6.82 (td, *J* = 7.3, 0.8 Hz, 1H), 6.73 (d, *J* = 8.5 Hz, 2H), 4.33 (s, 2H), 4.06 (brs, 1H), 3.88 (d, *J* = 0.6 Hz, 3H); ¹³C NMR (101 MHz, CDCl₃): δ 158.9, 148.3, 131.5, 129.4, 128.9, 117.6, 114.1, 112.9, 55.4, 47.9; The spectroscopic data matched that previously report.^[8]



***N*-(4-chlorobenzyl)aniline (4g)**^[8], Colourless oil; ¹H NMR (400 MHz, CDCl₃): δ 7.40–7.33 (m, 1H), 7.32 (s, 3H), 7.22–7.17 (m, 2H), 6.80–6.73 (m, 1H), 6.65–6.60 (m, 2H), 4.32 (s, 2H), 4.06 (brs, 1H); ¹³C NMR (101 MHz, CDCl₃): δ 147.9, 138.1, 133.0, 129.4, 128.8, 127.6, 117.9, 113.0, 47.7; The spectroscopic data matched that previously report.^[8]



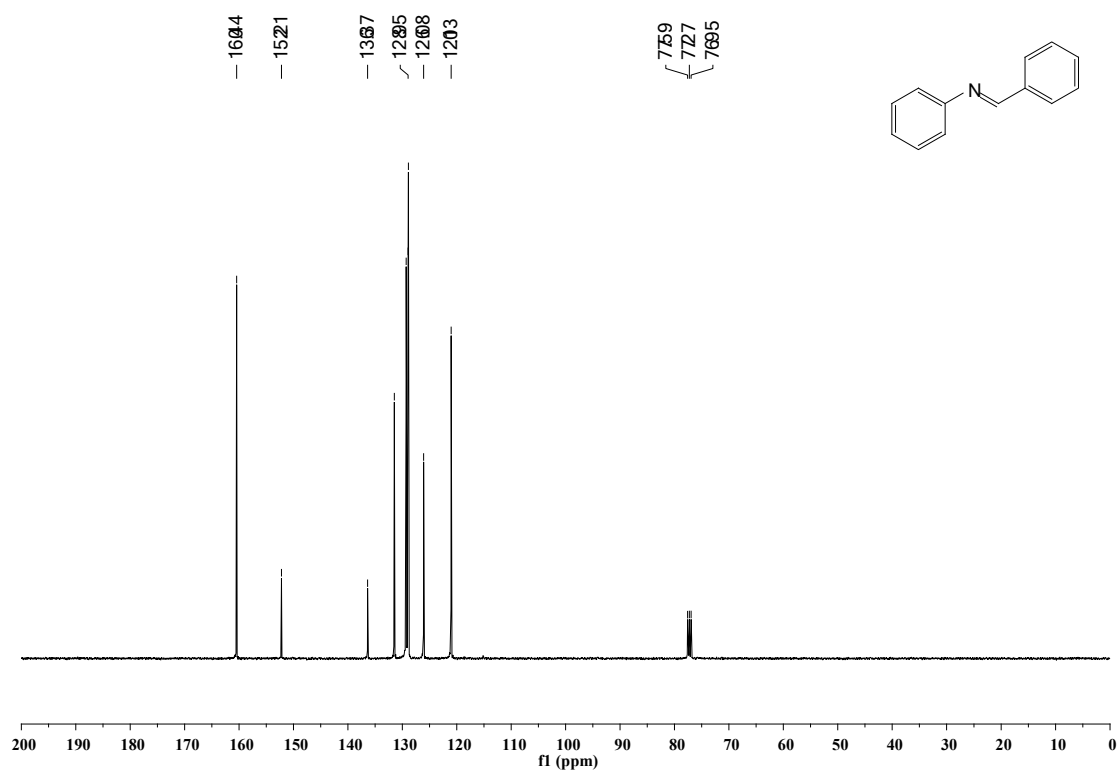
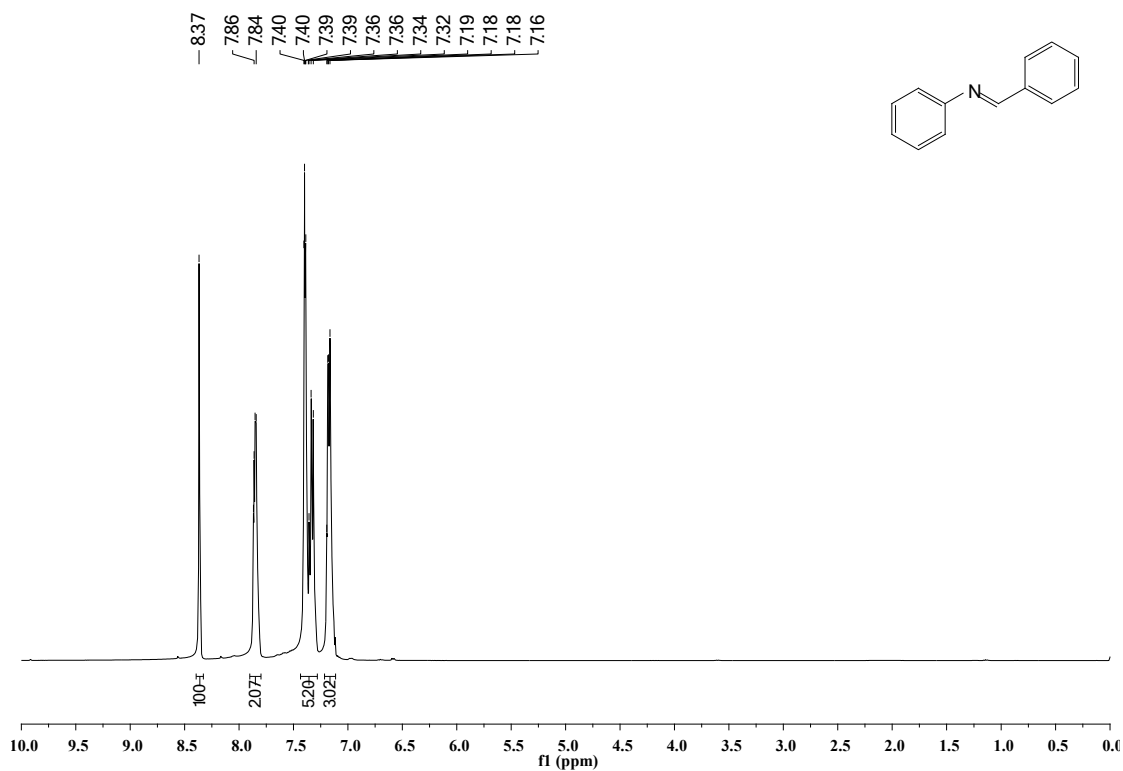
4-chloro-*N*-(4-fluoro-2-methylbenzyl)aniline (4h), White solid; ¹H NMR (400 MHz, CDCl₃): δ 7.03–6.94 (m, 3H), 6.90 (dd, *J* = 9.8, 2.7 Hz, 1H), 6.75 (td, *J* = 8.4, 2.8 Hz, 1H), 6.41–6.32 (m, 2H), 4.07 (s, 2H), 3.86 (brs, 1H), 2.17 (s, 3H); ¹³C NMR (101 MHz, CDCl₃): δ 161.6 (d, *J* = 243.4 Hz), 146.5, 138.9 (d, *J* = 6.6 Hz), 131.7 (d, *J* = 7.7 Hz), 131.3 (d, *J* = 3.2 Hz), 129.7, 122.5 (d, *J* = 30.0 Hz), 114.3 (d, *J* = 22.2 Hz), 113.9, 113.7, 46.1, 18.2; HRMS (*m/z*): calcd. for C₁₄H₁₄ClFN [M+H], 250.0793; found, 250.0789.

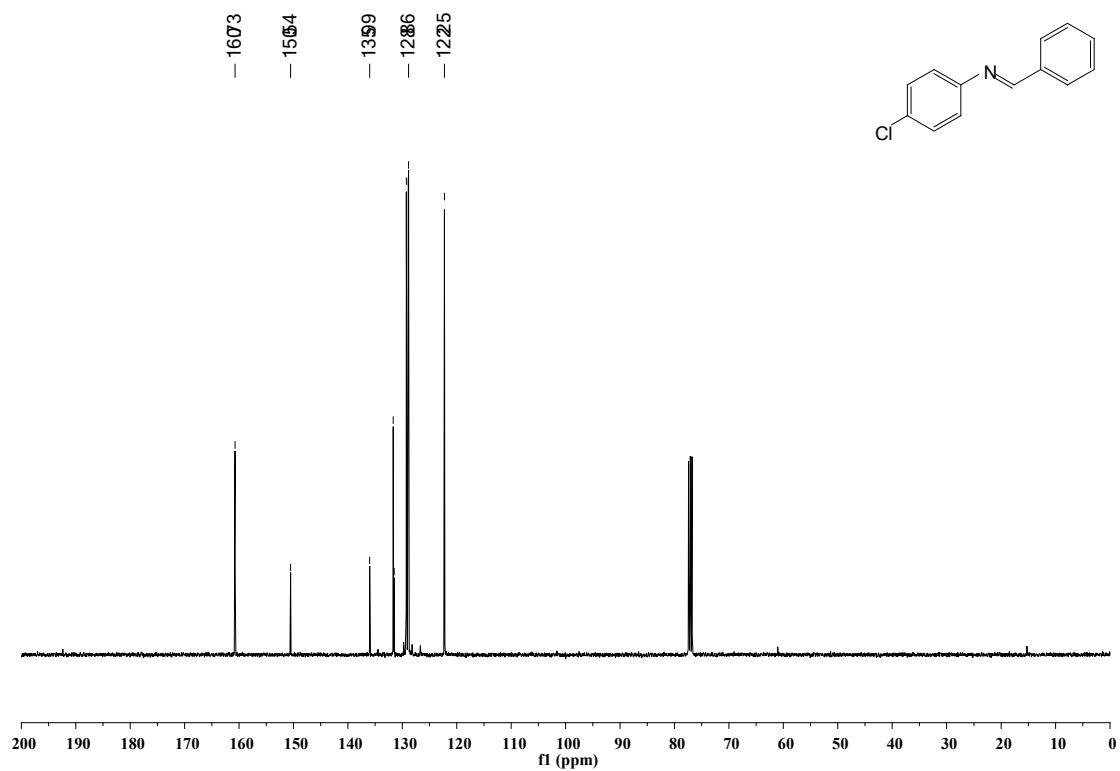
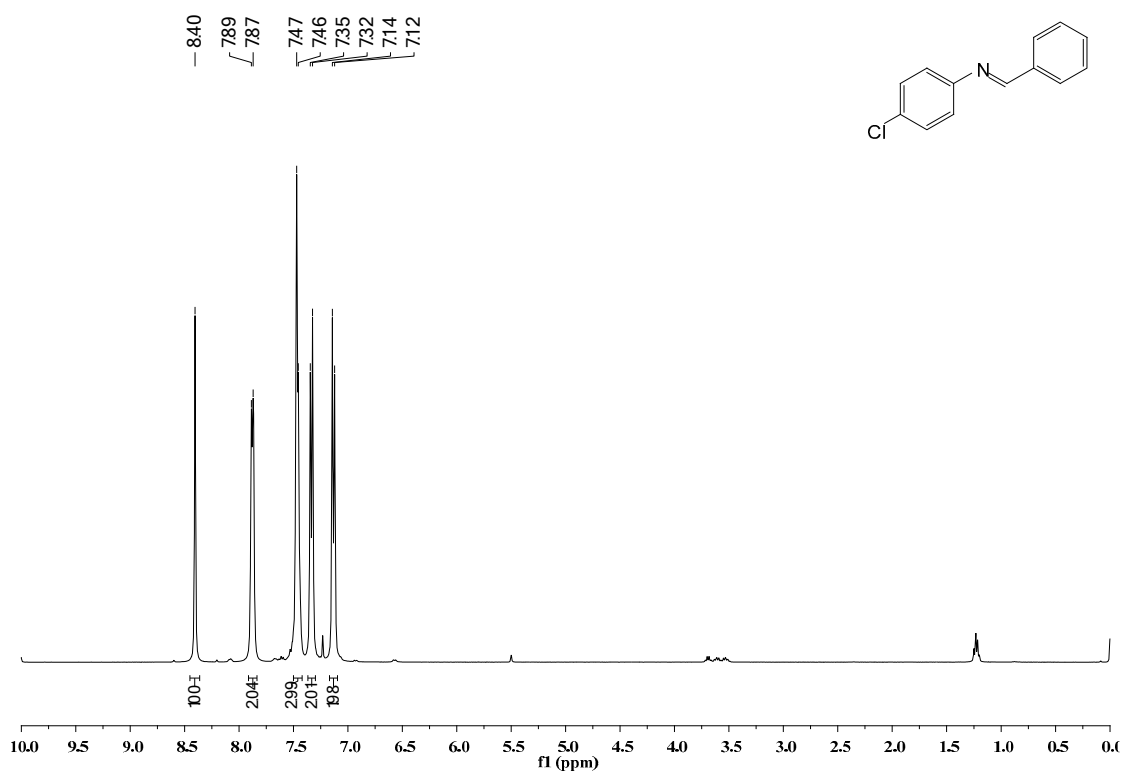


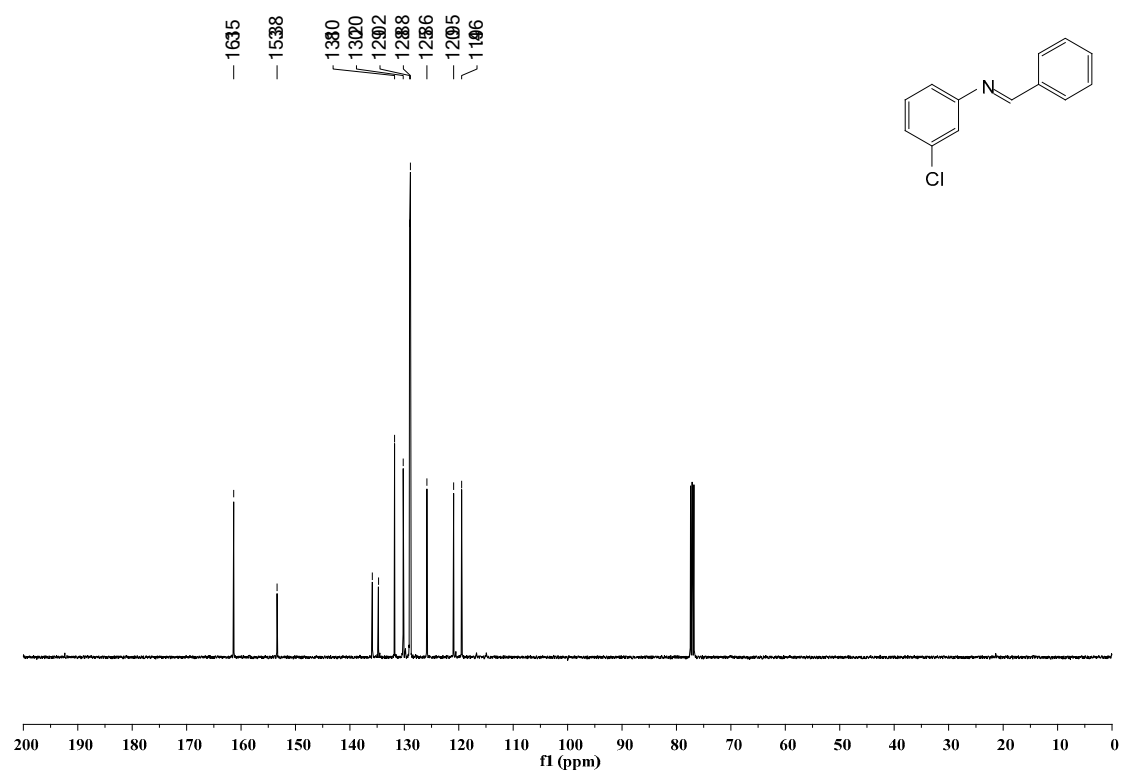
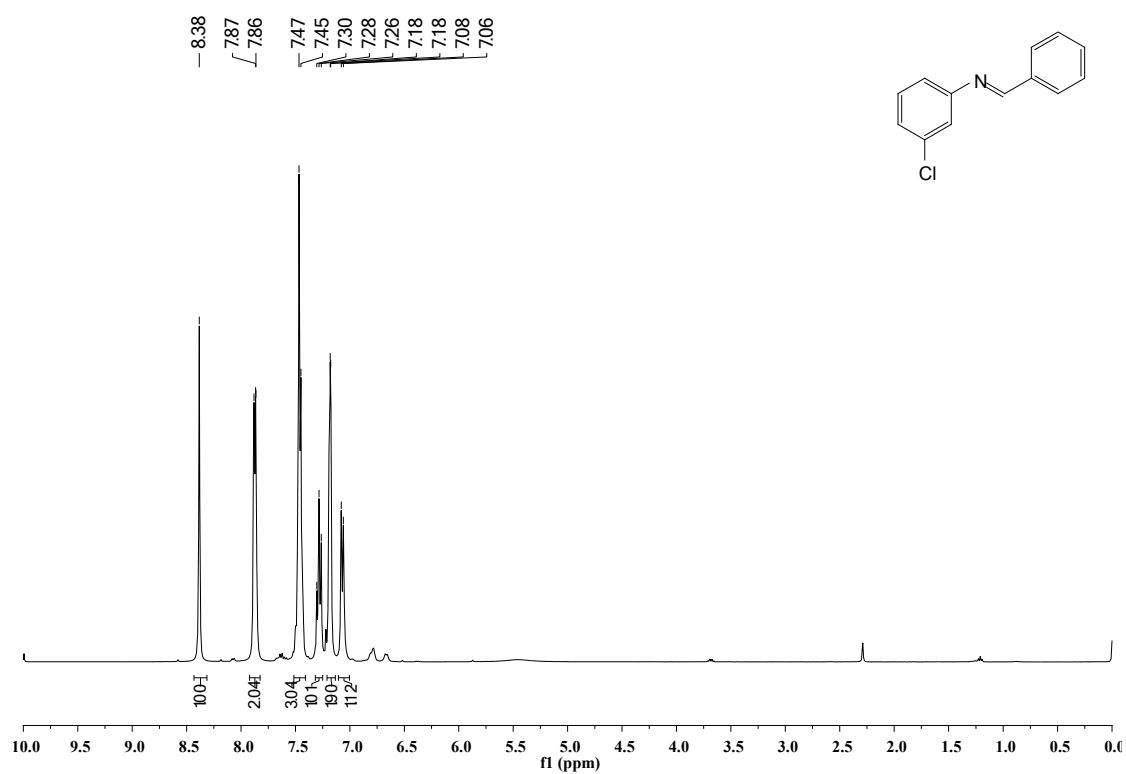
***N*-(naphthalen-2-ylmethyl)aniline (4i)**^[8], Yellow solid; ¹H NMR (600 MHz, CDCl₃): δ 7.03–6.94 (m, 3H), 6.90 (dd, *J* = 9.8, 2.7 Hz, 1H), 6.75 (td, *J* = 8.4, 2.8 Hz, 1H), 6.41–6.32

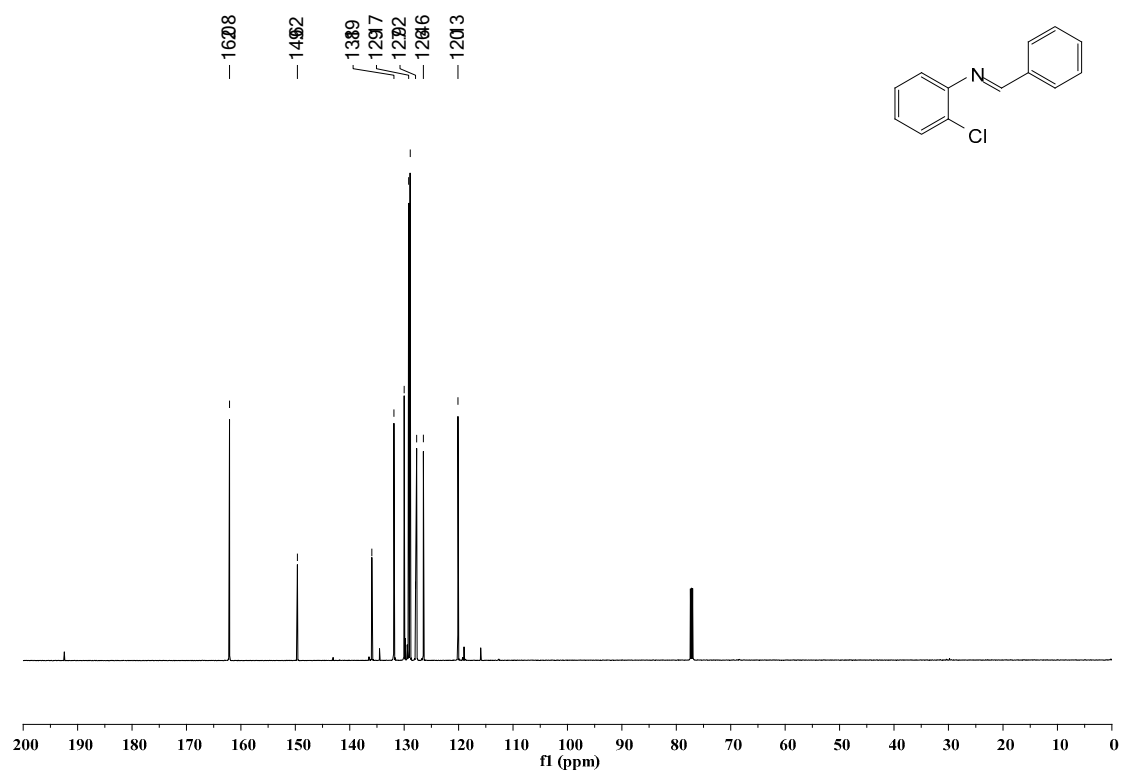
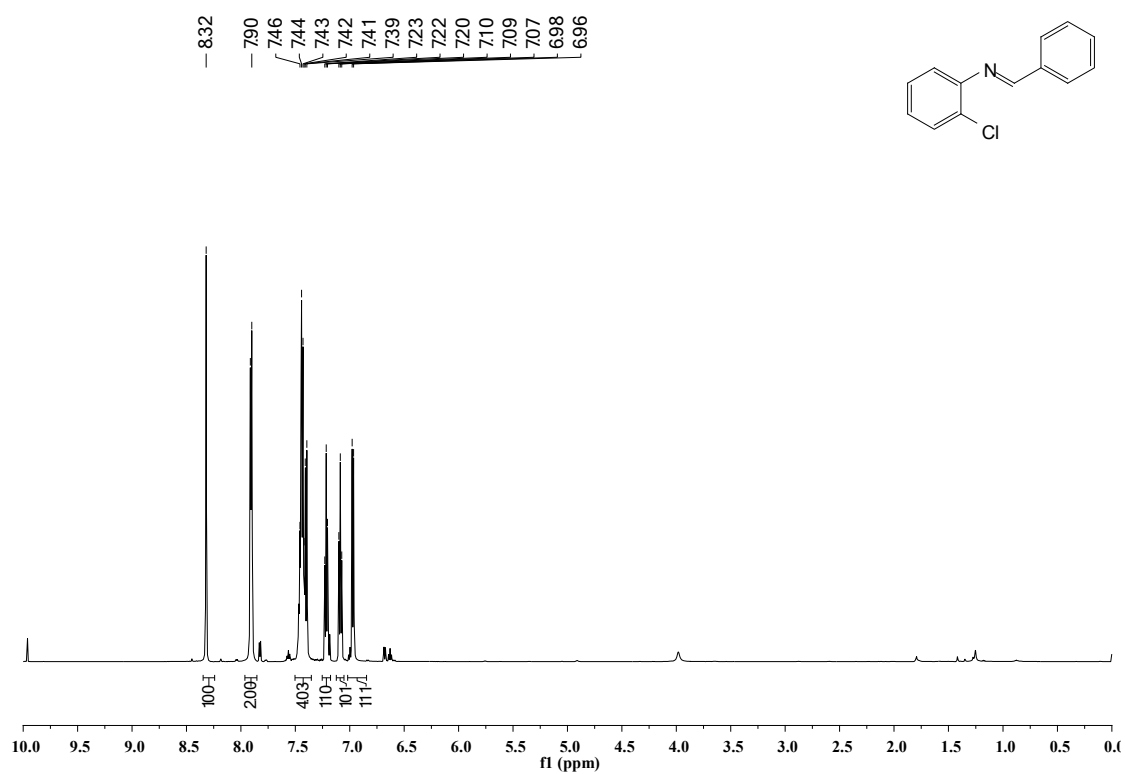
(m, 2H), 4.07 (s, 2H), 3.86 (brs, 1H), 2.17 (s, 3H); ^{13}C NMR (151 MHz, CDCl_3): δ 146.9, 135.8, 132.3, 131.6, 128.1, 127.2, 126.6, 126.6, 124.9, 124.6, 124.6, 124.6, 116.4, 111.7, 47.2; The spectroscopic data matched that previously report.^[8]

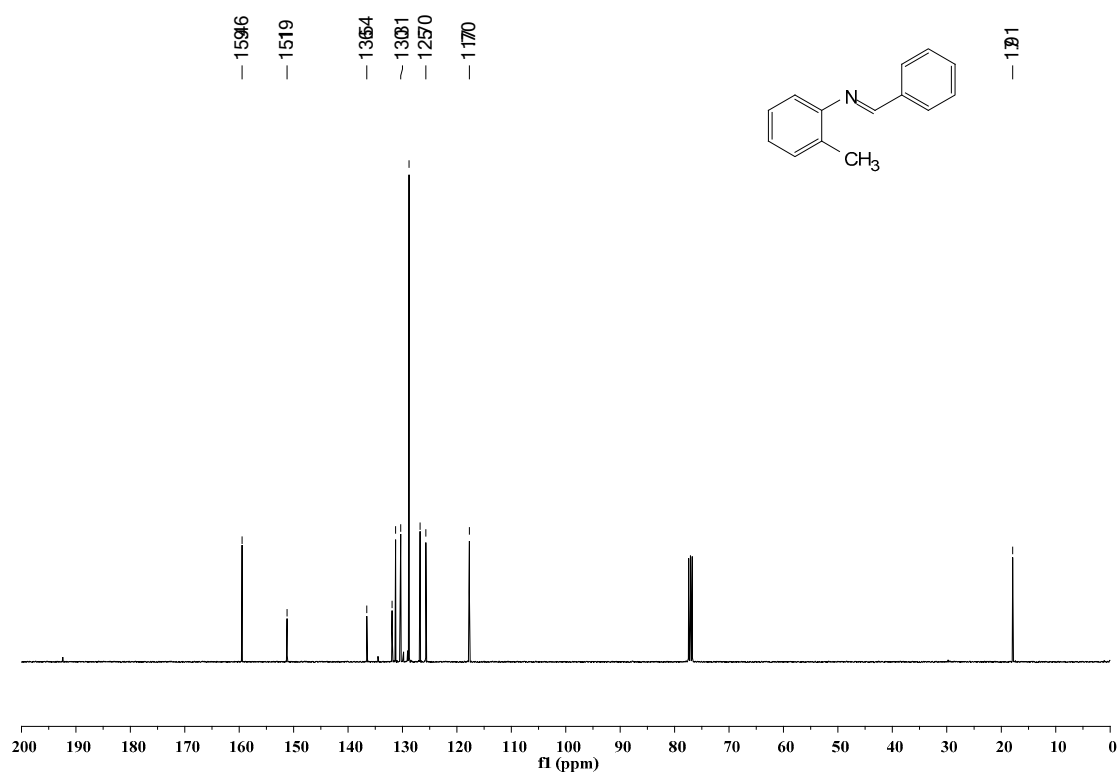
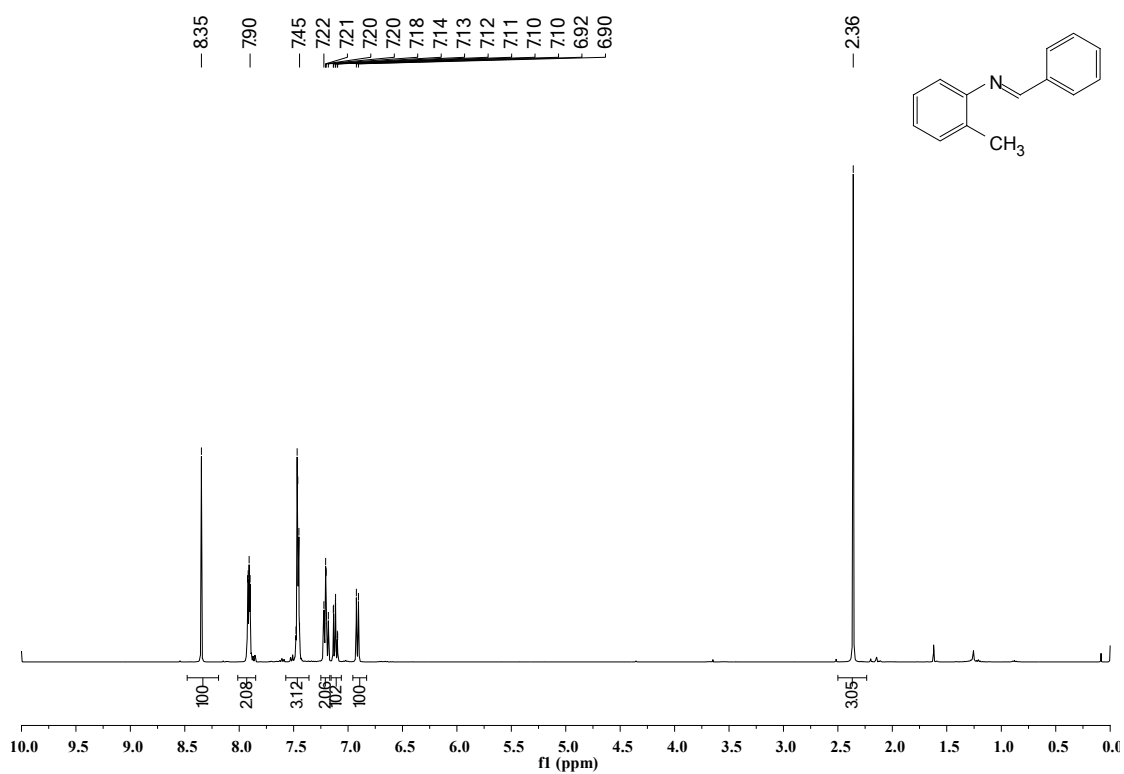
^1H and ^{13}C NMR spectra of products

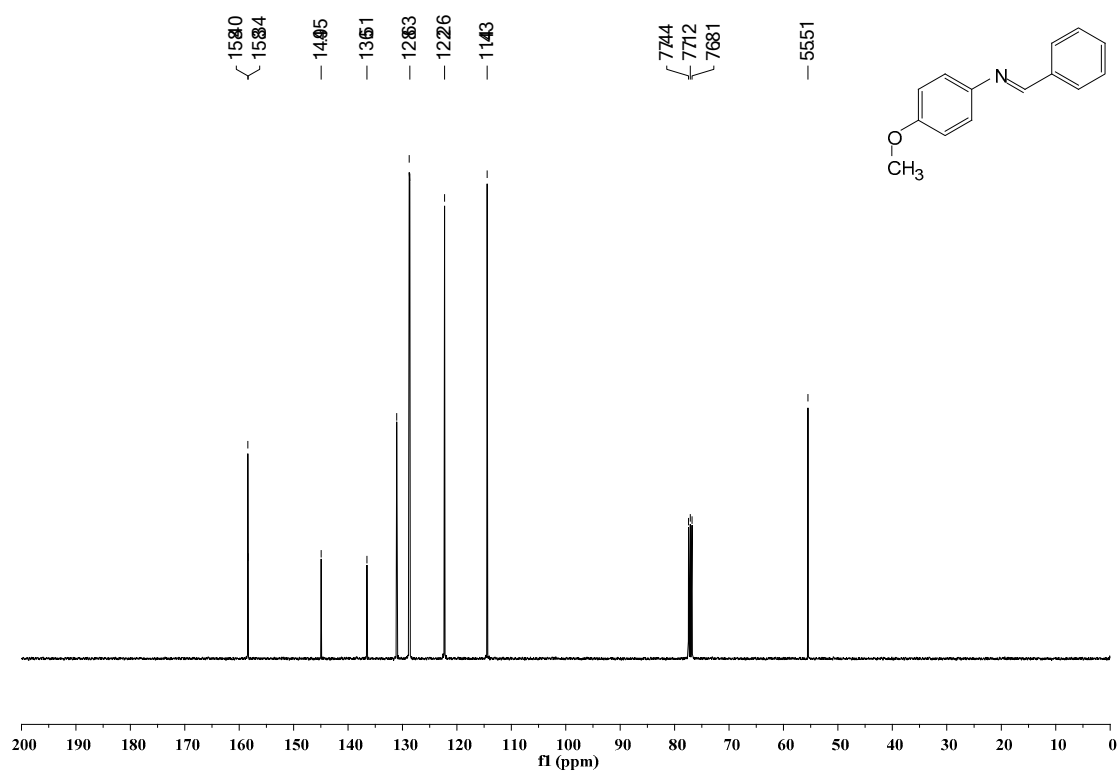
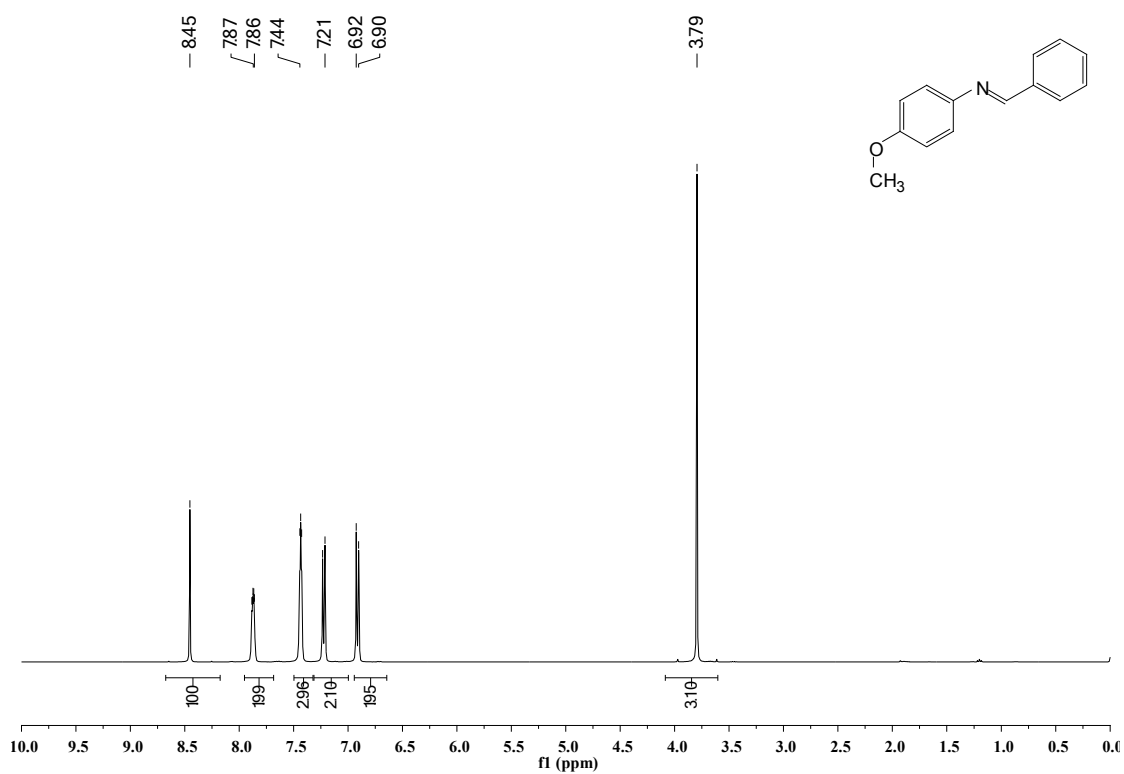


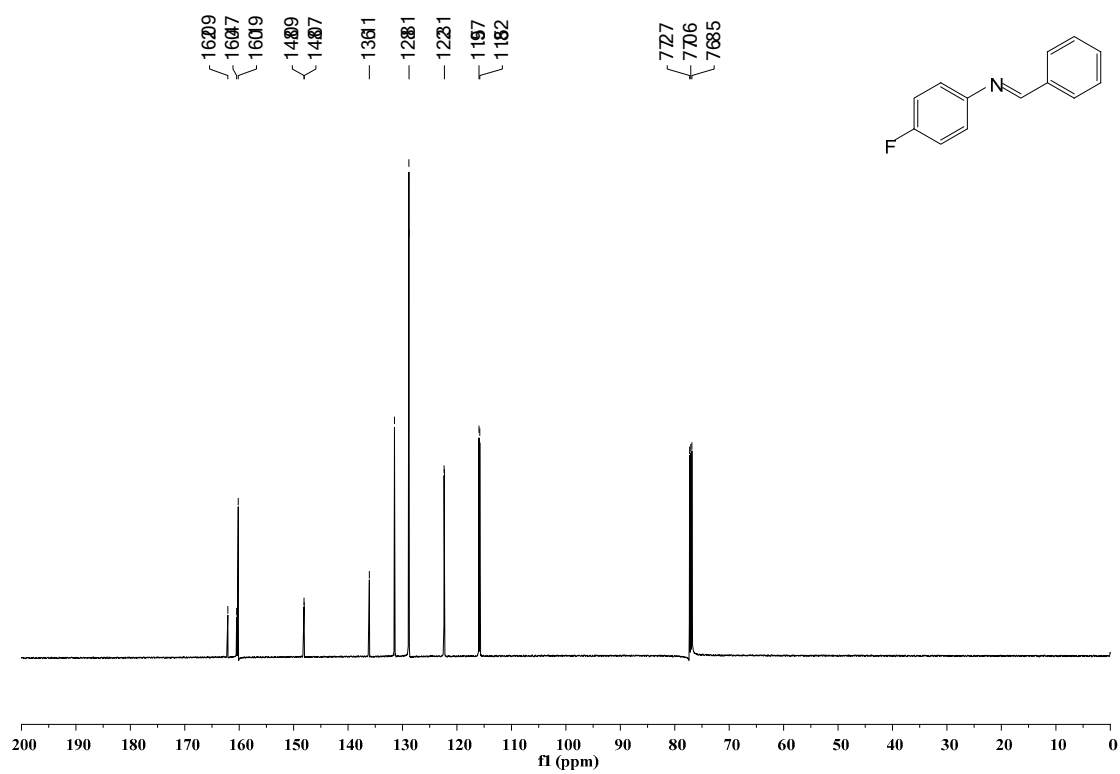
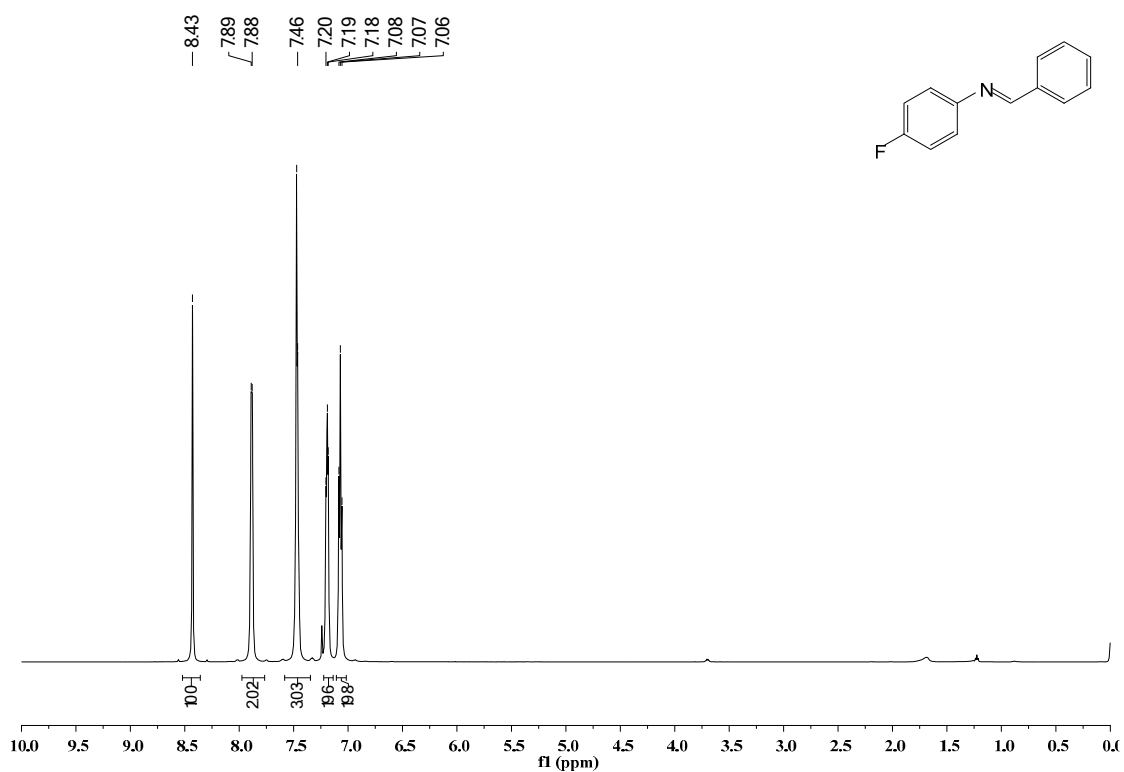


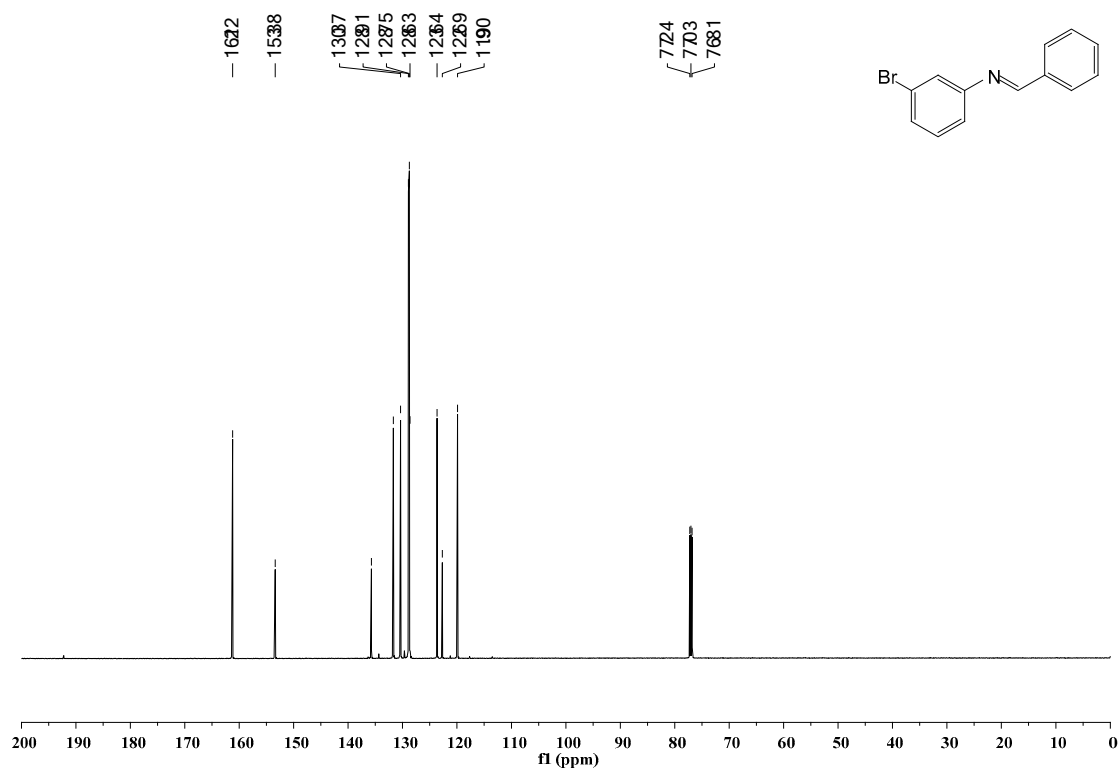
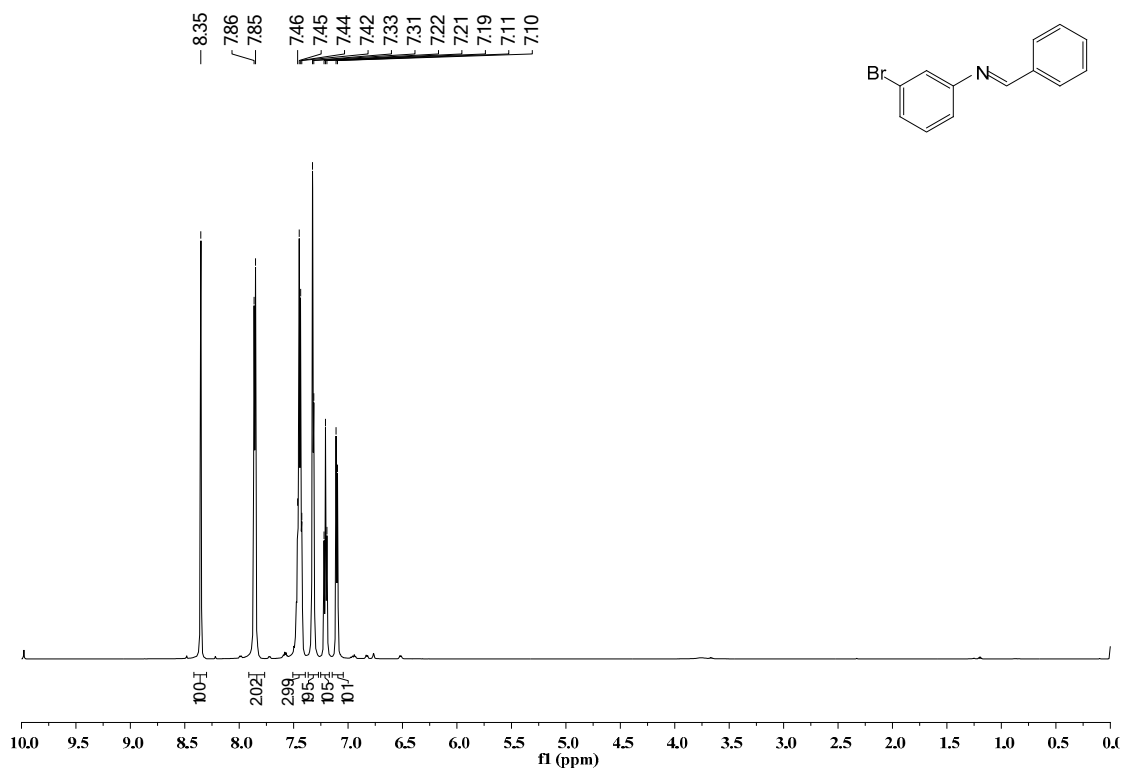


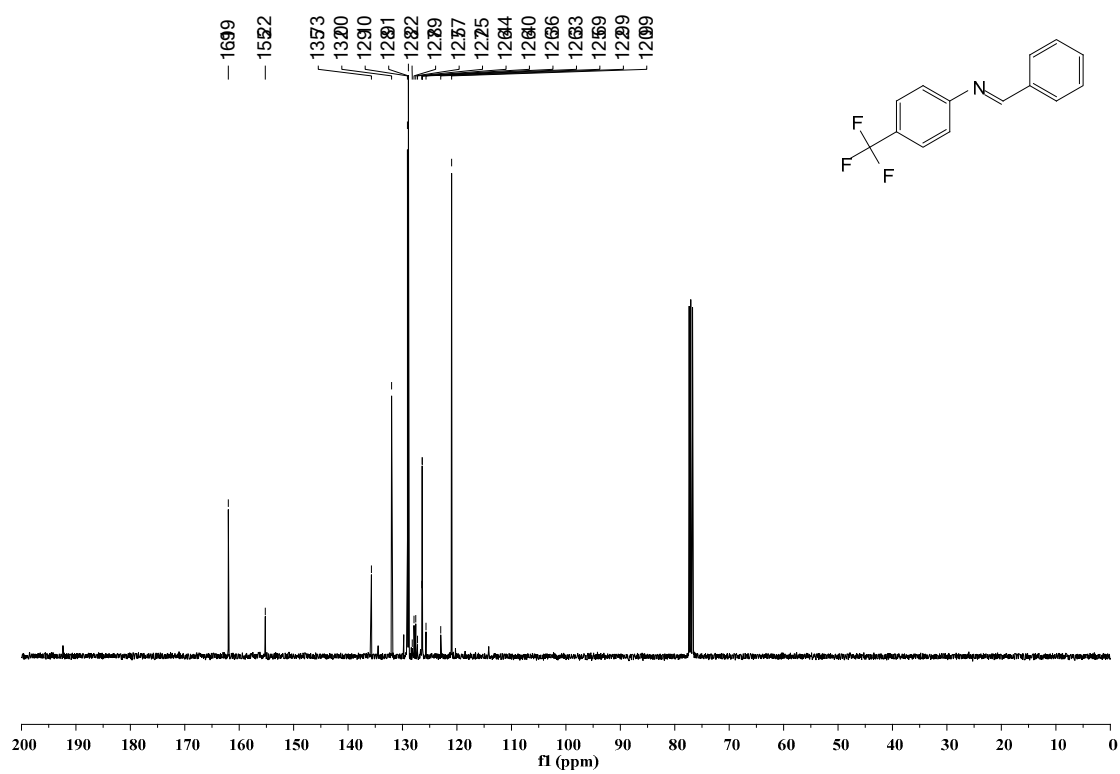
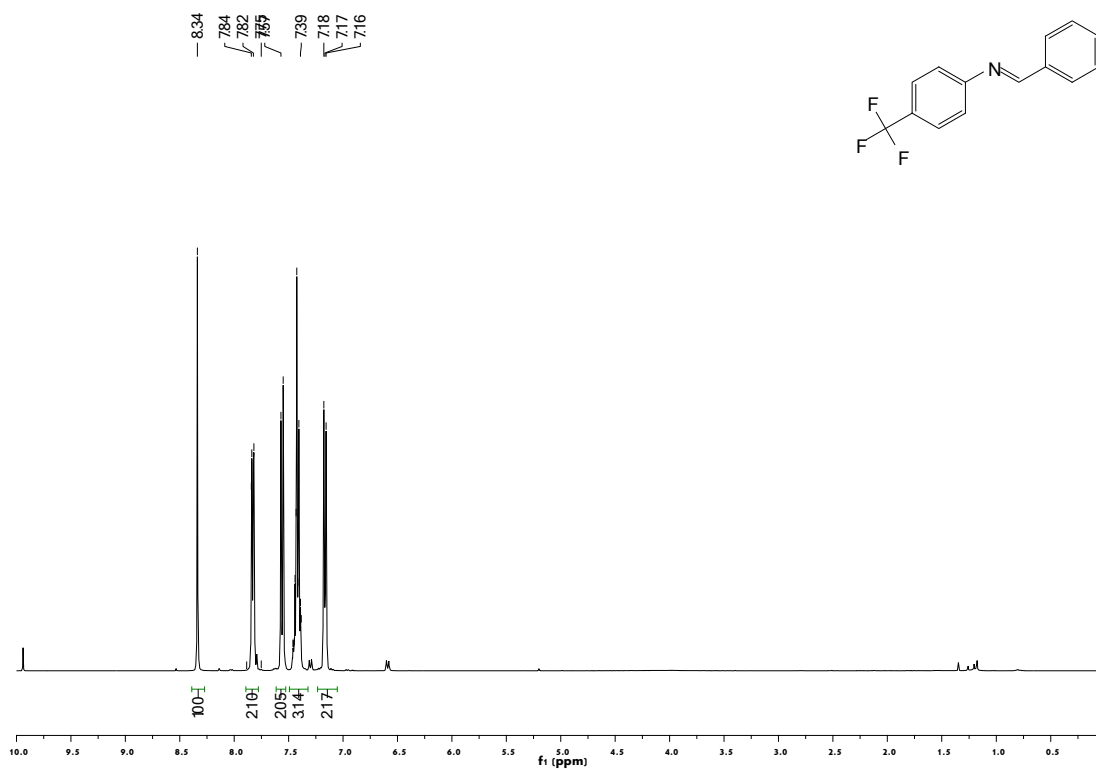


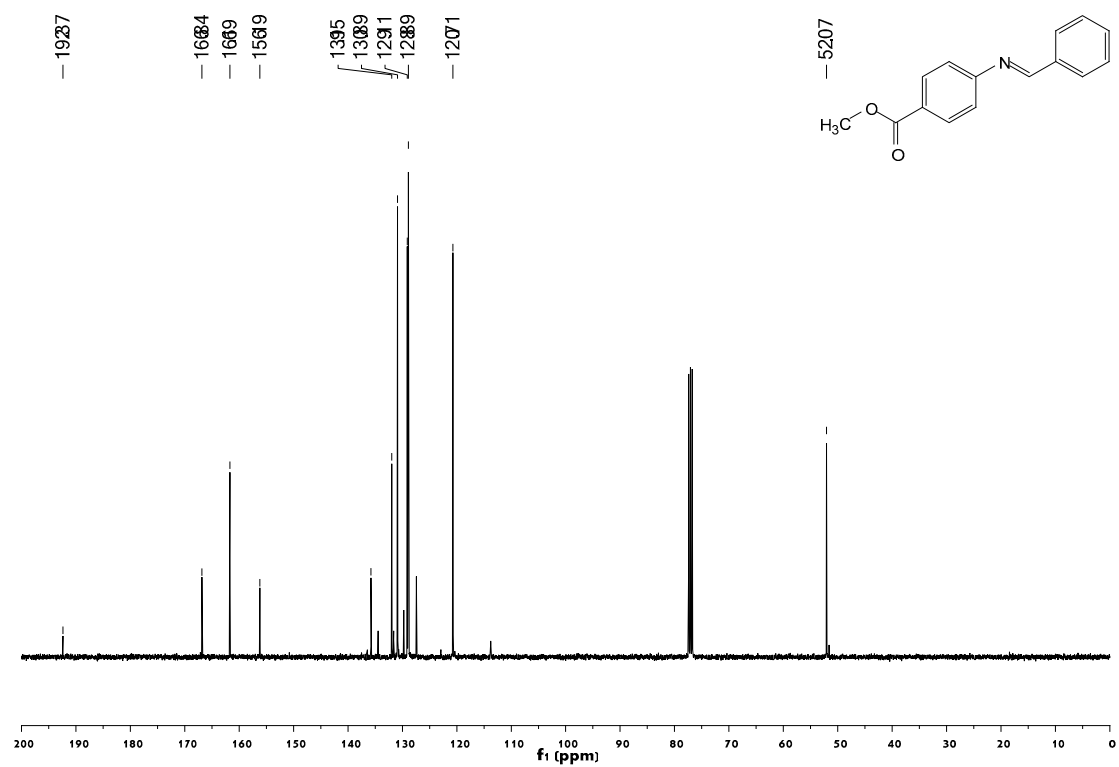
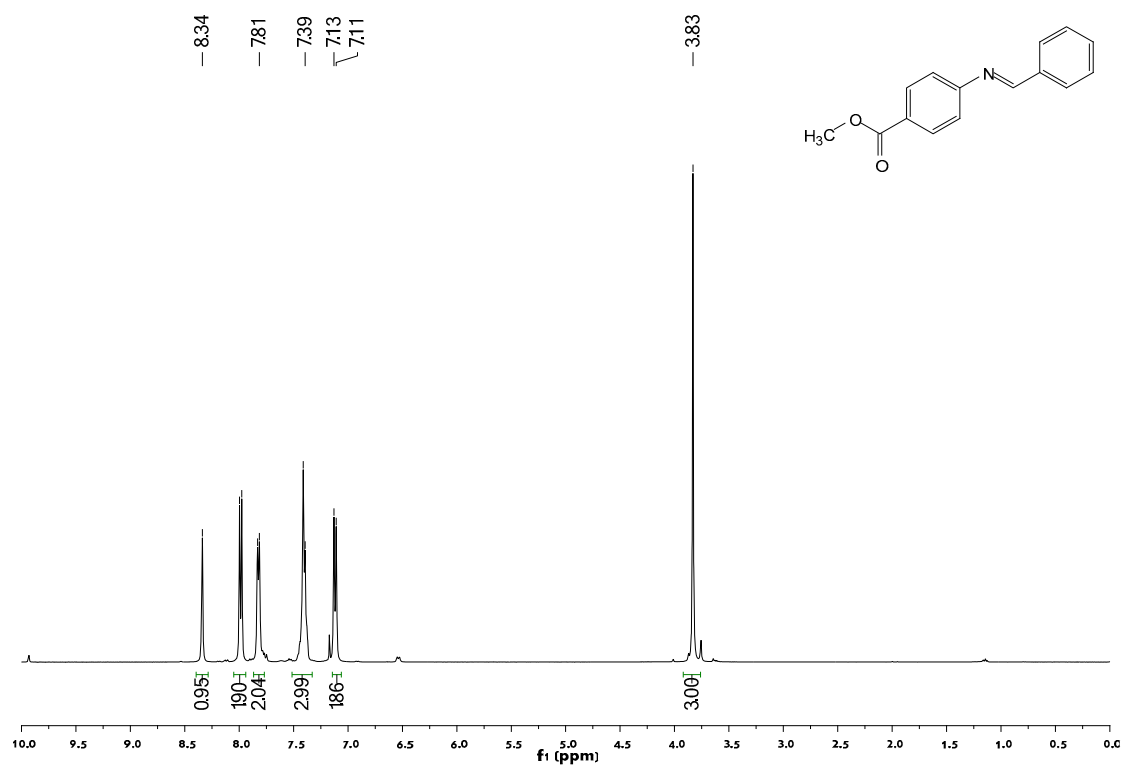


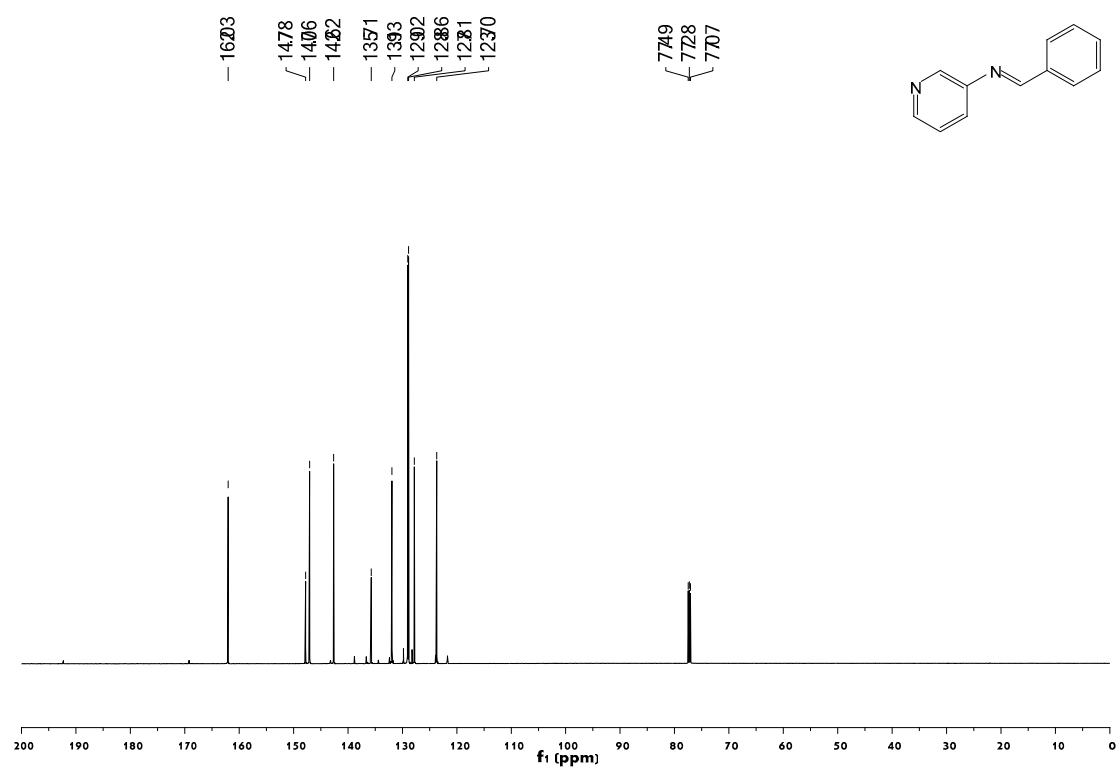
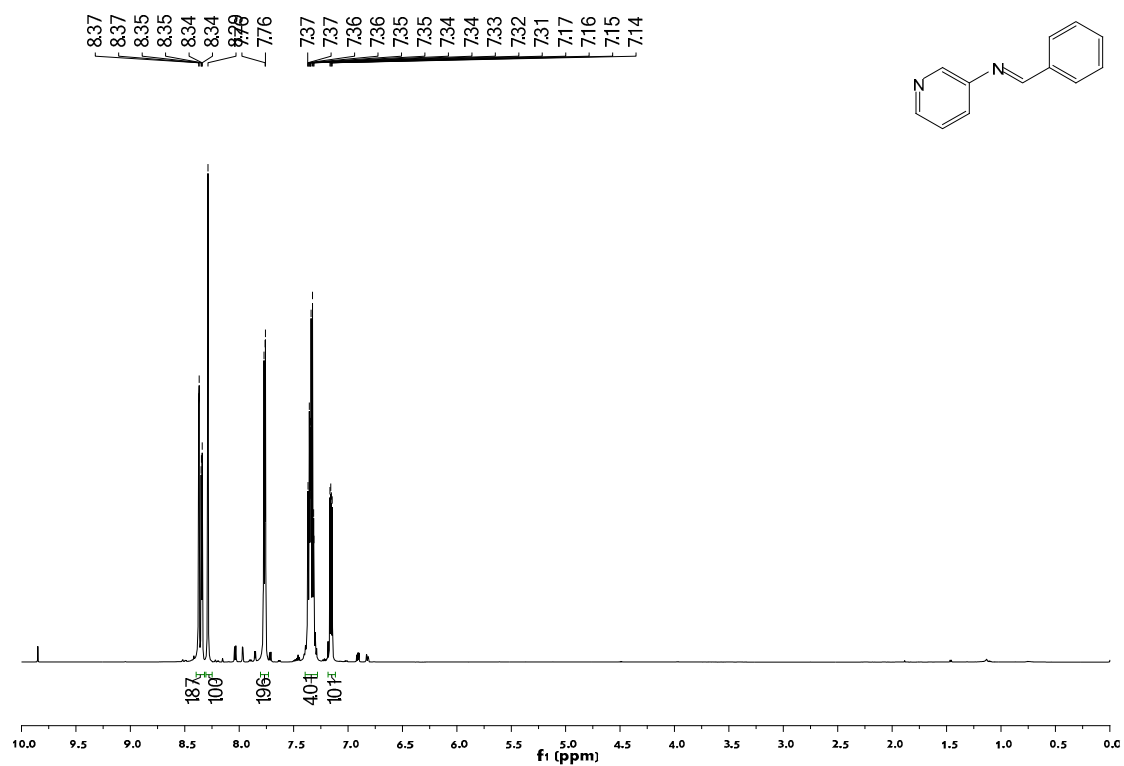


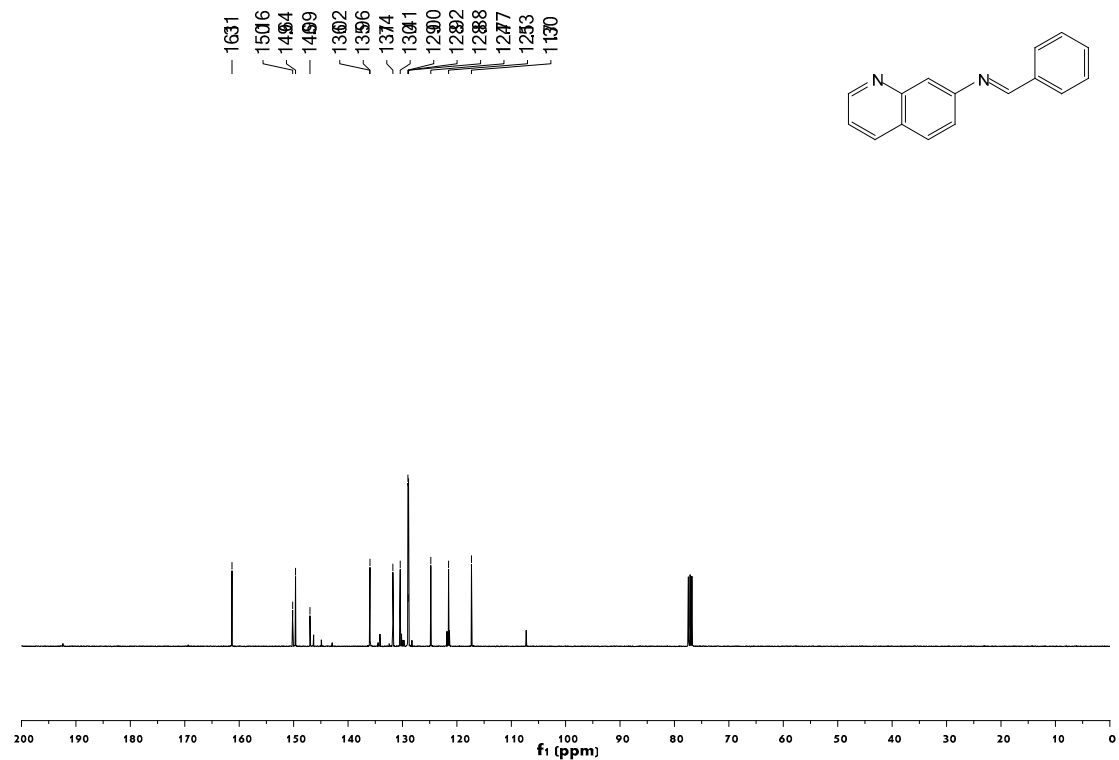
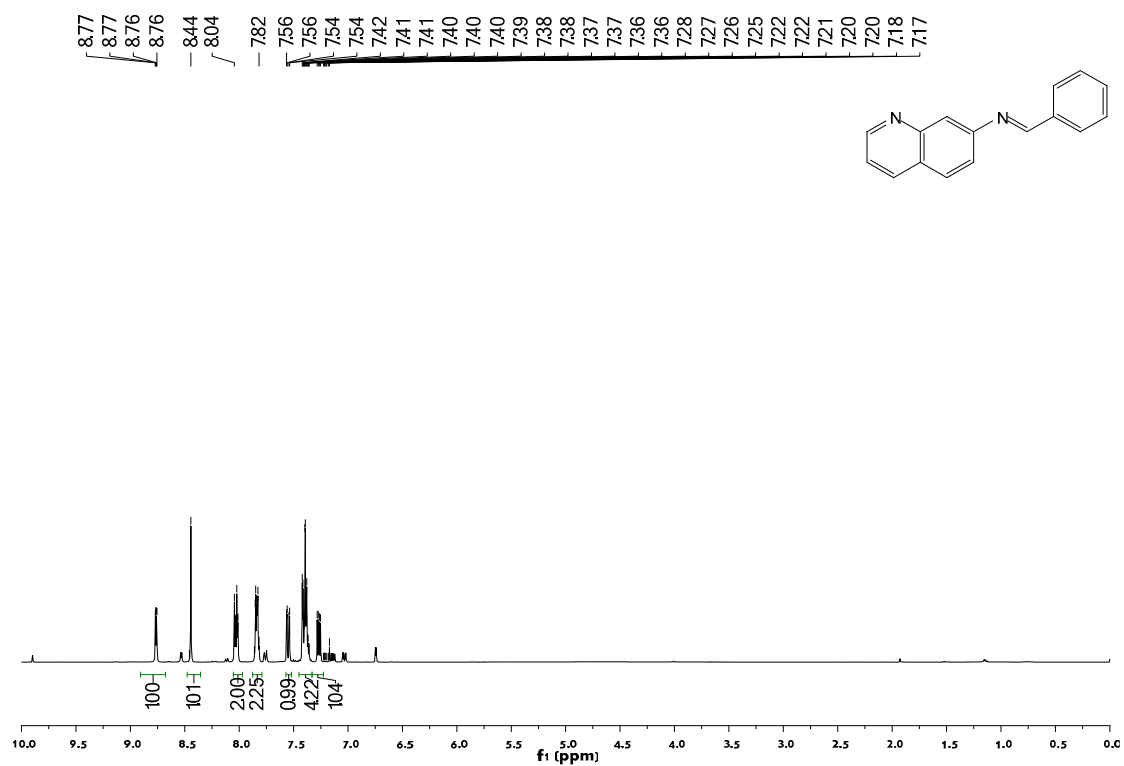


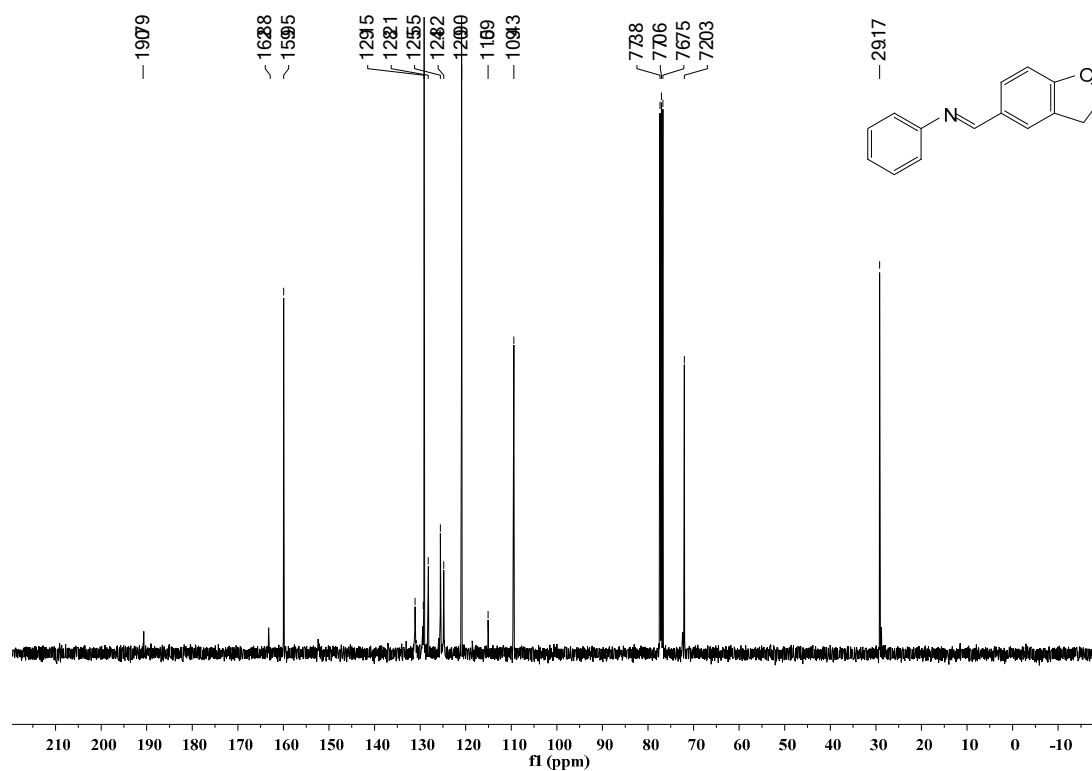
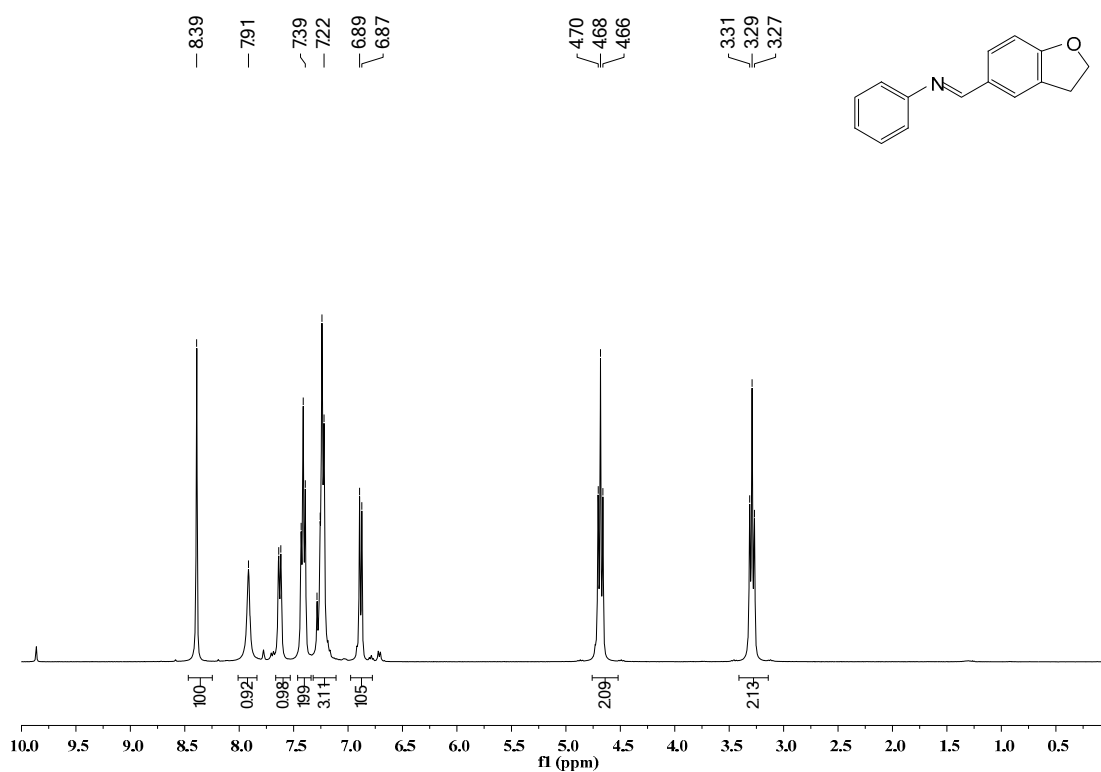


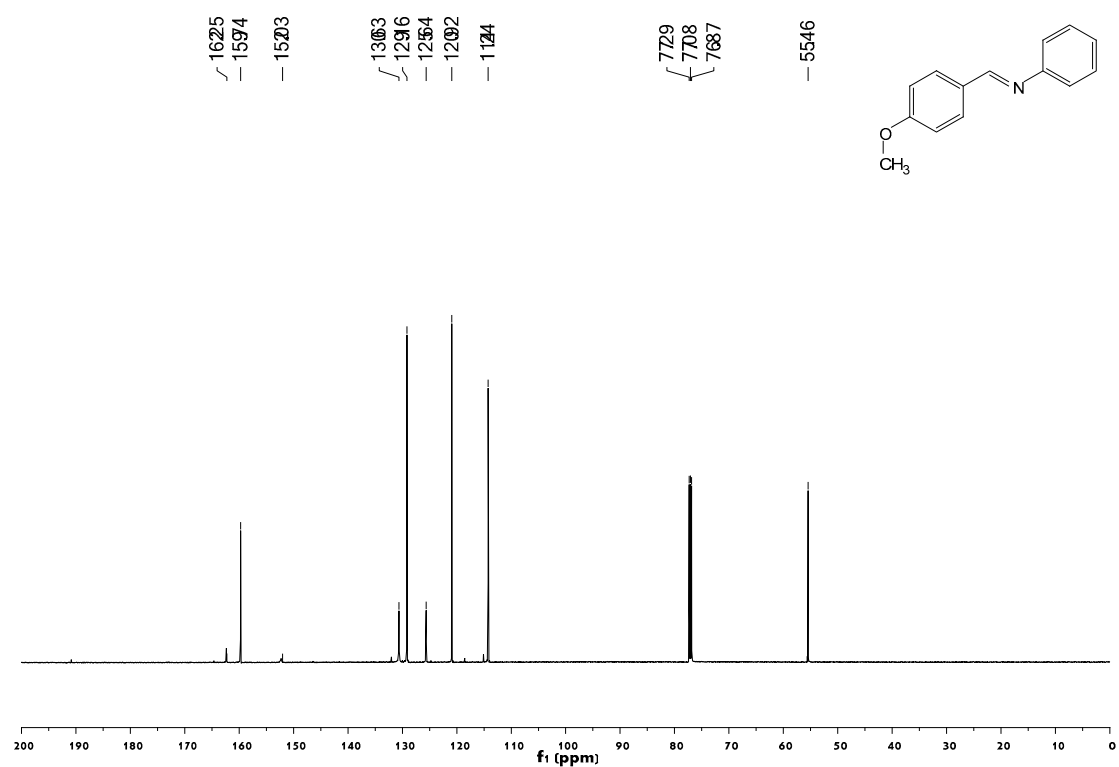
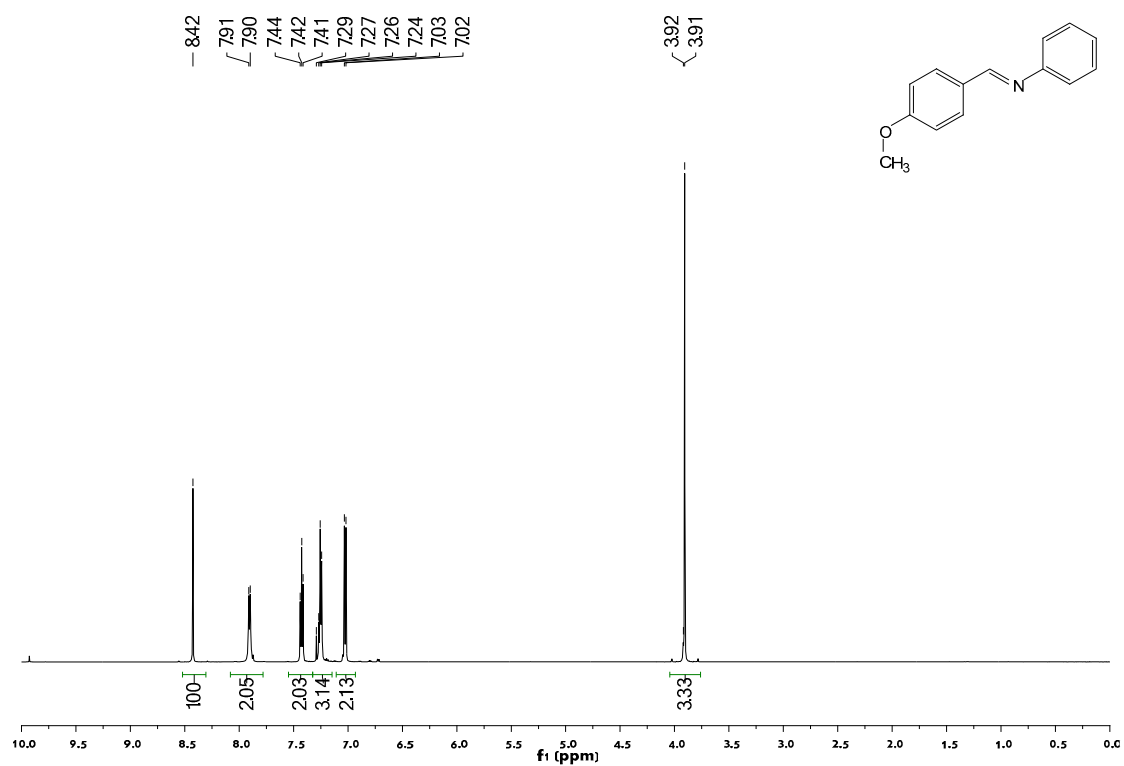


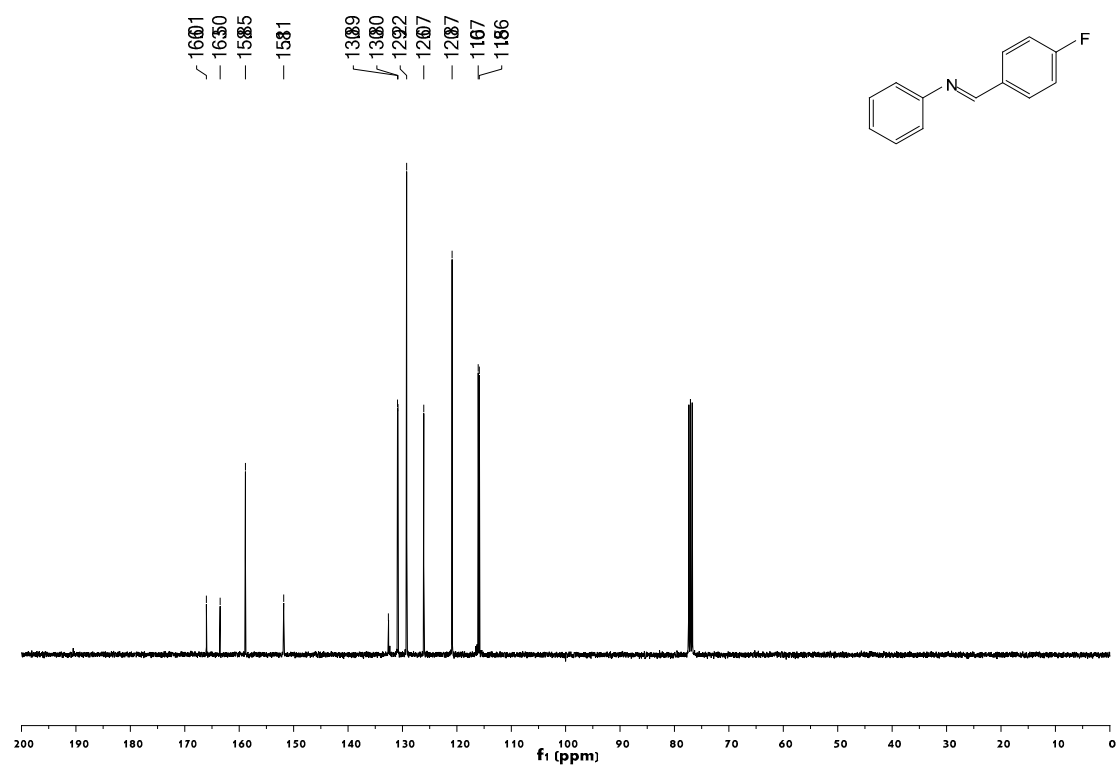
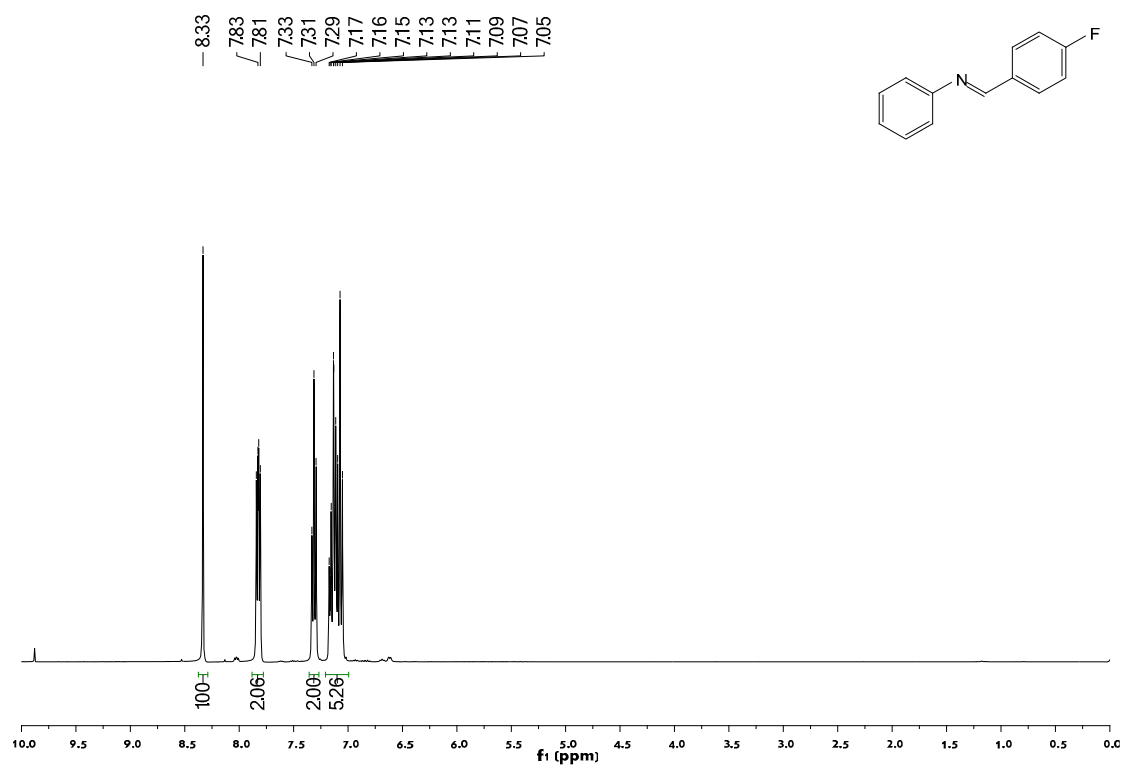


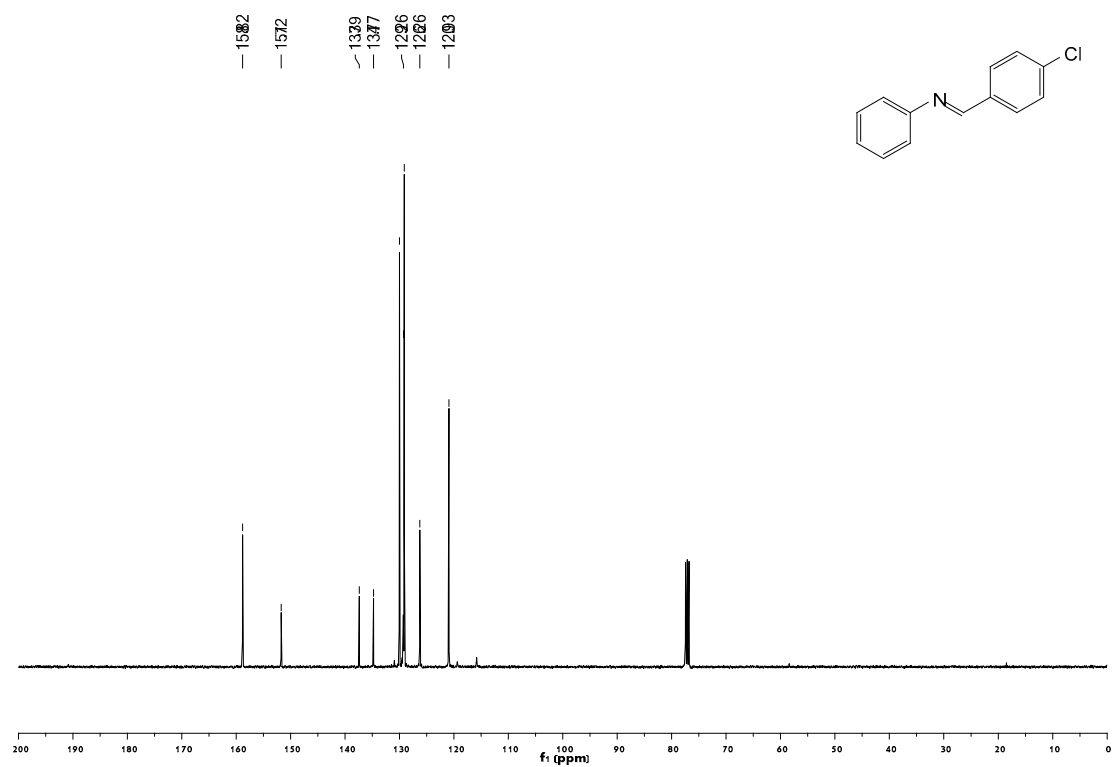
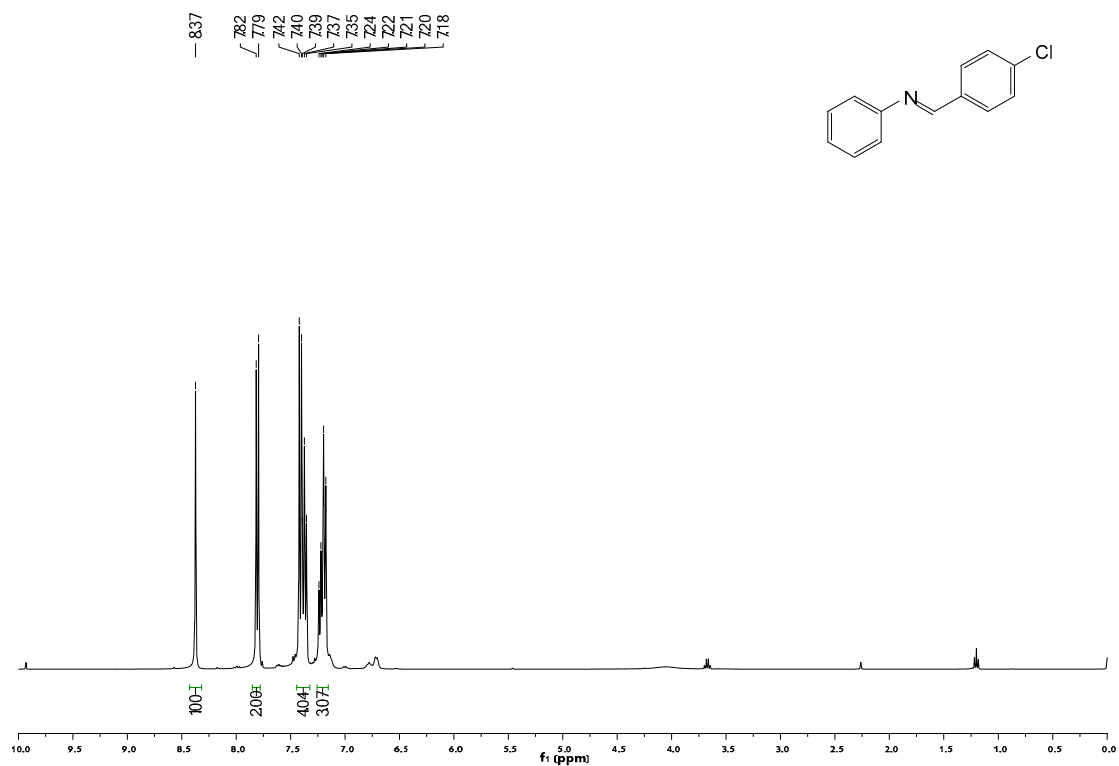


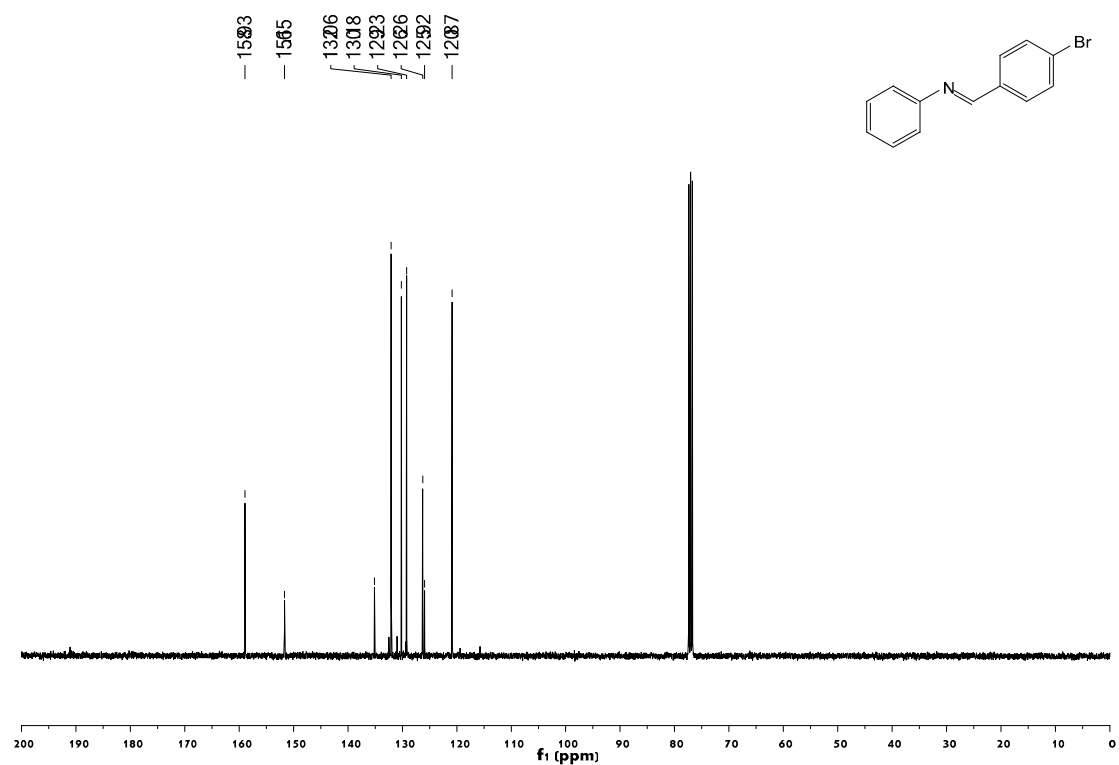
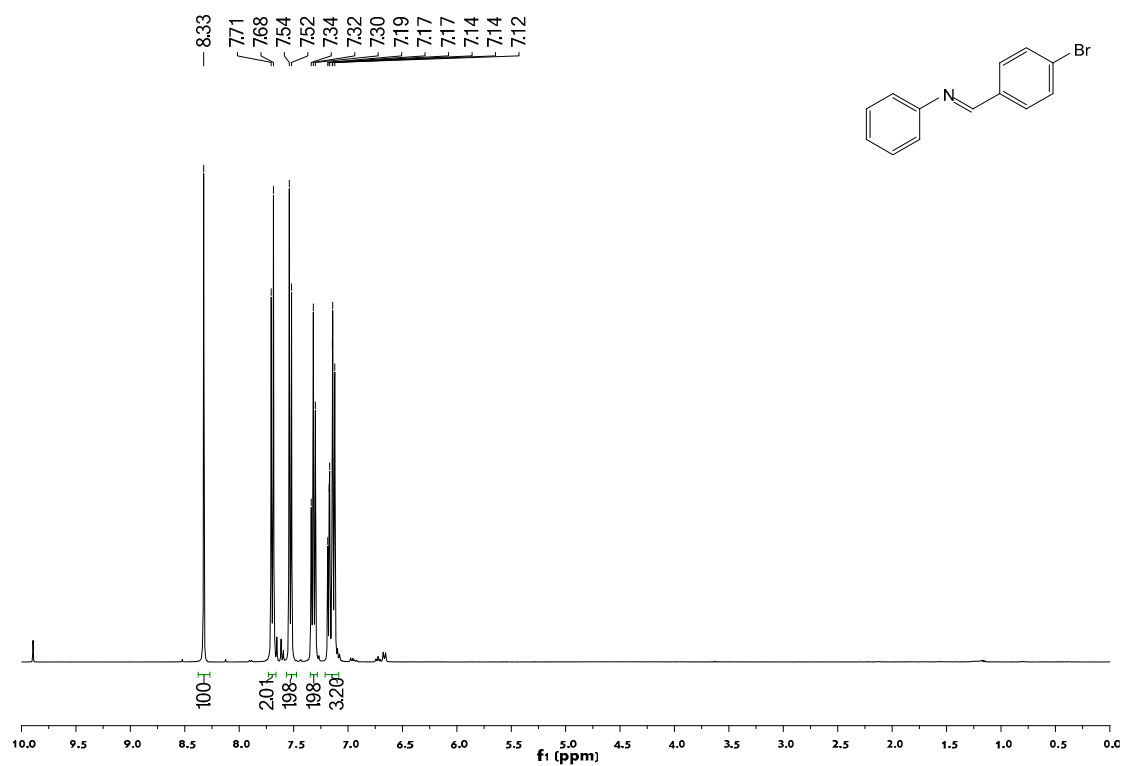


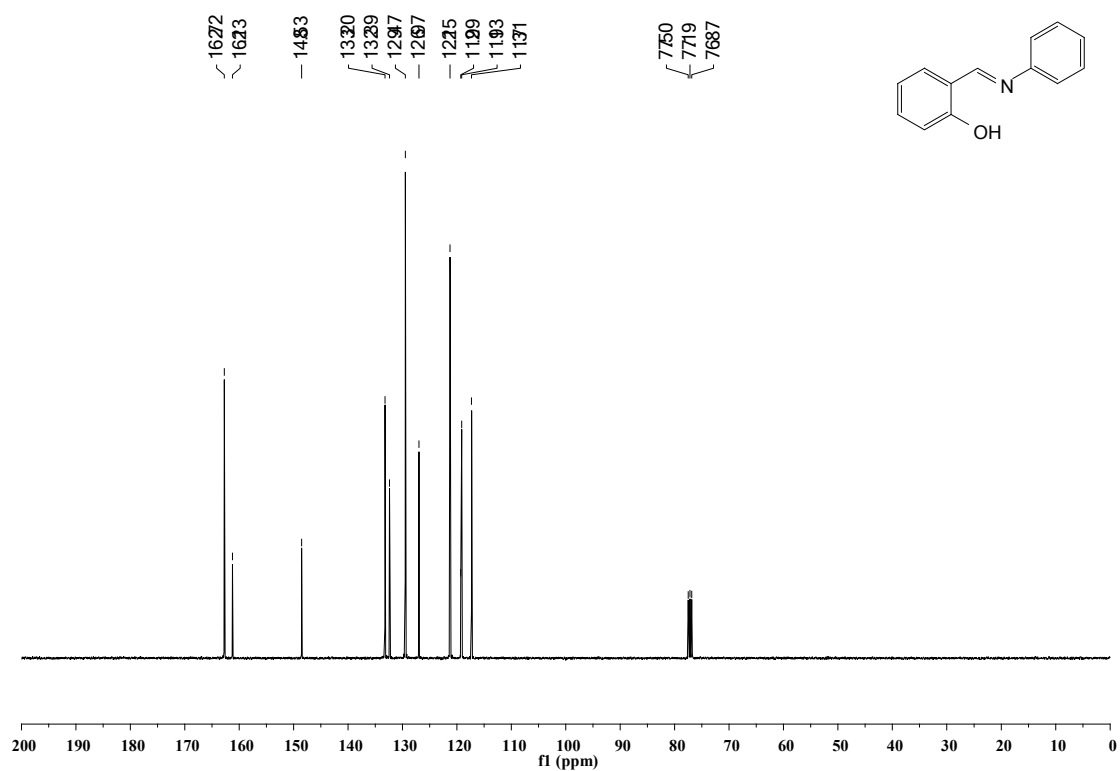
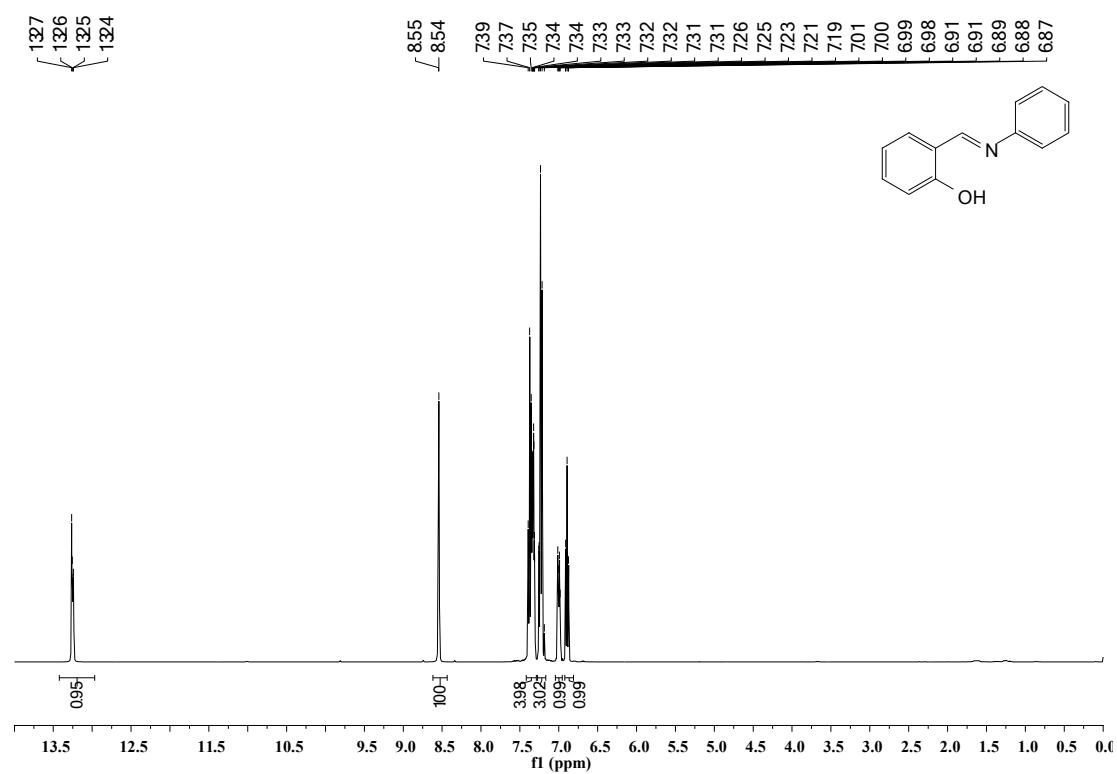


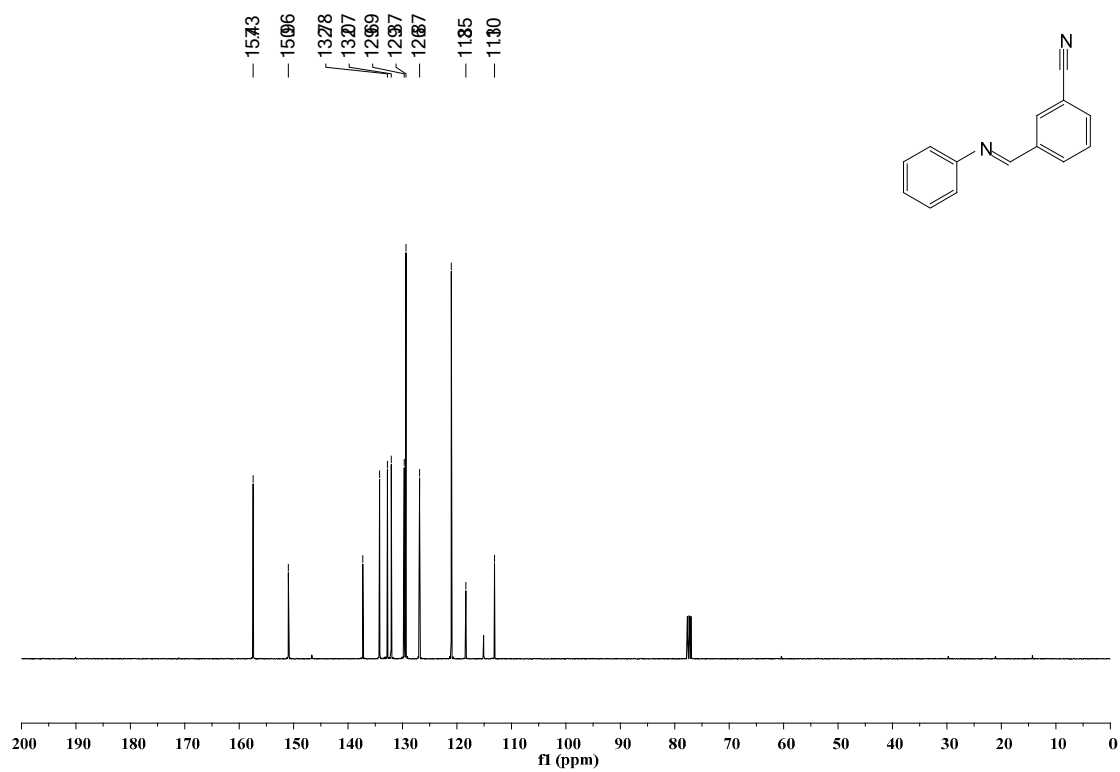
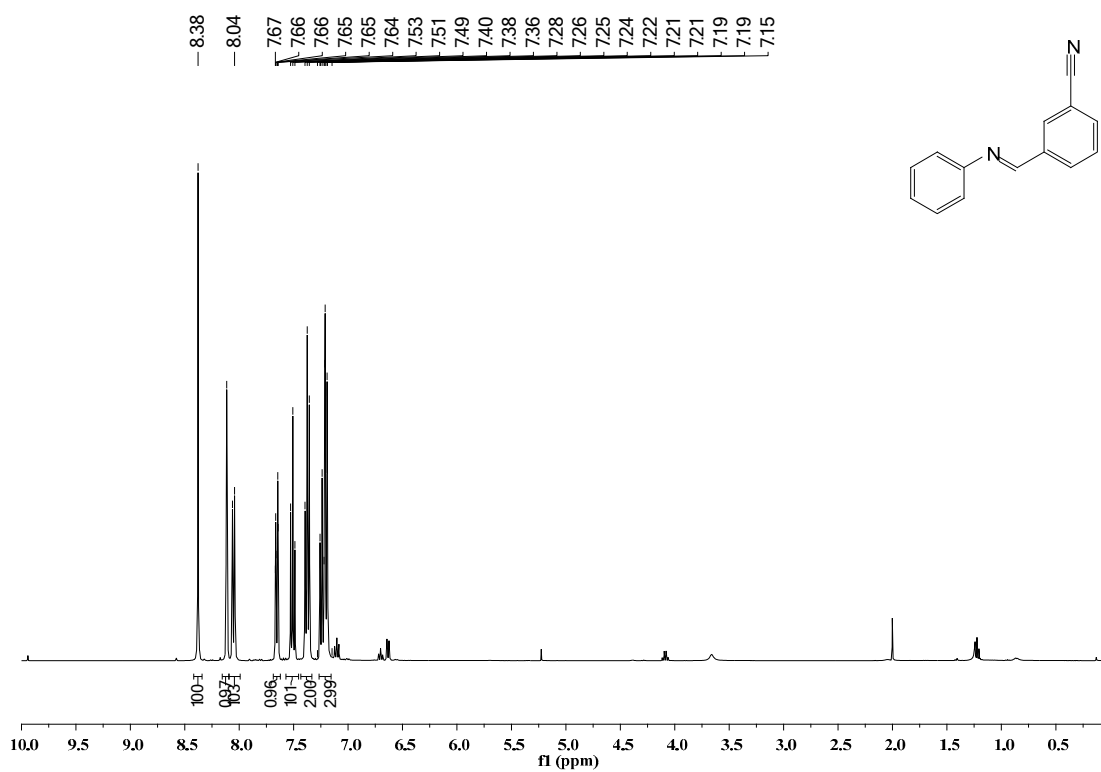


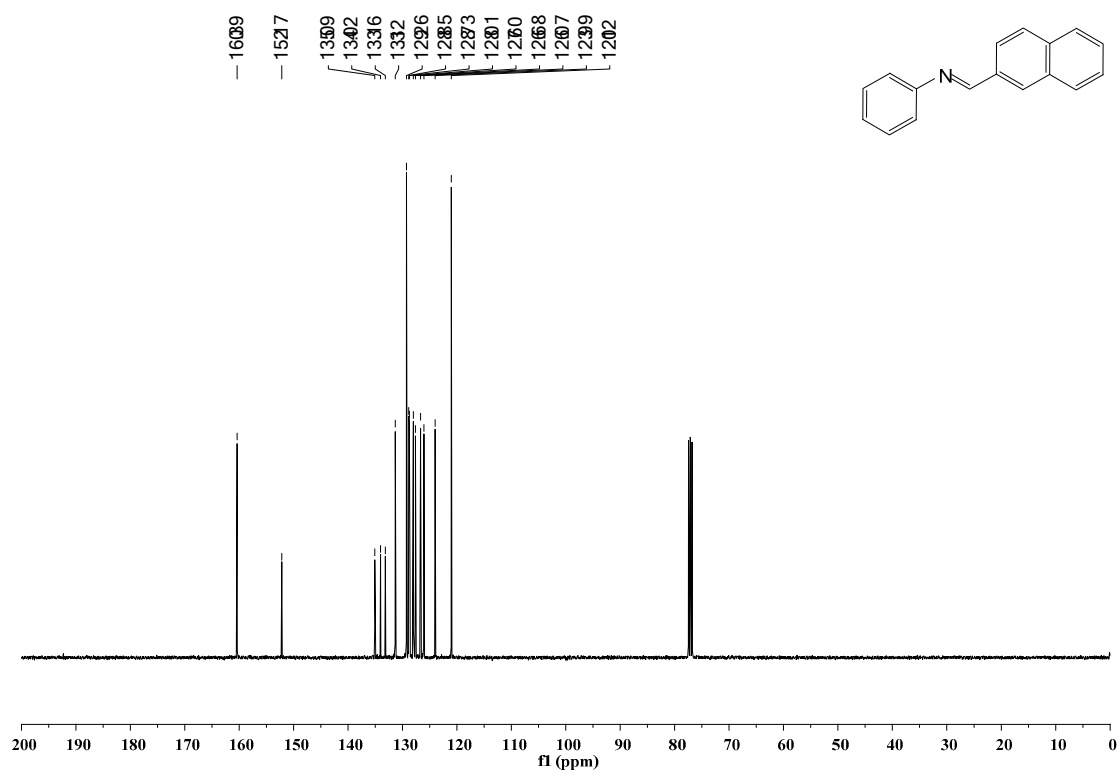
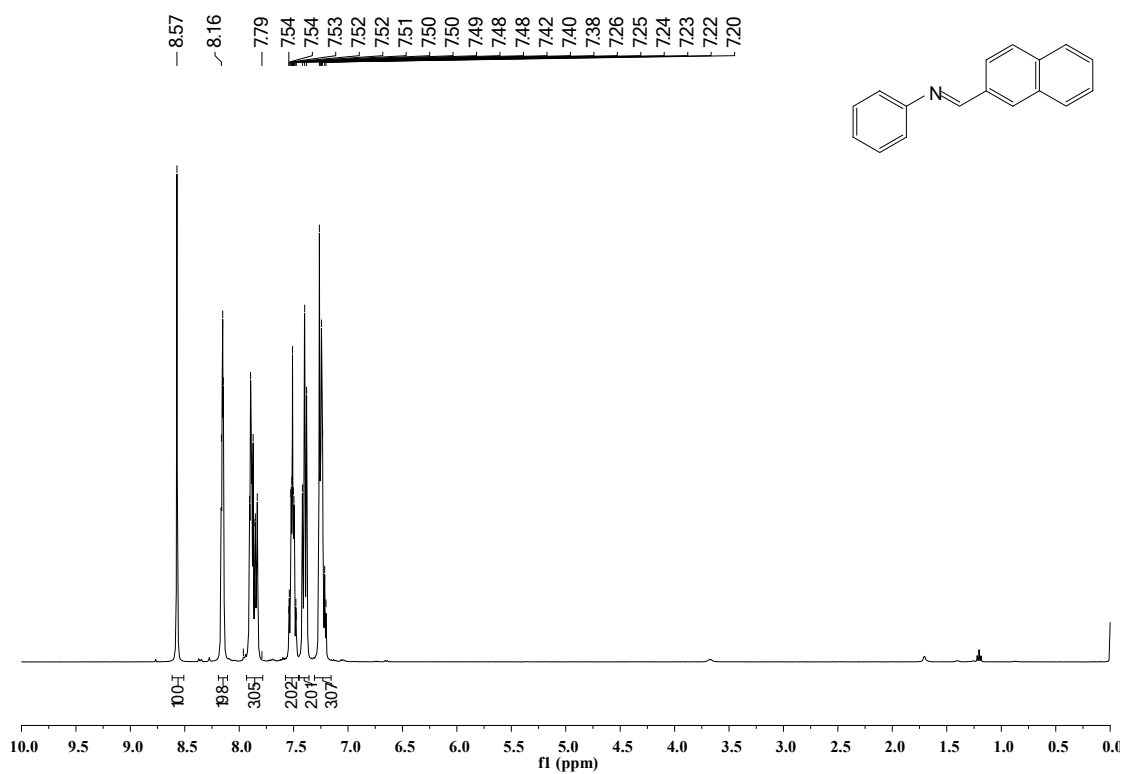


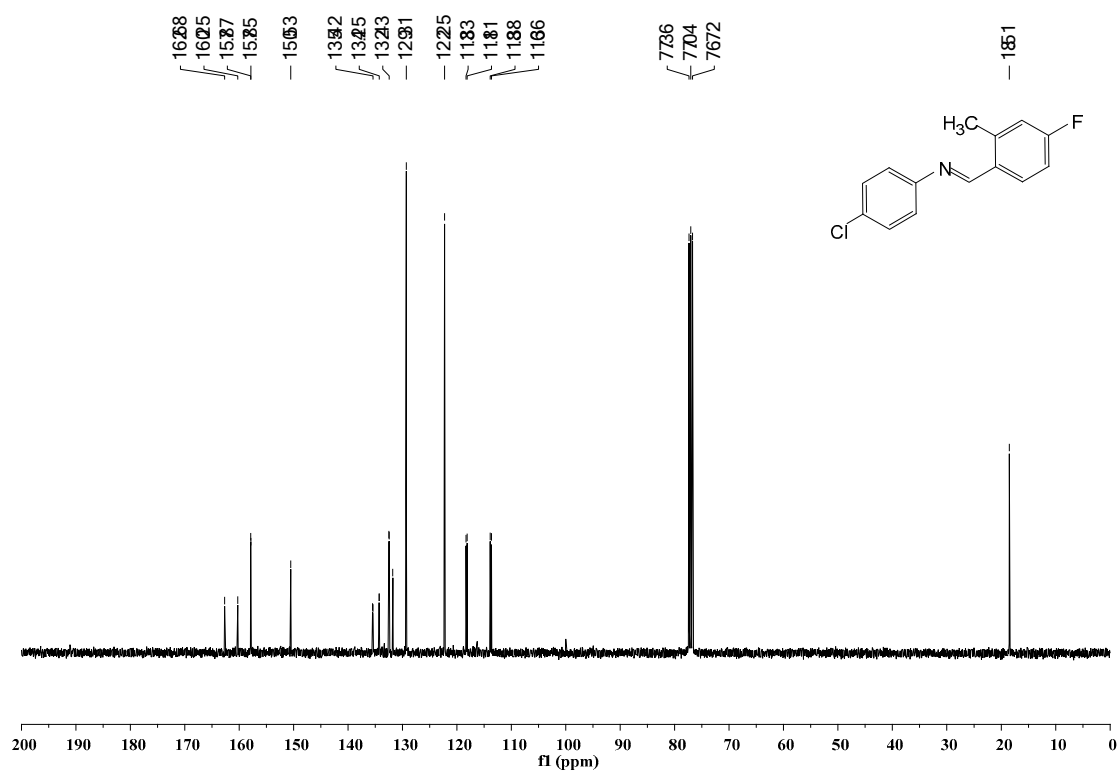
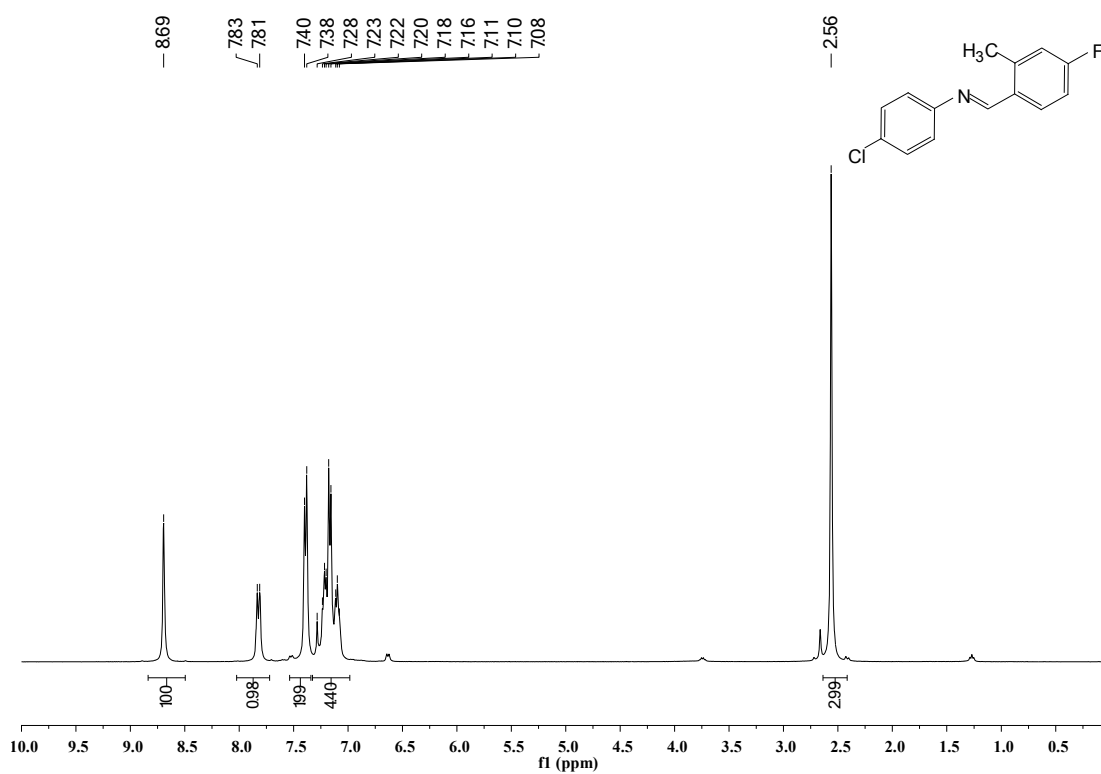


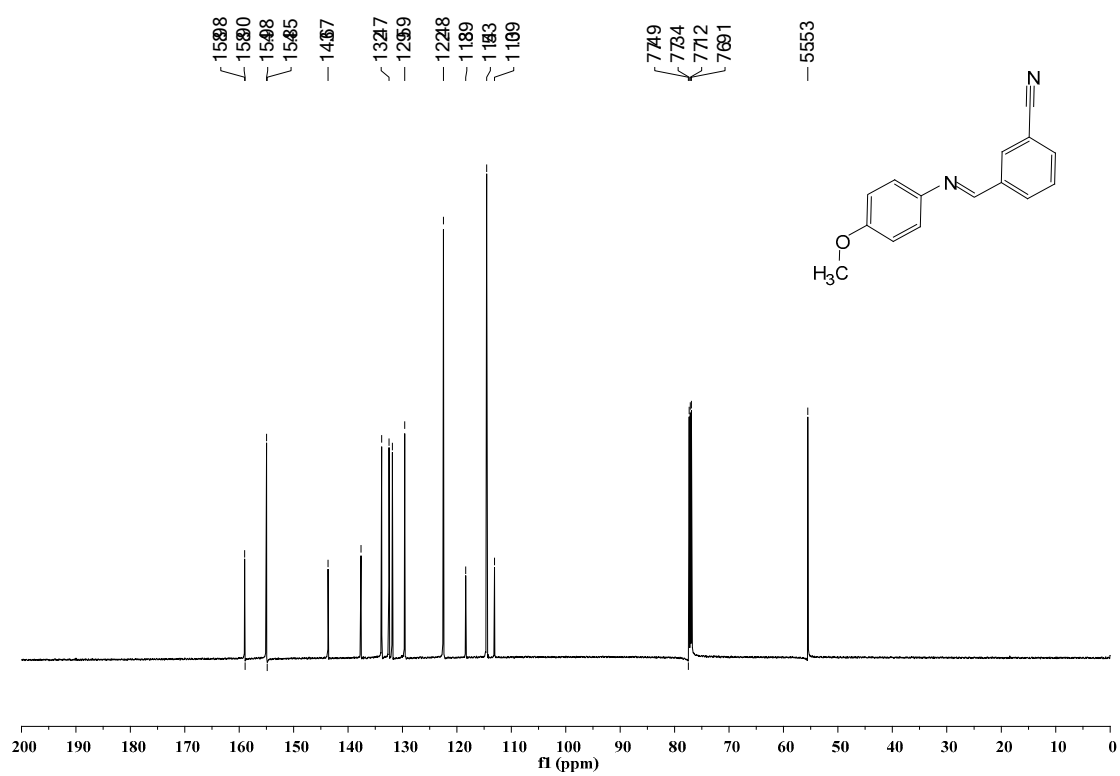
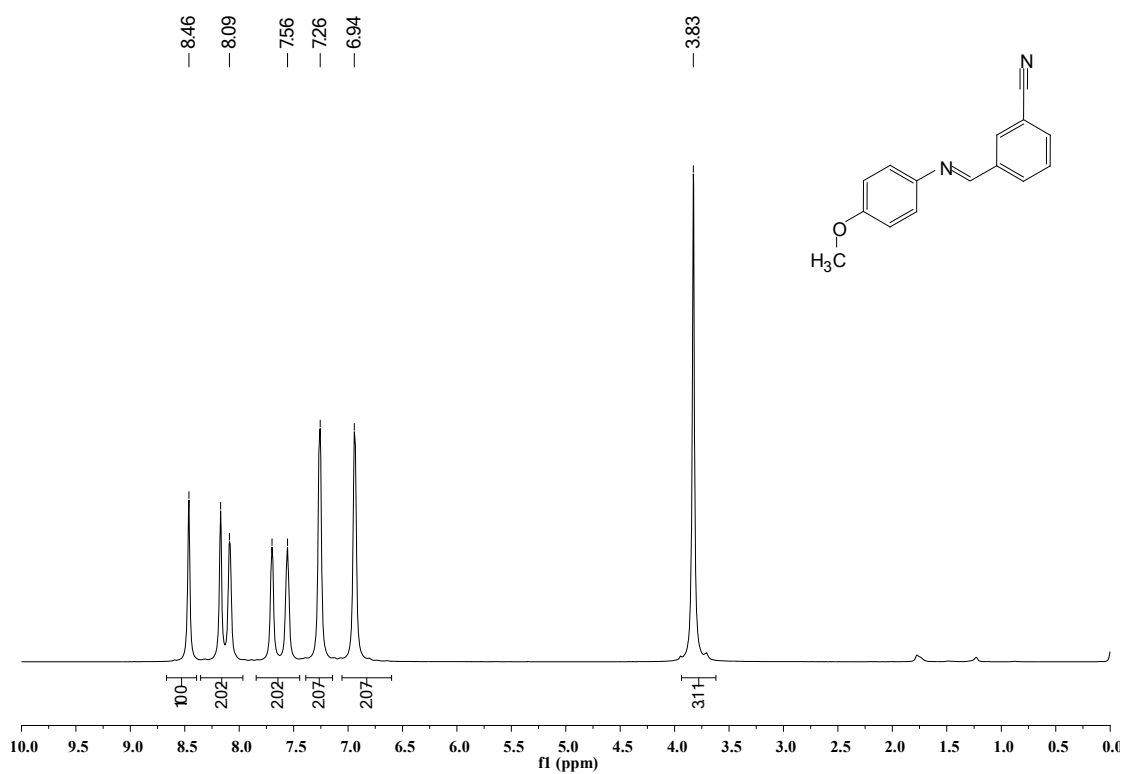


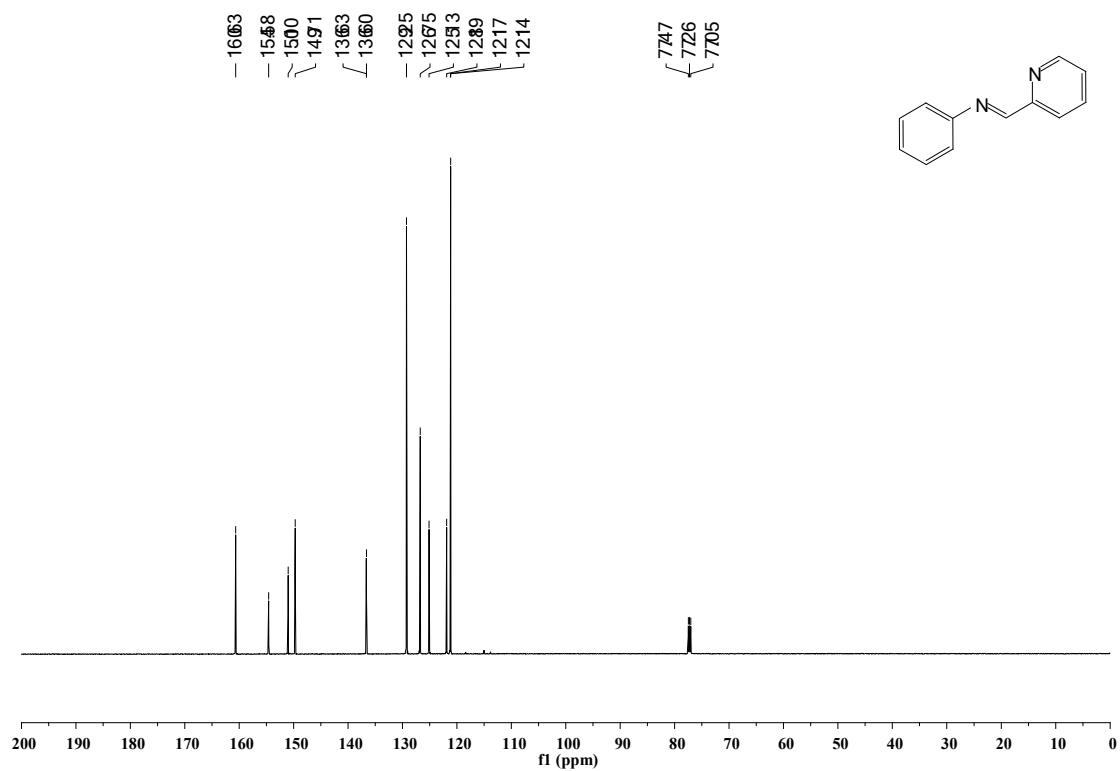
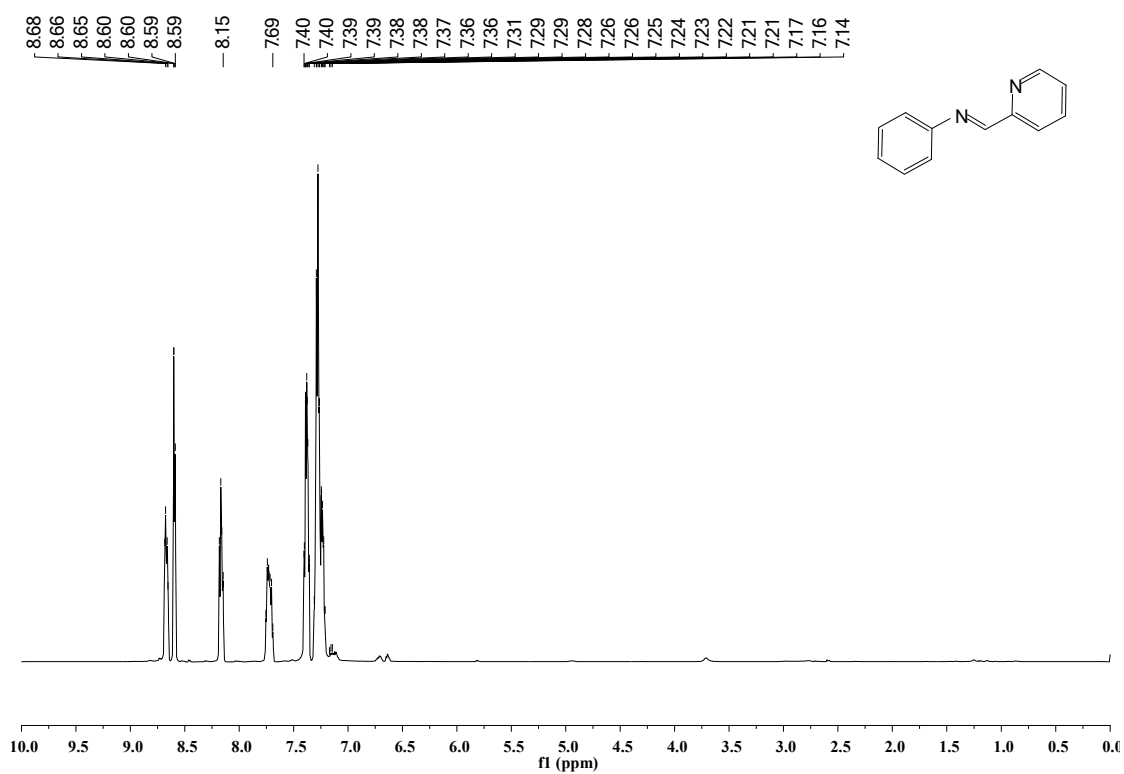


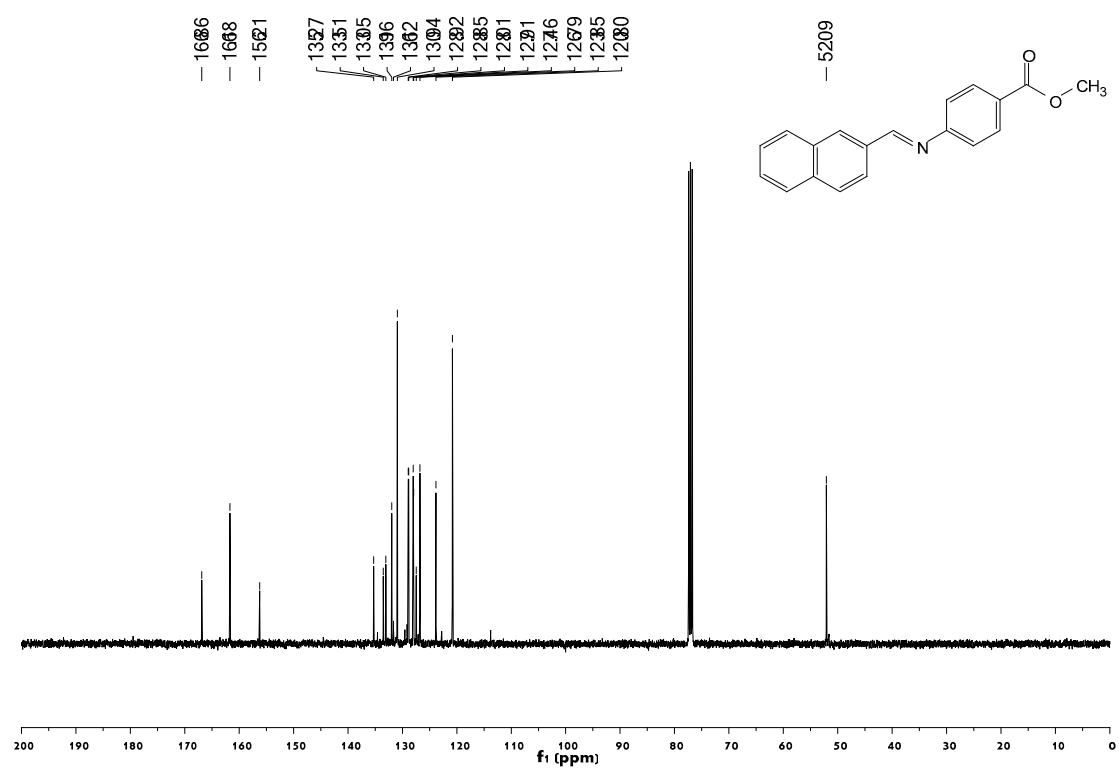
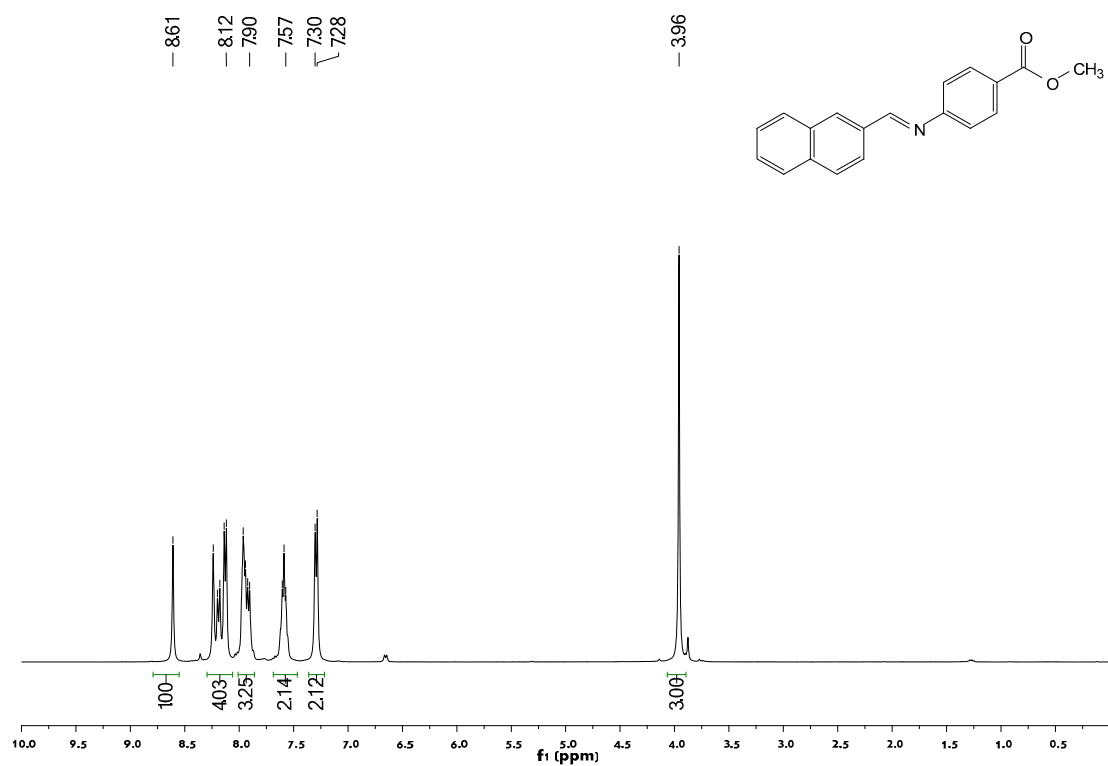


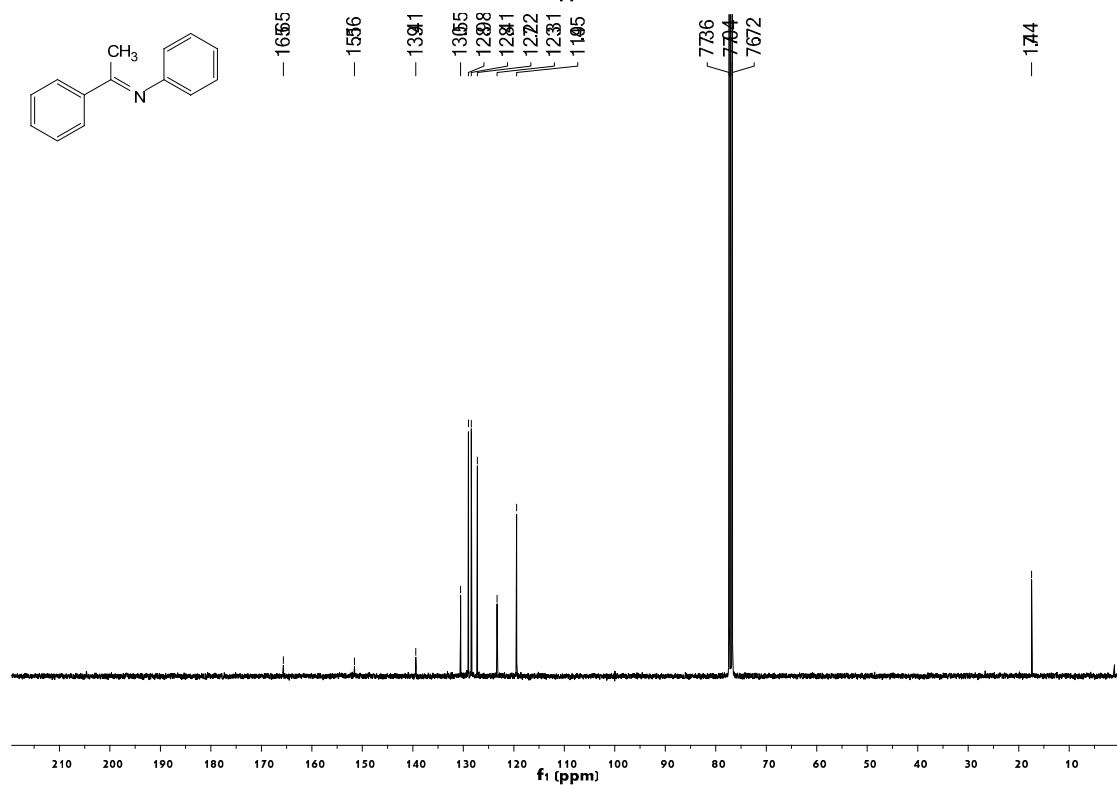
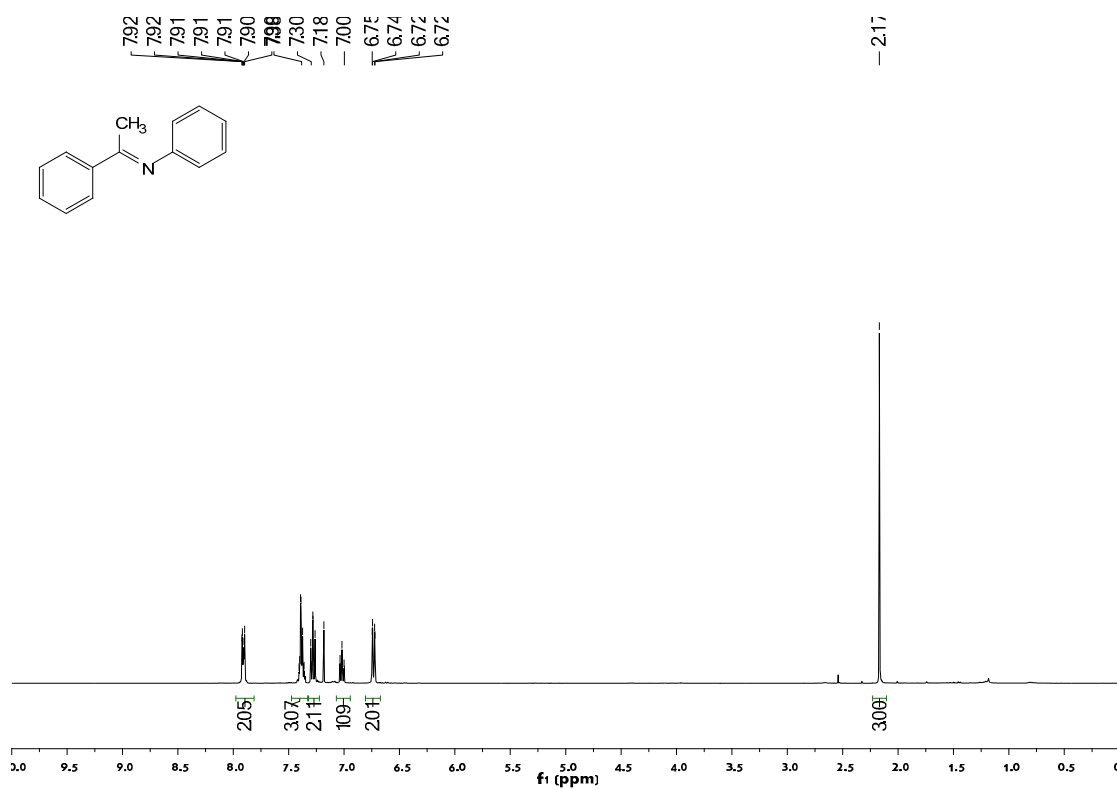


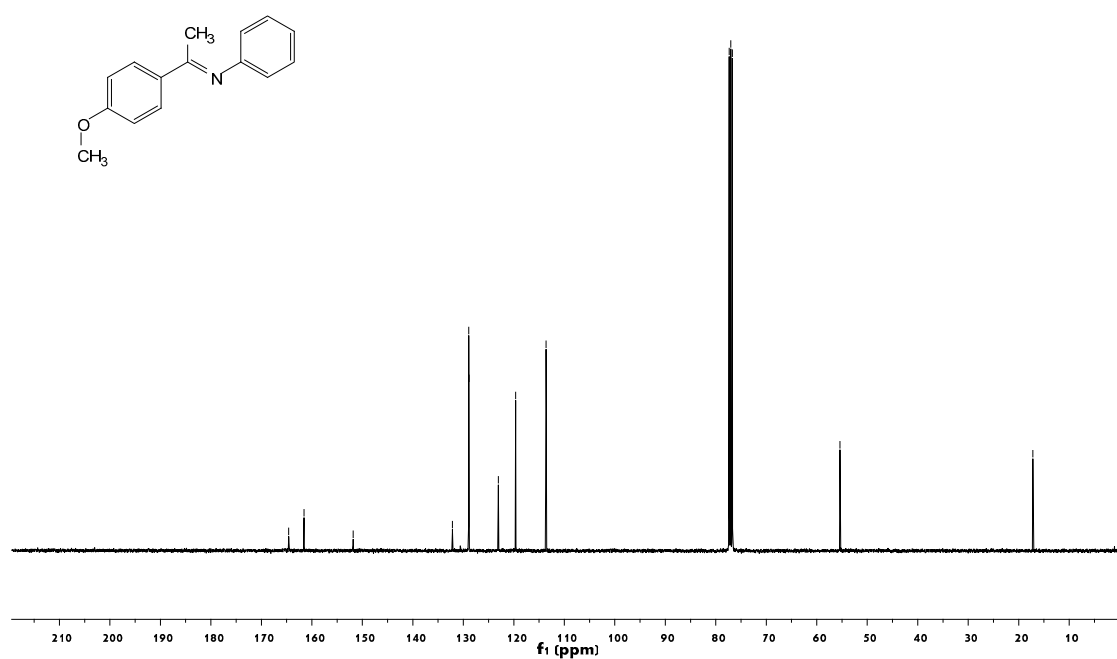
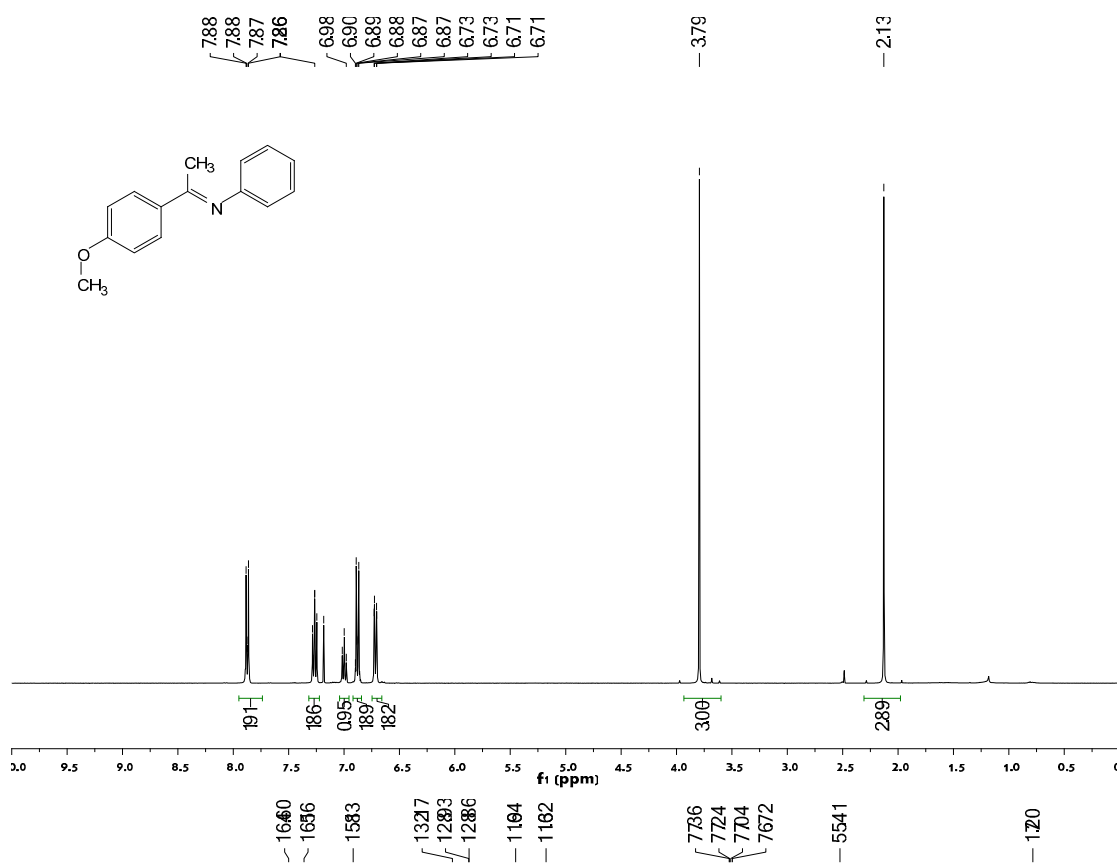


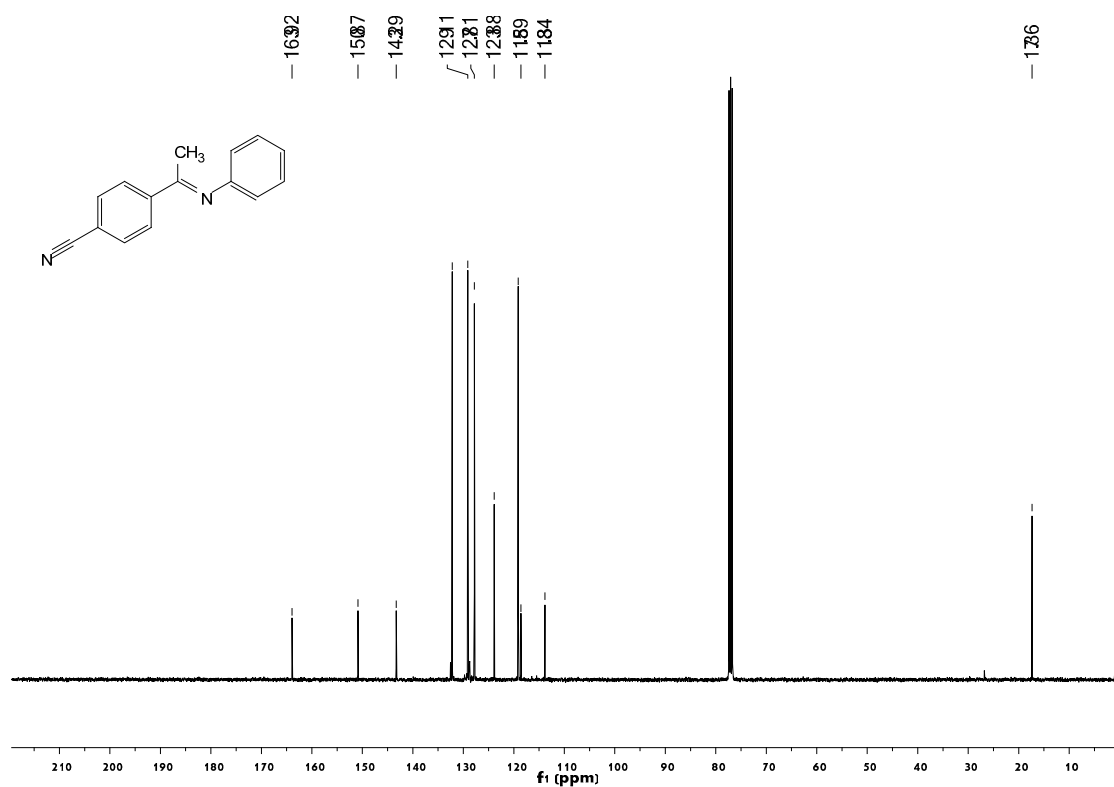
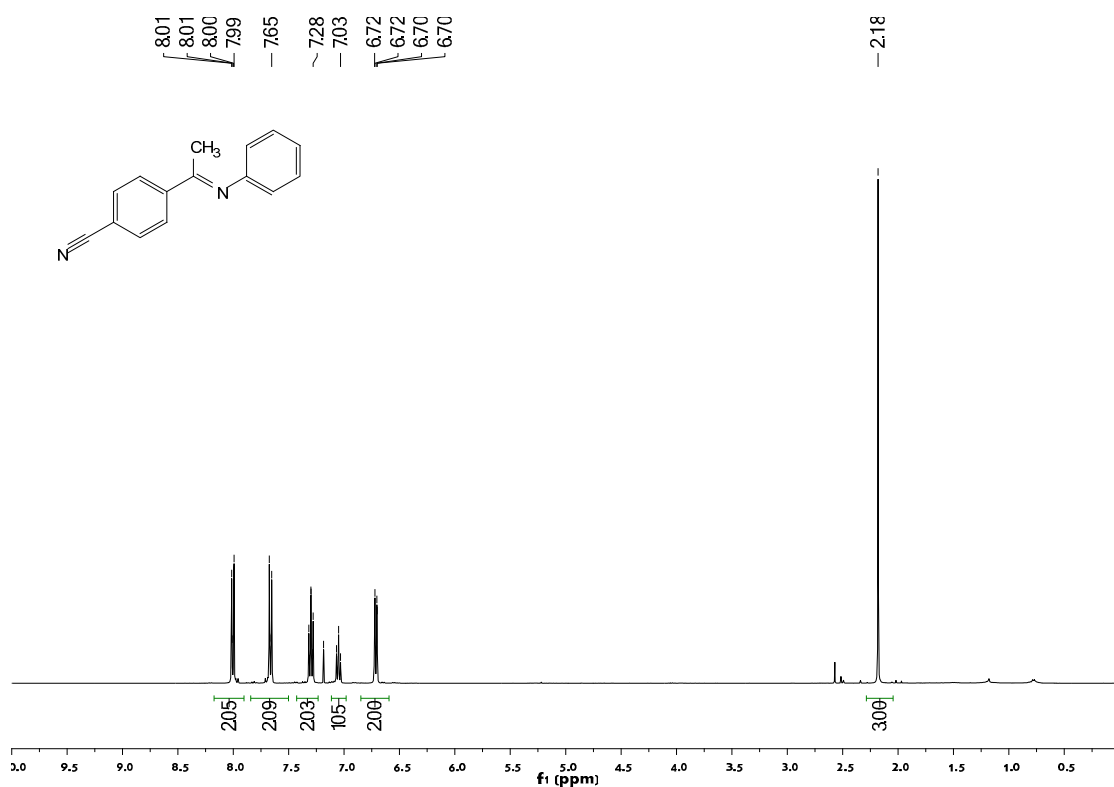


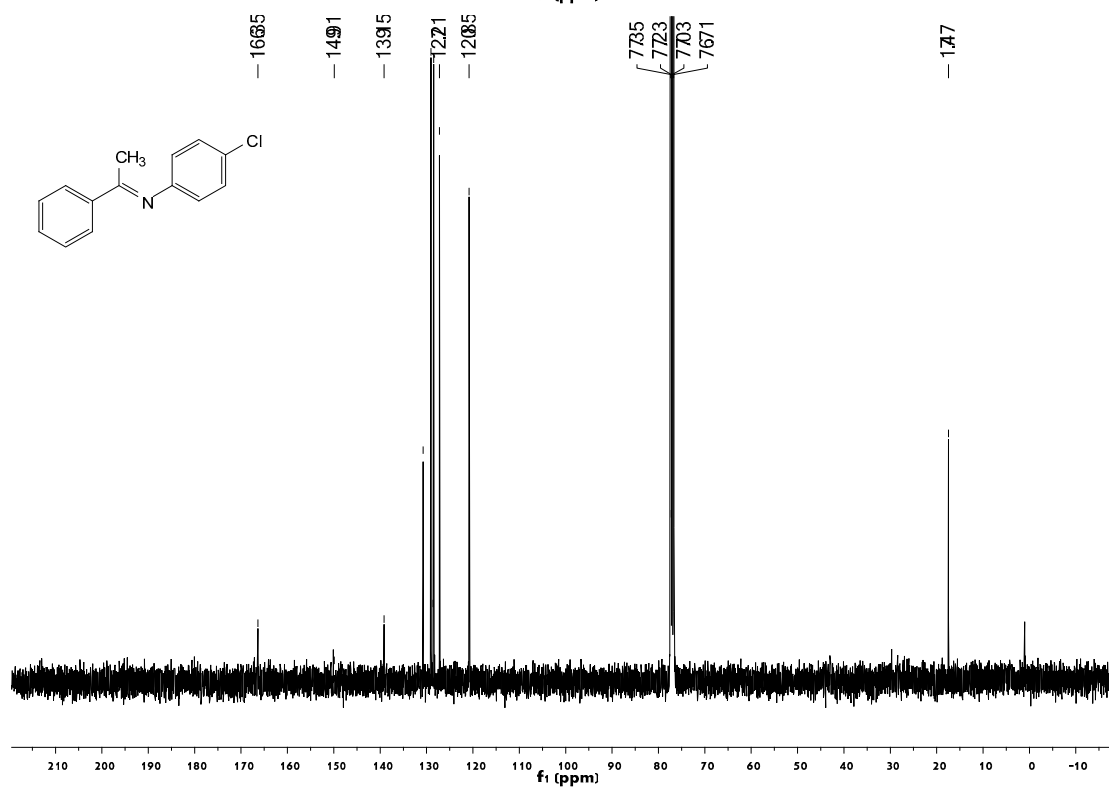
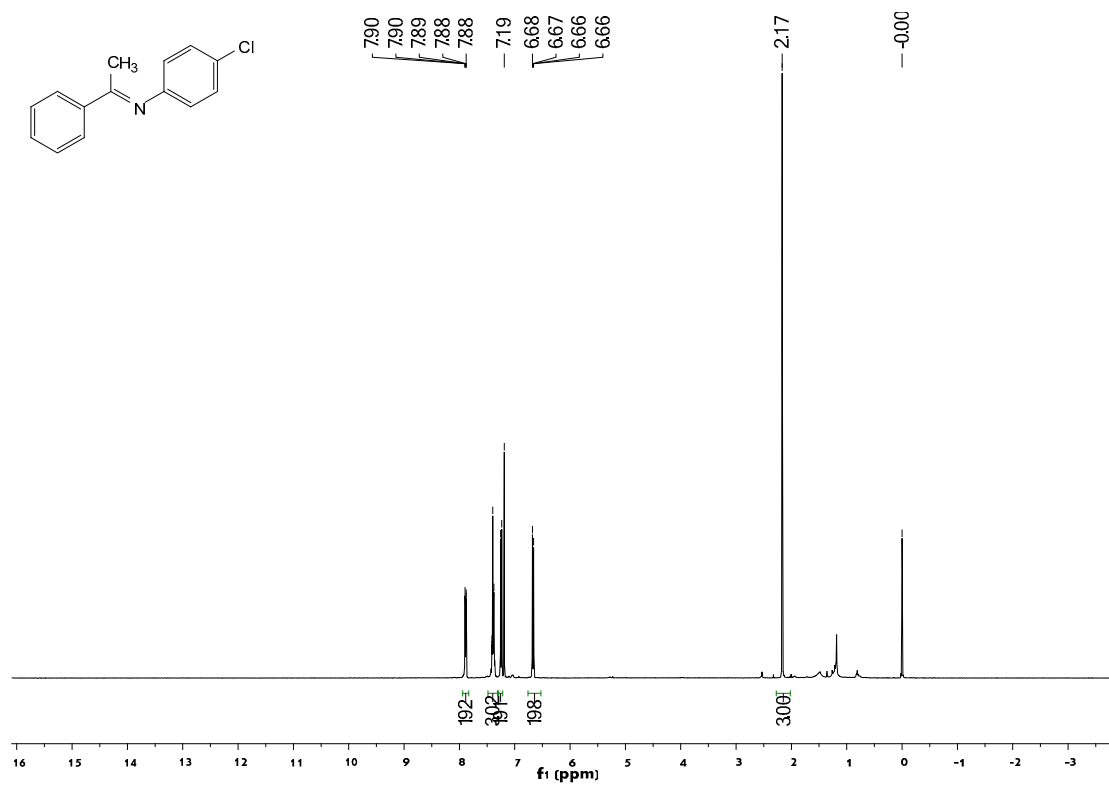


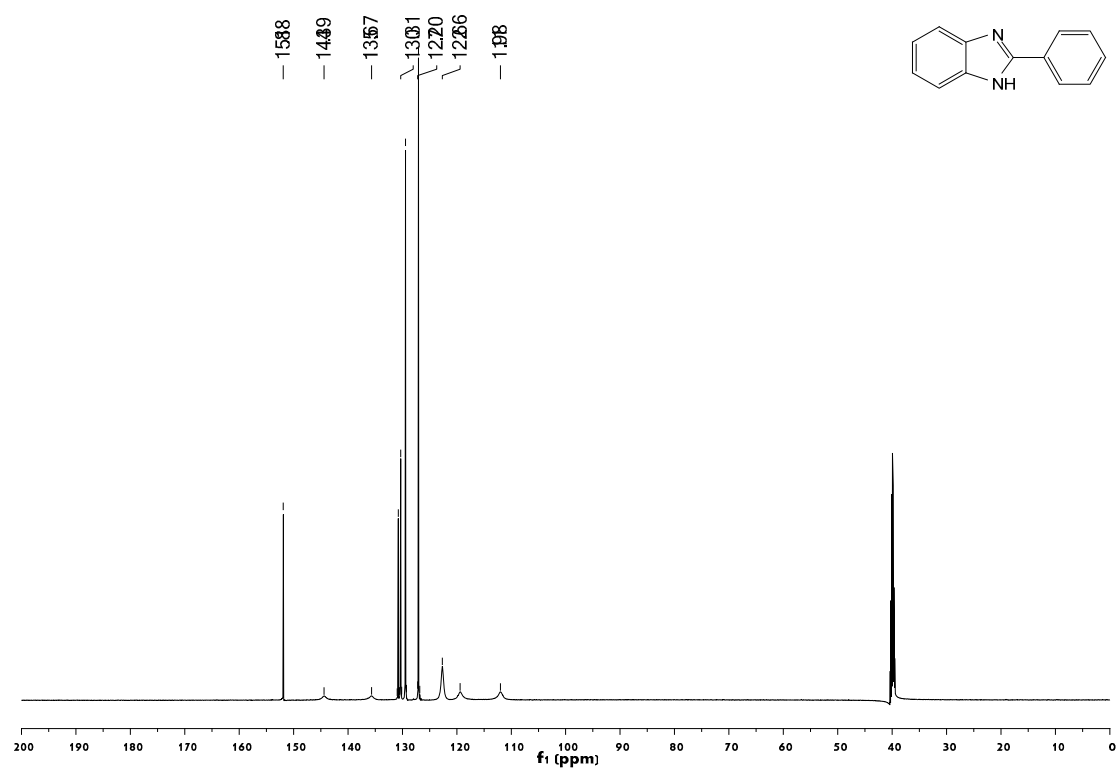
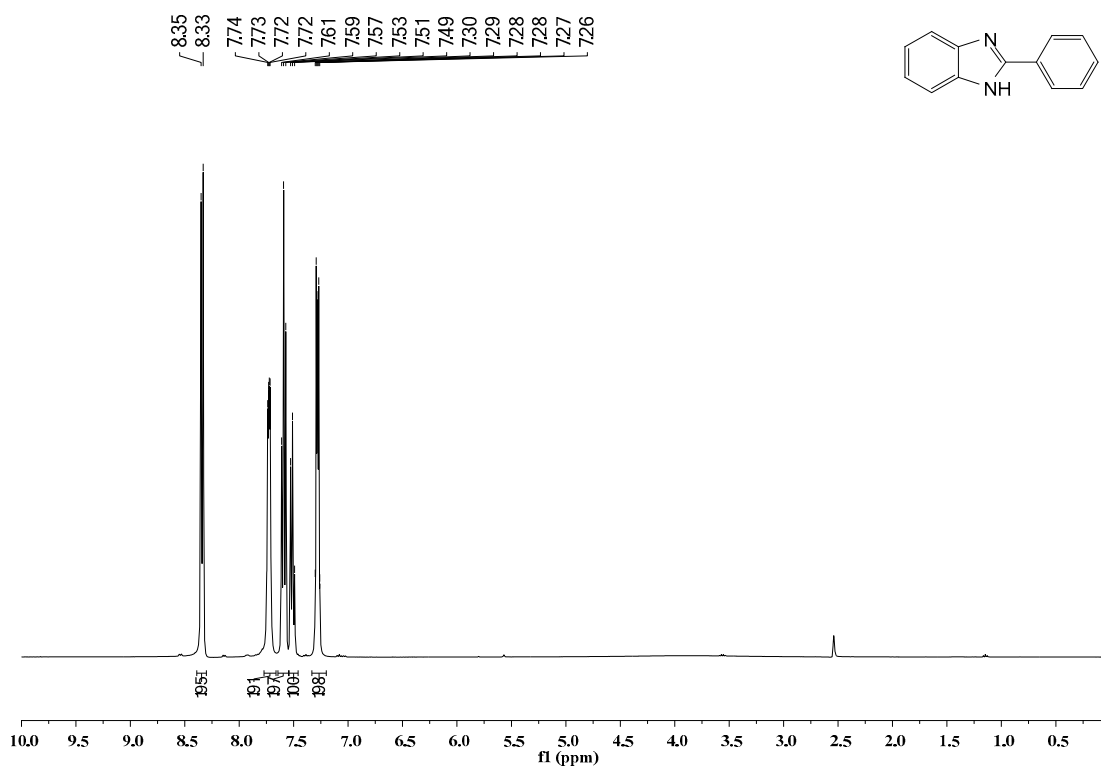


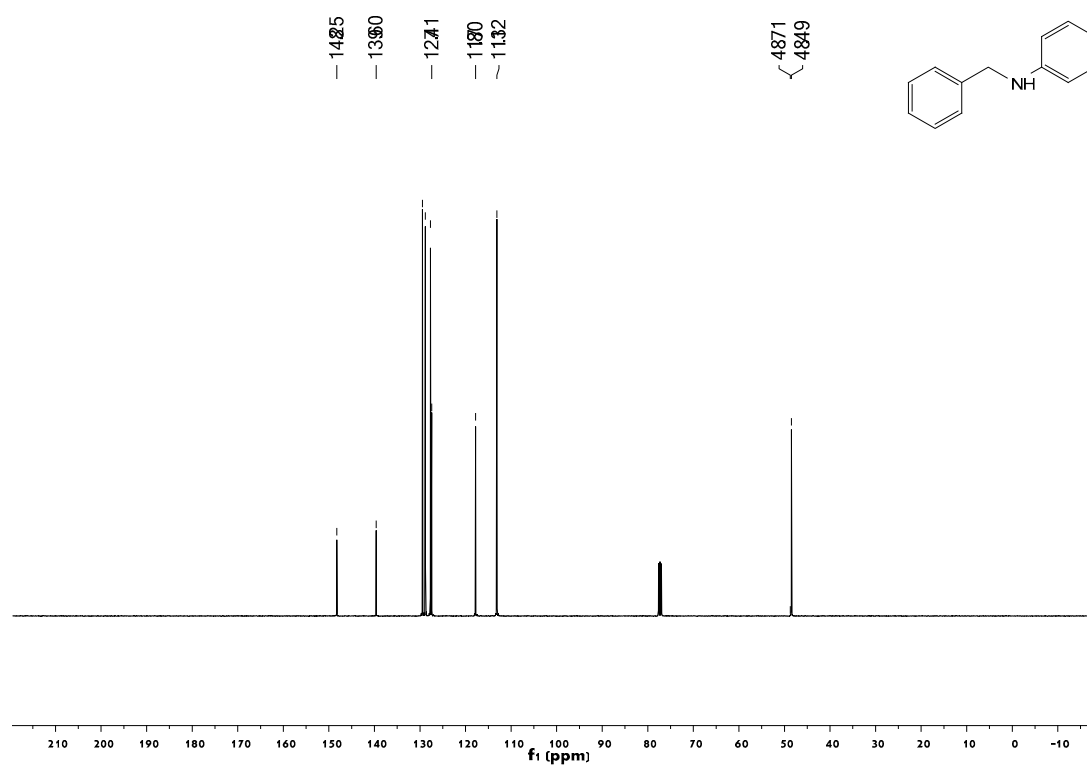
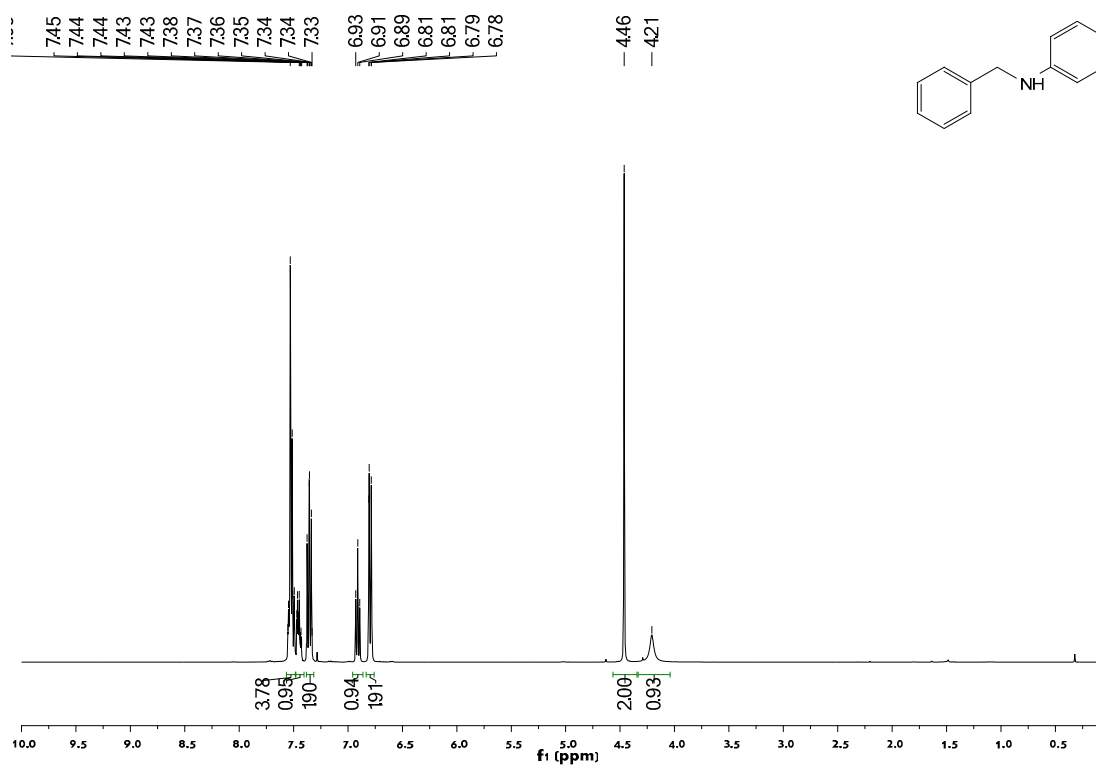


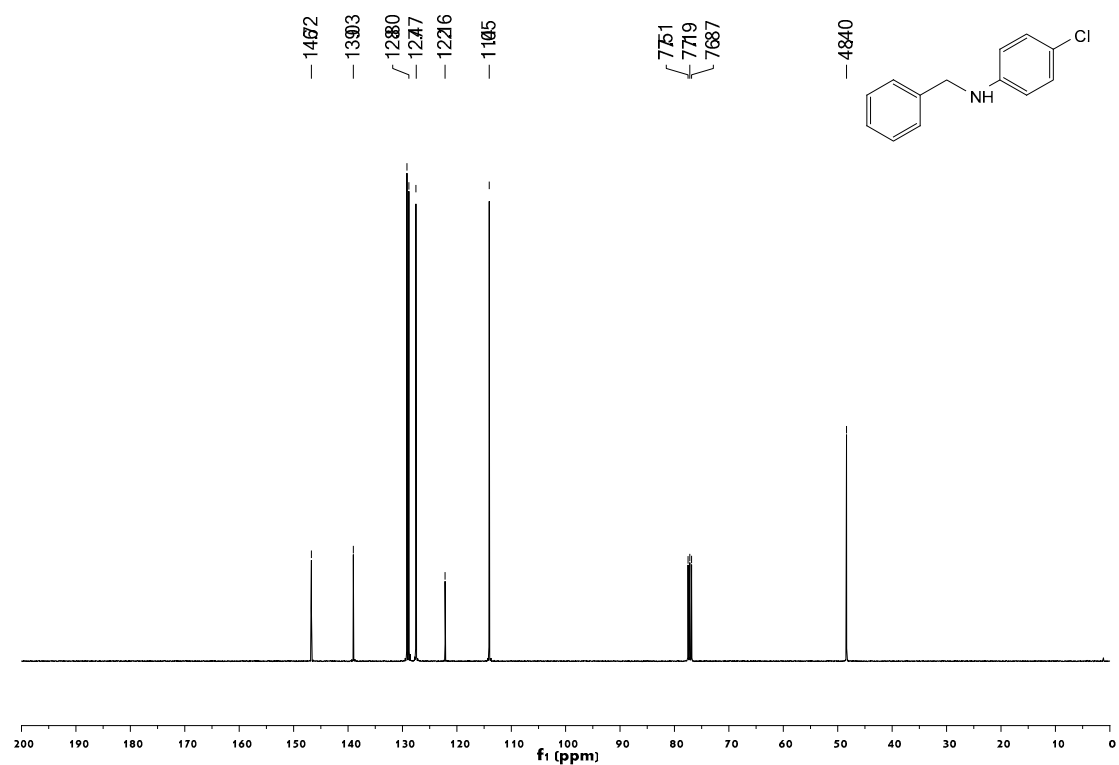
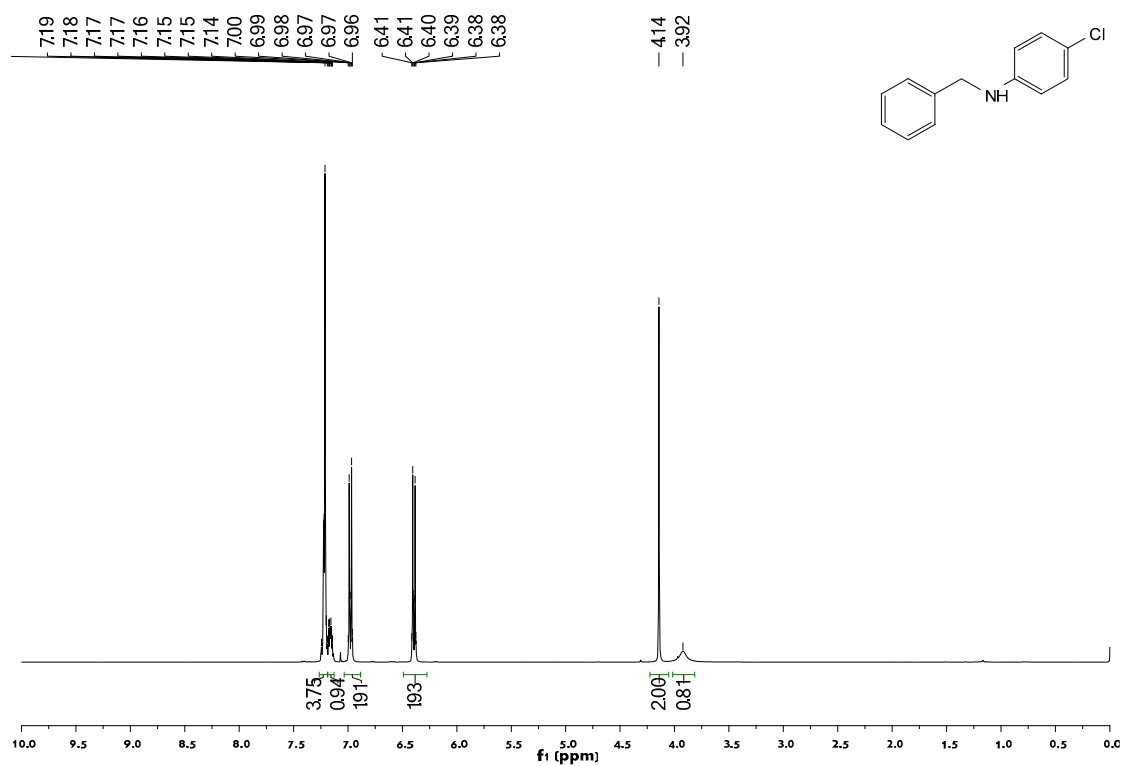


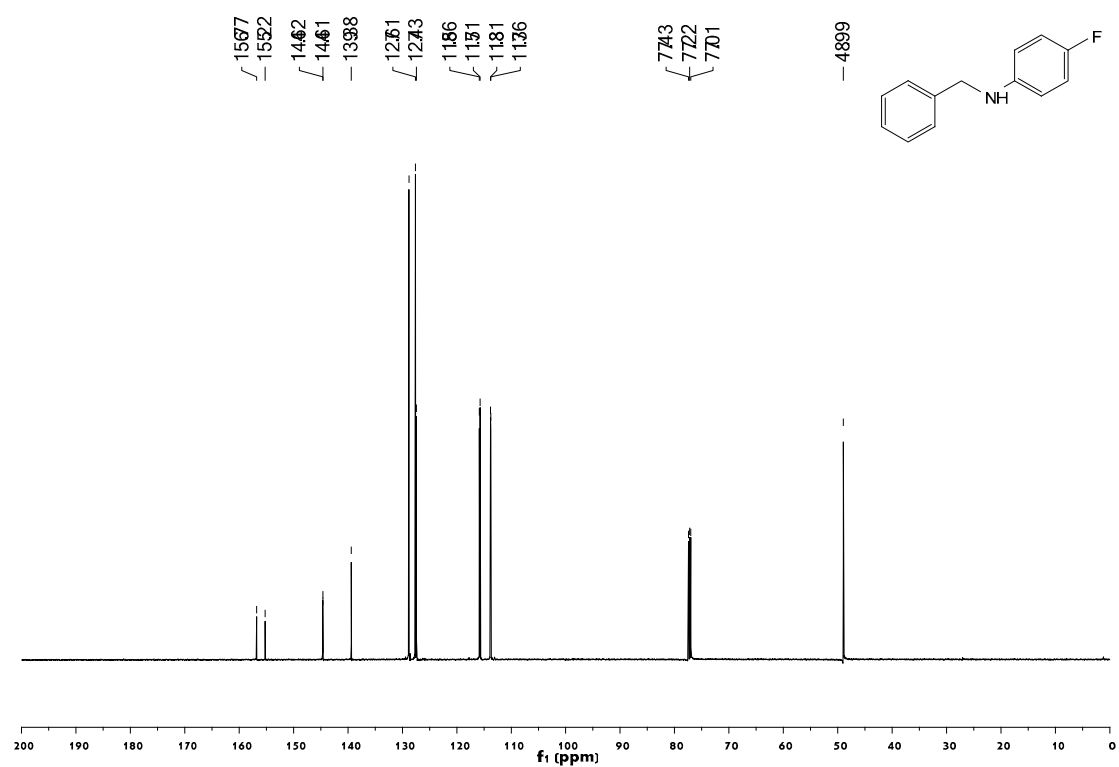
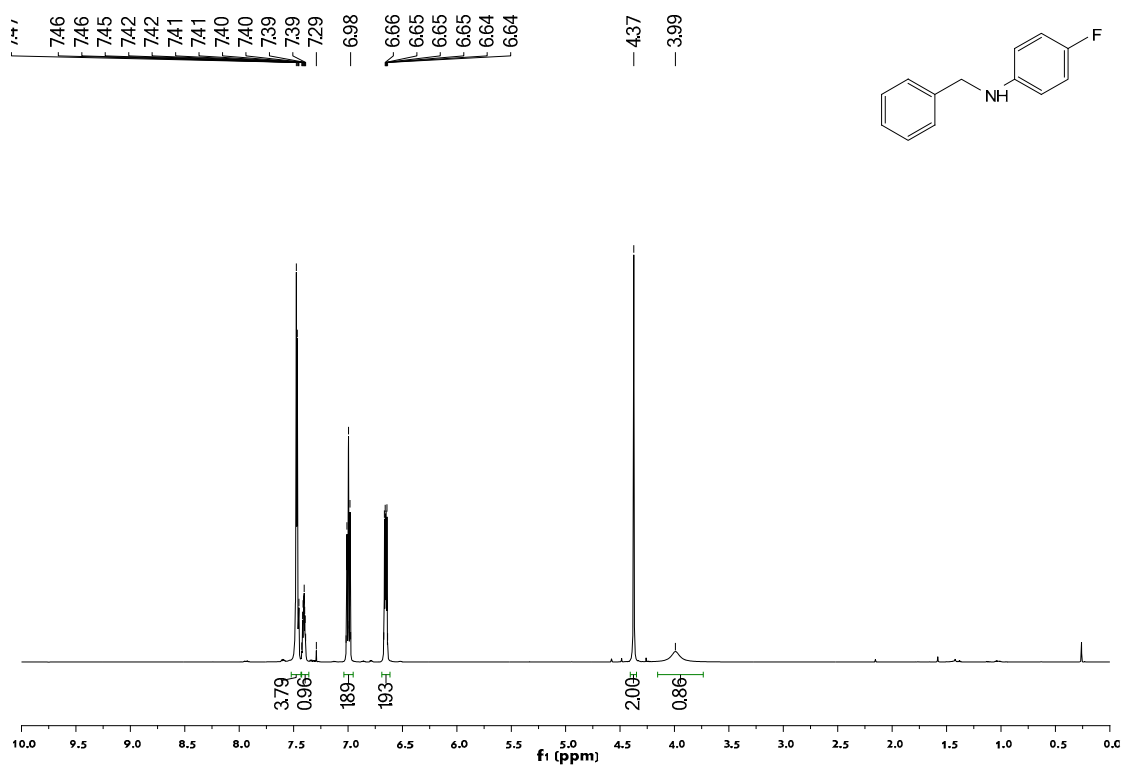


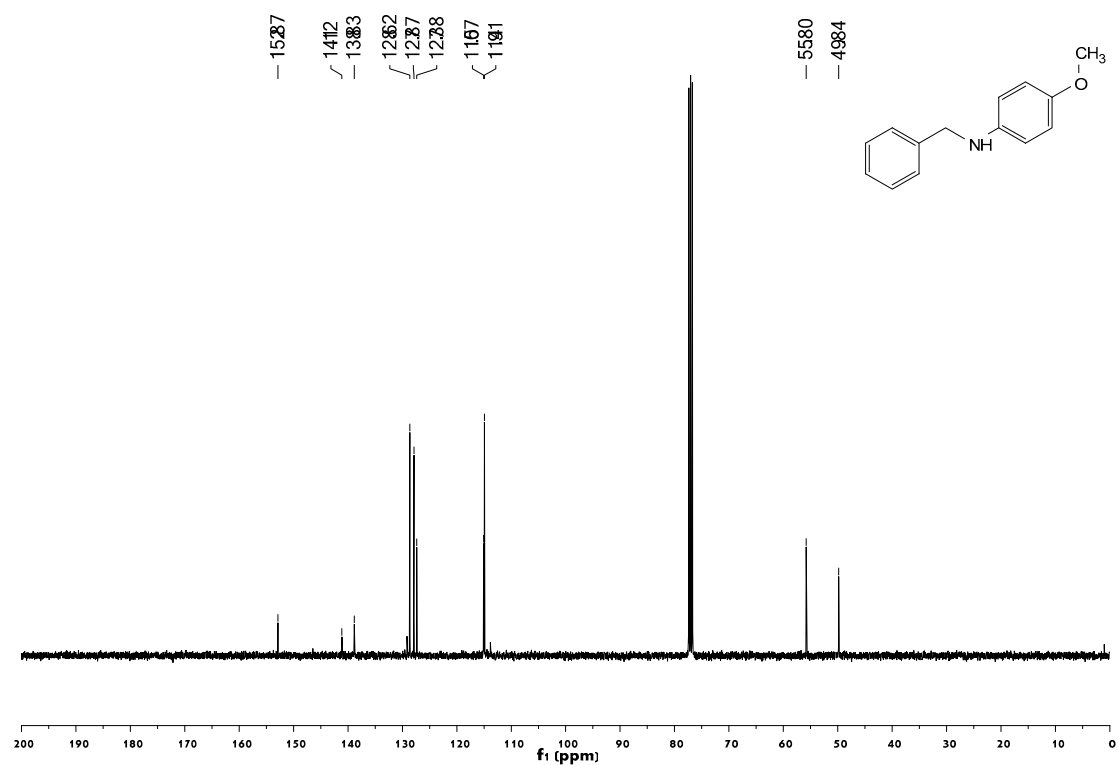
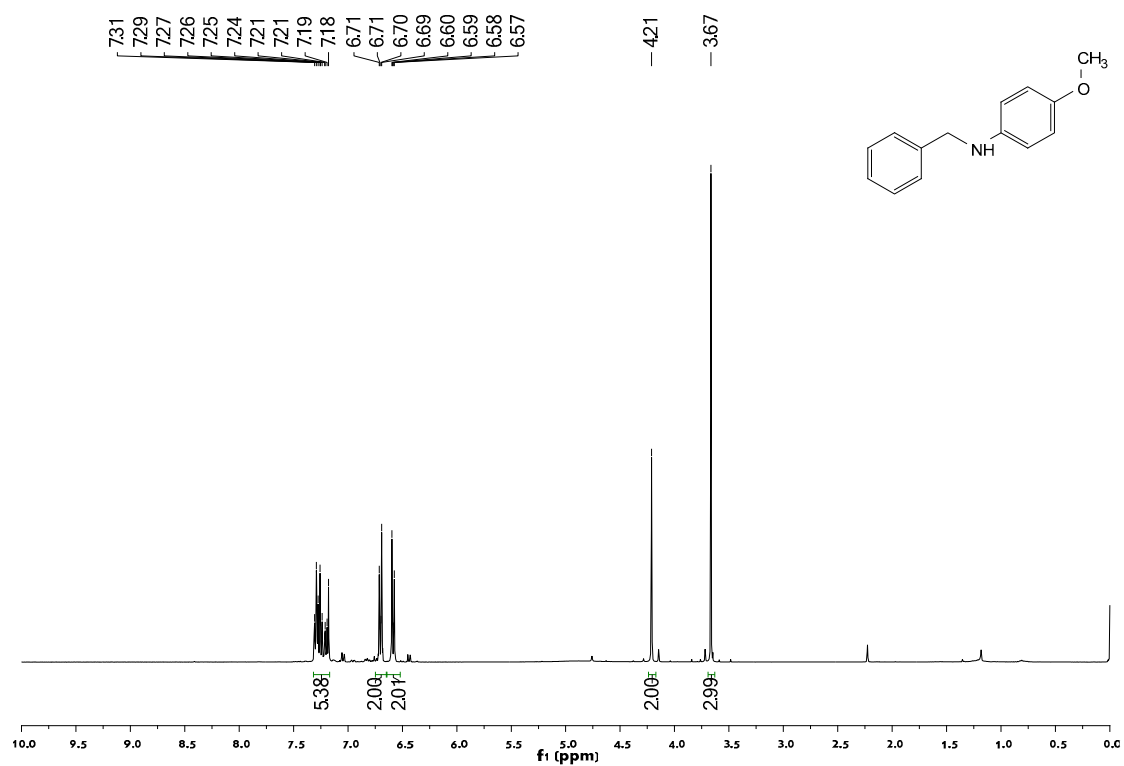


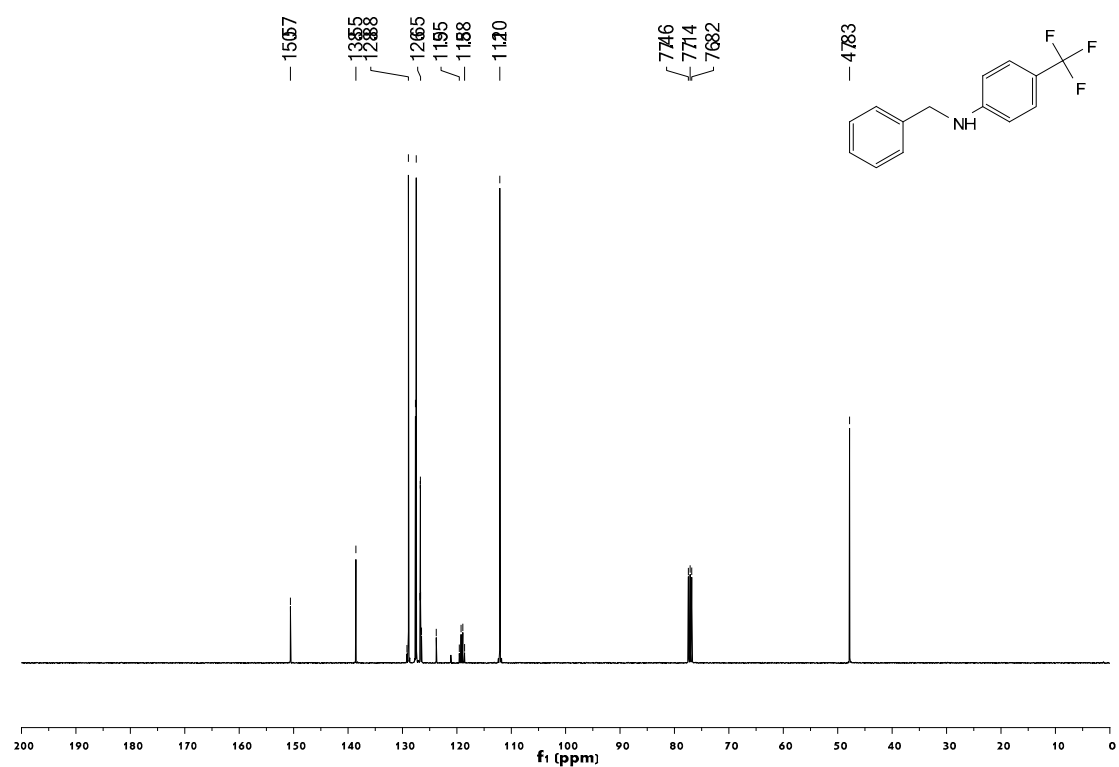
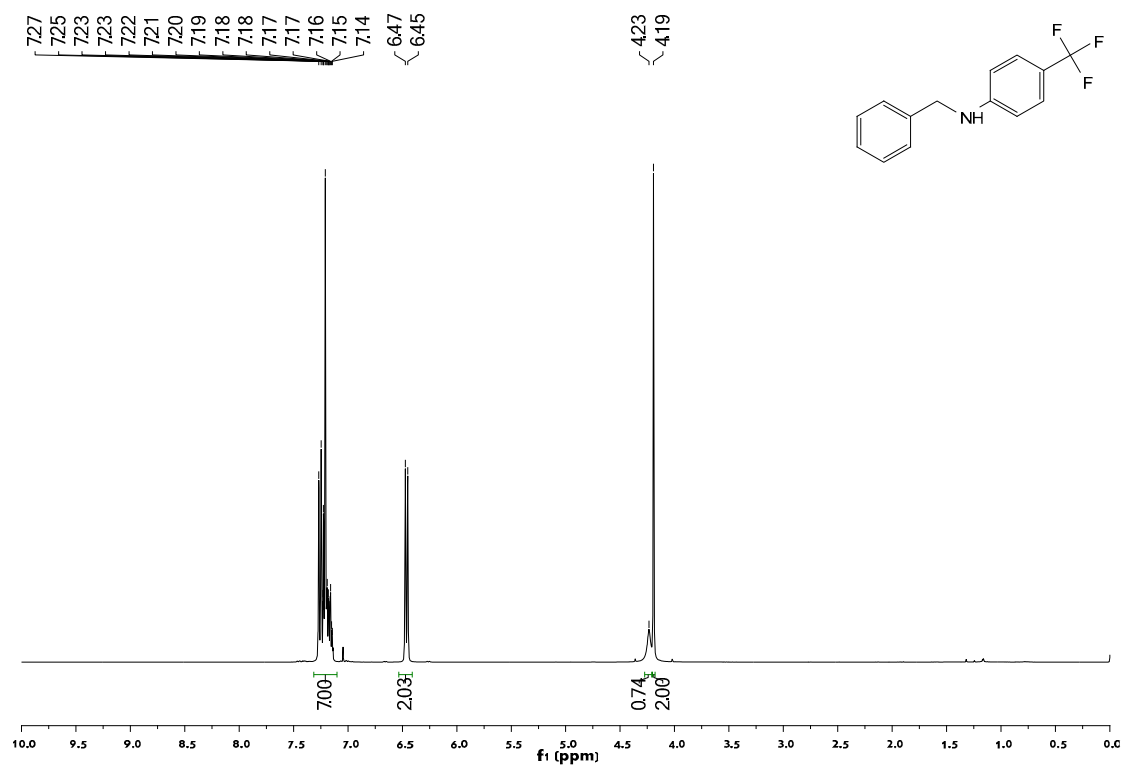


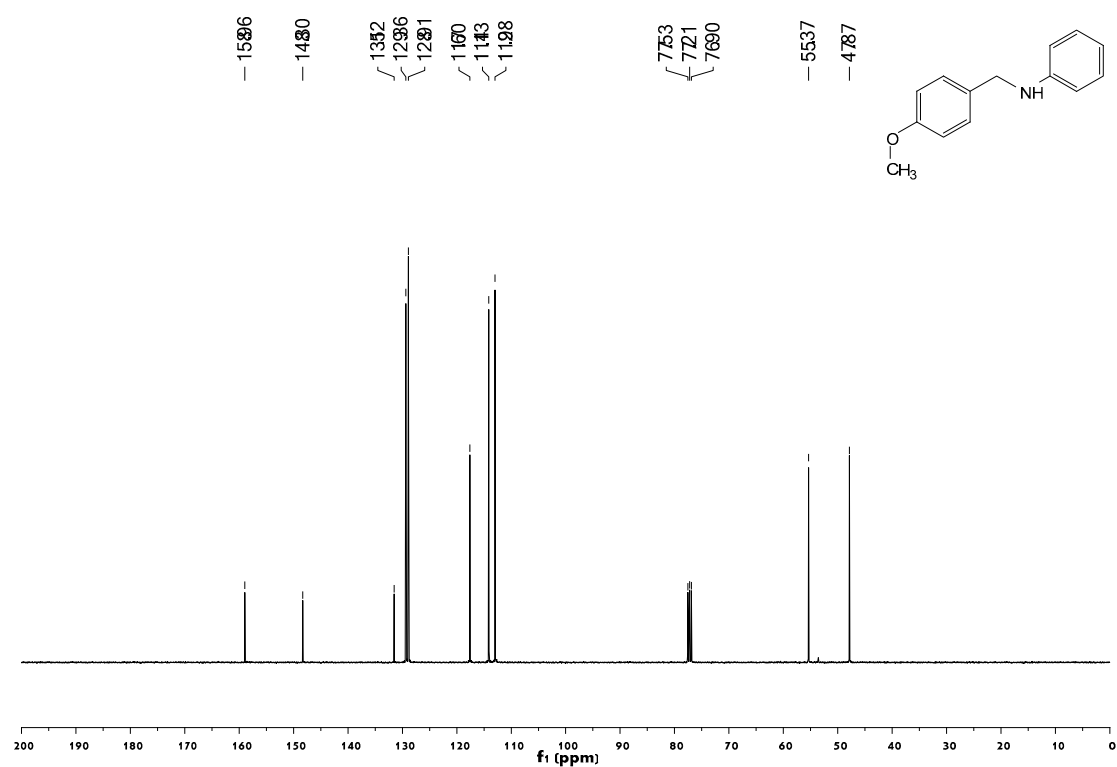
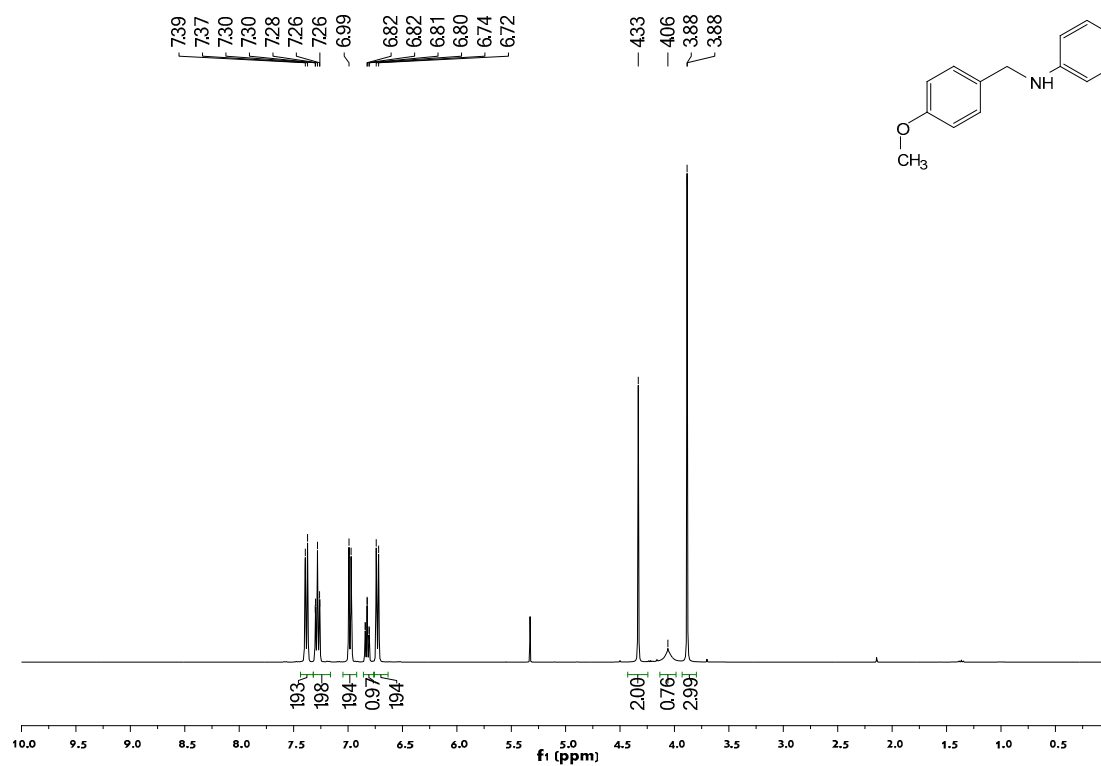


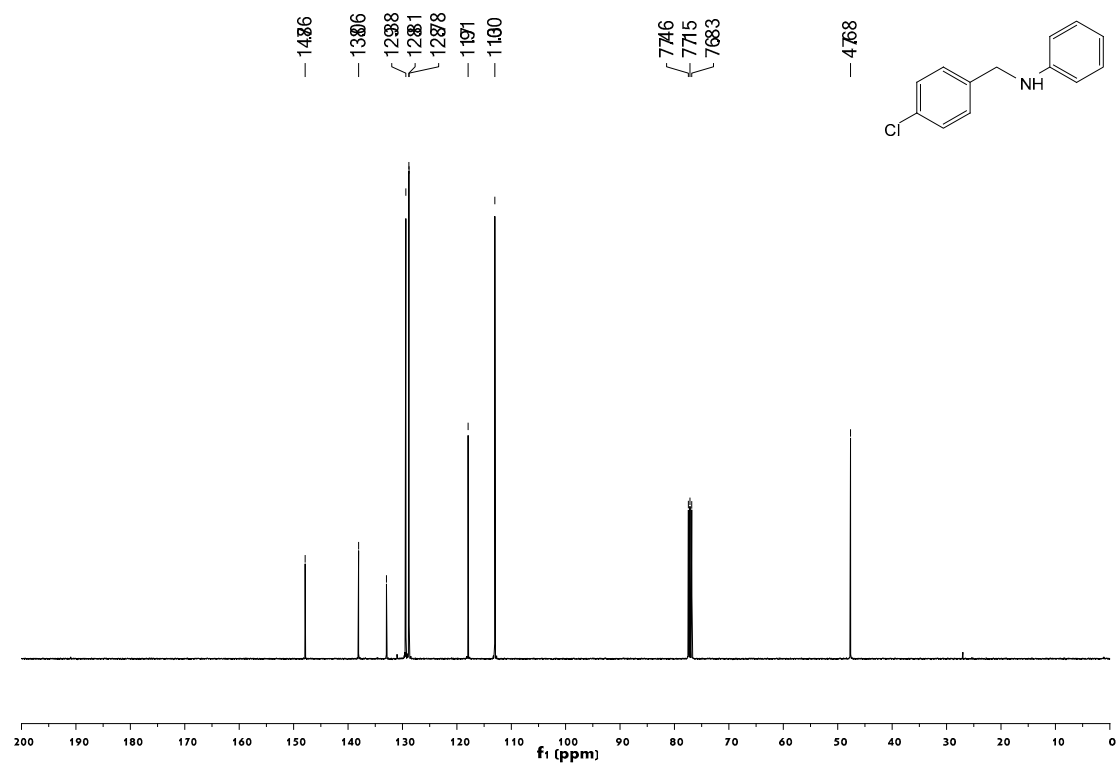
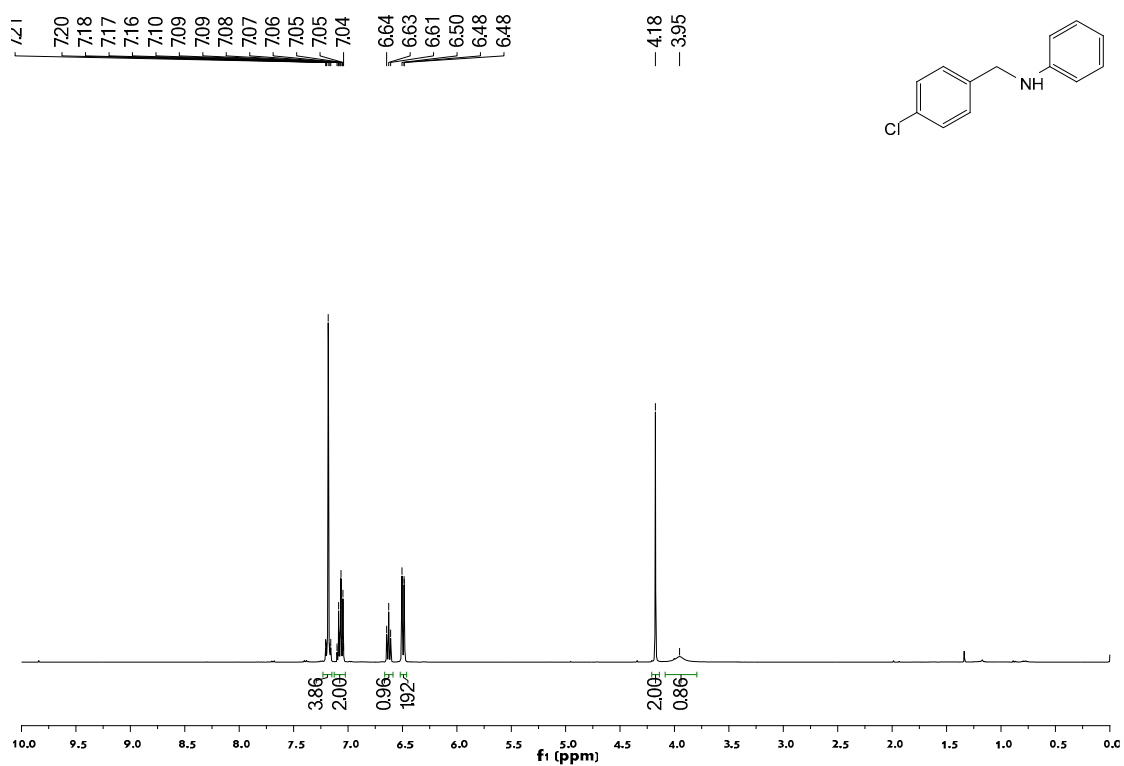


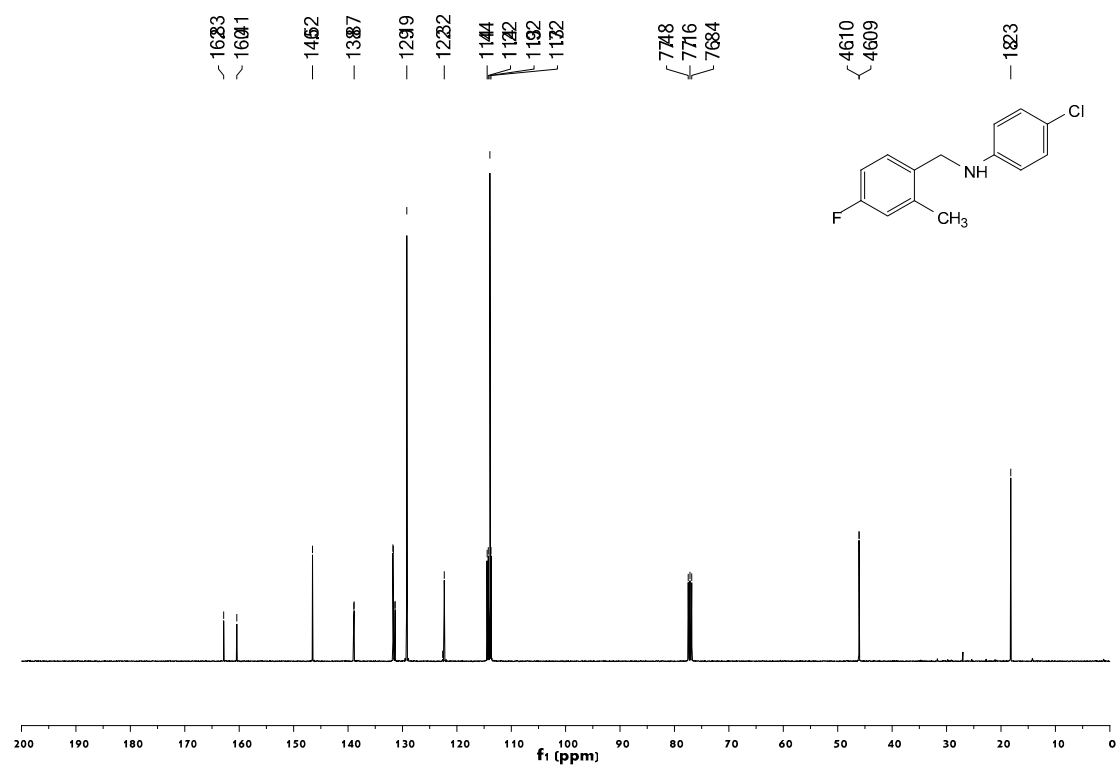
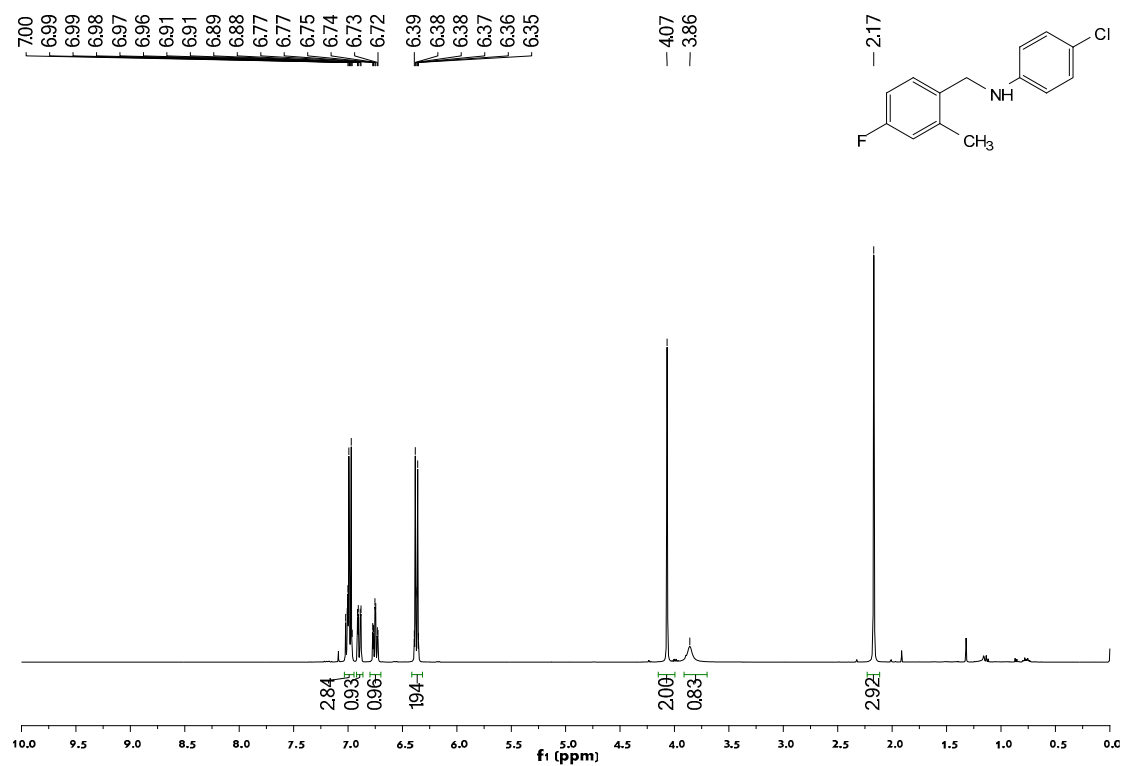


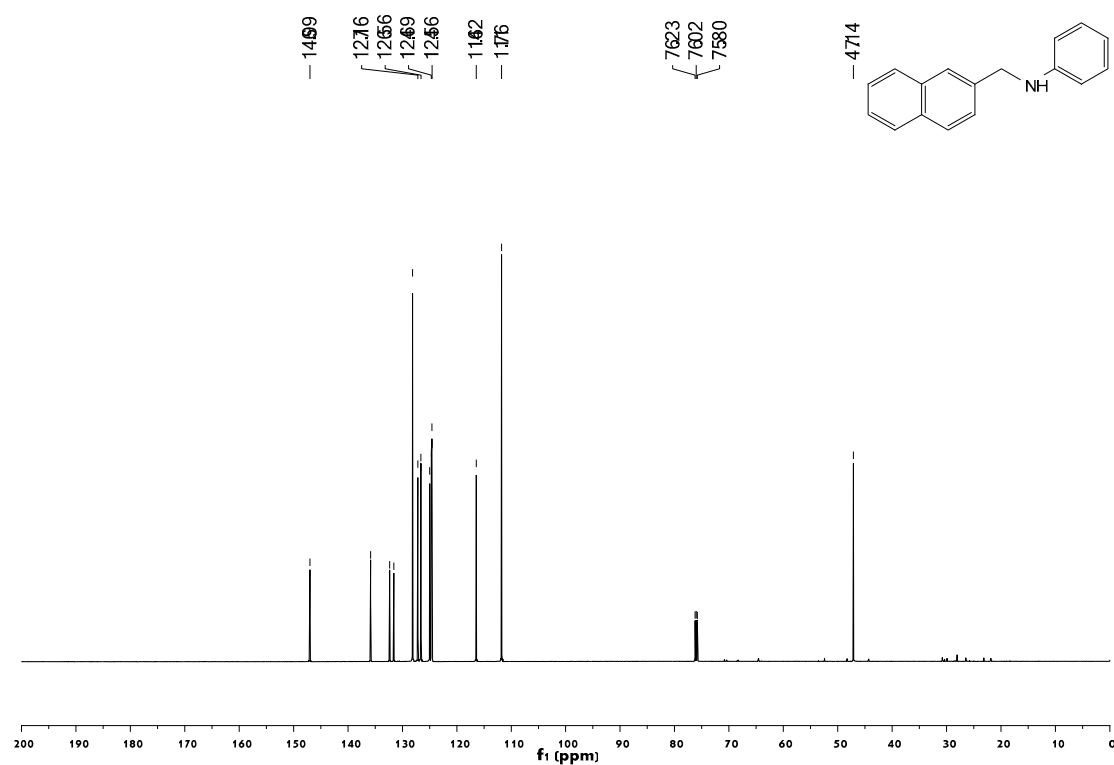
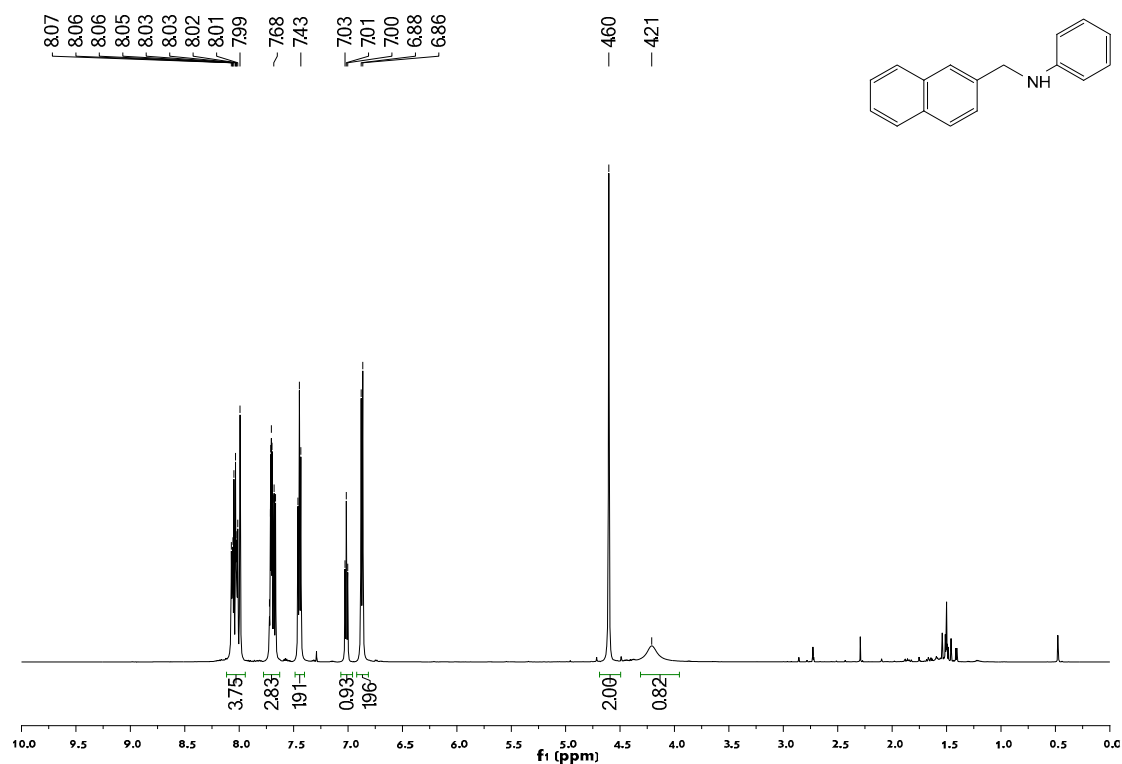












8. Reference

- [1] T. Schwob, R. Kempe, *Angew. Chem. Int. Ed.* **2016**, *55*, 15175–15179; *Angew. Chem.* **2016**, *128*, 15400–15404.
- [2] Y. Zhang, F. Lu, H. -Y. Zhang, J. Zha, *Catal. Lett.* **2017**, *147*, 20–28.
- [3] L. Tang, H. Sun, Y. Li, Z. Zha, Z. Wang, *Green Chem.* **2012**, *14*, 3423–3428.
- [4] J. Yang, *Dalton Trans.* **2017**, *46*, 5003–5007.
- [5] L. Wang, C. Cao, C. Cao, *Magnetic Resonance in Chemistry* **2015**, *53*, 520–525.
- [6] B. Turan, K. Şendil, E. Şengül, M. S. Gültekin, P. Taslimi, İ. Gulçin, C. T. Supuran, *Journal of Enzyme Inhibition*

and Medicinal Chemistry **2016**, *31*, 79-88.

- [7] B. Chen, C. Zhang, L. Niu, X. Shi, H. Zhang, X. Lan, G. Bai, *Chem. Eur. J.* **2018**, *24*, 3481-3487
- [8] L. Fan, J. Jia, H. Hou, Q. Lefbvre, M. Pueping, *Chem. Eur. J.* **2016**, *22*, 16437-16440
- [9] N. Mršić, A. J. Minnaard, B.L. Feringa, J. G. deVries, *J. Am. Chem. Soc.*, **2009**, *131*, 8358-8359.
- [10] I. Tsuneo, I. Noriyuki, Y. Kazuhiro, *Org. Lett.* **2006**, *8*, 2289-2292.
- [11] Z.Wang, X. Ye, S. Wei, P. Wu, A. Zhang, J. Sun, *Org. Lett.*, **2006**, *8*, 999-1001.



© 2018 by the authors. Submitted for possible open access publication under the terms and conditions of the Creative Commons Attribution (CC BY) license (<http://creativecommons.org/licenses/by/4.0/>).